UNIVERSITÀ DEGLI STUDI DI MILANO

Agriculture, Environment and Bionergy PhD Course
XXXVI Cycle

Department of Agricultural and Environmental Sciences – Production, Landscape, Agroenergy

Identification of genes related to biotic stress resistance in grapevine

AGR/03 - ARBORICOLTURA GENERALE E COLTIVAZIONI ARBOREE

PhD student: Valentina Ricciardi

Tutor: Prof.ssa Gabriella De Lorenzis

Doctoral coordinator: Prof. Piero Attilio Bianco

A.A. 2022-2023

Andare a sentimento.

“The song you heard singing in the leaf when you were a child is singing still”.

Mary Oliver

Abstract

Downy mildew (*Plasmopara viticola*) and powdery mildew (*Erysiphe necator*) are some of the biggest threats affecting grapevine production. Part of the solution to the problem could be the development of breeding programs for resistant varieties.

In this context, the aim of this PhD project has been the identification of new resistance and susceptibility genes for future exploitation in the development of grapevine resistant varieties.

To do that, the project has been divided in different work packages. The first one was about the genome assembly and study of Mgaloblishvili, the first identified downy mildew resistant *Vitis vinifera* variety. In the genome, three resistance loci, *Rpv29*, *Rpv30* and *Rpv31*, were successfully identified and analyzed for gene content and expression during *P. viticola* infection.

The second work package was about the validation assay of *VviLBDIf7*, a candidate gene of susceptibility to downy mildew. Similarly, the third work package was dedicated to the screening for new candidate genes of susceptibility to downy mildew, starting from a previously published RNA-sequencing experiment and focusing on nitrogen metabolism. Both in the second and third work package a transient RNA interference (RNAi) approach based on the exogenous application of dsRNA was applied, and *VviLBDIf7* was proved to be a promising candidate S gene.

Finally, the fourth work package was about a Genome Wide Association Study (GWAS) for the identification of new resistance loci to downy mildew and powdery mildew. The study was conducted on a population of *V. vinifera* varieties originated in the Caucasus and neighboring regions, one of the two domestication centers of grapevine. Four new loci where identified and analyzed for gene content. Interesting new candidate genes of resistance were hypothesized.

All together, these results will contribute to the increase of knowledge on plant-pathogen interaction and, hopefully, to viticulture sustainable disease management.

Contents

Contents 1
Chapter 1: General introduction 3
1.1 Grapevine is one of the most important fruit crops 3
1.2 Botany and Biology of grapevine plants 3
1.3 Downy mildew and powdery mildew are some of the worst diseases affecting grapevine 4
1.4 Insights on downy mildew and powdery mildew resistance sources and mechanisms 8
1.5 Resistance genes and susceptibility genes for durable resistant grape varieties 12
1.5.1 Grapevine DM and PM Resistance loci (R loci) 12
1.5.2 Grapevine DM and PM Susceptibility genes (S-genes) 14
1.6 Caucasian *V. vinifera* cultivars are a unique germplasm source for DM resistance 15
Aim of the PhD project 18
Chapter 2: Mgaloblishvili genome assembly and identification of its downy mildew resistance loci 22
2.1 Introduction 22
2.2 Materials and Methods 24
2.3 Results 29
2.4 Discussion 40
2.5 Conclusions 45
Chapter 3: *VviLBDIf7* as a candidate gene of susceptibility to *Plasmopara viticola* 46
3.1 RNAi of a Putative Grapevine Susceptibility Gene as a Possible Downy Mildew Control Strategy 46
3.1.1 Introduction 47
3.1.2 Material and Methods 51
3.1.3 Results 59
3.1.4 Discussion 65
3.1.5 Conclusion 70
Chapter 4: Mining grapevine nitrogen metabolism to identify candidate genes of susceptibility to downy mildew 73
4.1 Influence of Nitrogen on Grapevine Susceptibility to Downy Mildew 73
4.1.1 Introduction 74
4.1.2 Material and Methods 76
4.1.3 Results 82
4.1.4 Discussion 90
4.1.5 Conclusions 94
4.2.1 Introduction 95

4.2.2 Material and Methods 96
4.2.3 Results 102
4.2.4 Discussion 106
4.2.5 Conclusions 109
Chapter 5: Identification of powdery mildew and downy mildew resistance loci in Caucasian germplasm 110
5.1 Introduction 110
5.2 Material and methods 113
5.3 Results 117
5.4 Discussion 126
5.5 Conclusions 133
Chapter 6: General conclusions and future perspectives 134
Supplementary materials 136
Chapter 2 136
Chapter 3 138
Chapter 5 138
References 140

Chapter 1: General introduction

1.1 Grapevine is one of the most important fruit crops

Grapevine (*Vitis vinifera* L.) is one of the most important fruits crops worldwide. Since ancient times, its history is closely intertwined with that of humans, due to its fruits widely cultivated and appreciated, and for the wine they allow to produce (Myles *et al.*, 2011). Nowadays, the world area dedicated to viticulture is 7.3 mha, with five Countries, respectively Spain, France, China, Italy and Turkey, representing 50% of this area. Grapes produced from these lands amount to about 77.8 mt, with 30% of this production coming from Europe (OIV & International Organisation of Vine and Wine, 2019, 2022).

1.2 Botany and Biology of grapevine plants

Grapevine species belong to the *Vitaceae* family, and most of the existing cultivars used for production belong to the *V. vinifera* species, whose origins have been traced back to be West Asiatic and European (Riaz *et al.*, 2018). The plant can be divided in two sections: roots, in cultivated wine grapes often represented by a rootstock, and the scion. The scion is divided in trunk, cordons and shoots, and the shoots are composed by buds, leaves, tendrils and clusters (Figure 1.1).

During juvenile phase, grapevine leaves are characterized by spiral phyllotaxis, while in the adult phase phyllotaxis switches to opposite type. In the cluster, berries develop from the pollination of flowers pistils. This fruit is composed by a maximum of four seeds (pips), surrounded by the endocarp, pulp (mesocarp) and the skin (exocarp) (Keller, 2015).

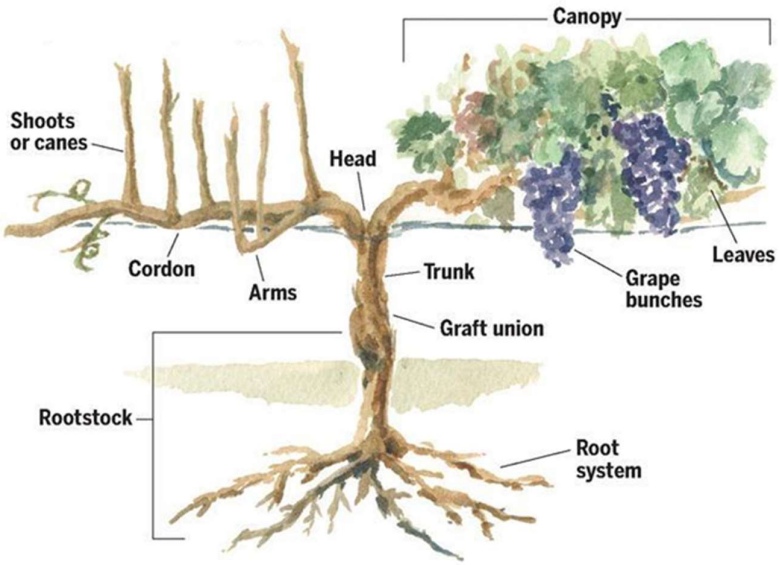

Figure 1.1 Representation of a grapevine plant (www.evineyardapp.com).

Almost all the cultivated grape varieties are hermaphrodite, self-fertile and easily crossable. Moreover, they are highly heterozygous. For this reason, the most preferred propagation is the vegetative one (clonal propagation through cuttings) (This, Lacombe and Thomas, 2006). This technique allows to maintain and multiplicate desirable genotypes and eases plant material transportation (Keller, 2015). Occasionally, asexual propagation gives rise to somatic mutations, genotype variants that sometimes lead to phenotype changes (clonal variants). This constitutes an additional source of genetic variability exploitable by breeding programs (This, Lacombe and Thomas, 2006).

From the genetic point of view, grapevine is a diploid organism. Its genome is about 475-500 Mb and is composed of nineteen chromosomes (Jaillon *et al.*, 2007).

1.3 Downy mildew and powdery mildew are some of the worst diseases affecting grapevine

Some of the biggest threats to grapevine production are downy mildew (DM) and powdery mildew (PM) diseases, caused respectively by the oomycete

Plasmopara viticola (Berk. et Curtis) Berl. and de Toni, and the ascomycete *Erysiphe necator* (Schwein).

P. viticola is a biotrophic pathogen which causes downy mildew to members of the family *Vitaceae*, in particular to the cultivated species *V. vinifera* (Bellin *et al*., 2009). The pathogen was first introduced in Europe at the end of the nineteenth century. At that time, France was attempting to replant French vineyards due to the destruction caused by phylloxera (*Daktulosphaira vitifoliae*). As a consequence, the Country introduced the pathogen as an accidental by-product of exchanges with North America (Gessler, Pertot and Perazzolli, 2011). From France, the pathogen spread across the continent, where it caused extensive damage to the grape industry. This is due to *P. viticola* ability of infecting all the plants green tissues, causing, under favourable weather conditions, extensive losses in grape yield (Yu *et al*., 2012). The yield losses are due to both quantitative and qualitative damages, with the quantitative damages caused by the ability of the oomycete to infect inflorescences and bunches, and the qualitative ones as a consequence of the leaf infection, that leads to defoliation (Figure 1.2) (Toffolatti *et al*., 2016). In temperate regions, where grapevine vegetative season is subjected to climatic conditions characterized by moderate temperature and recurrent rainfall, downy mildew usually manifests in the form of severe epidemics. As a consequence, the control of the disease is usually achieved by regular application of fungicides (Toffolatti *et al*., 2016).

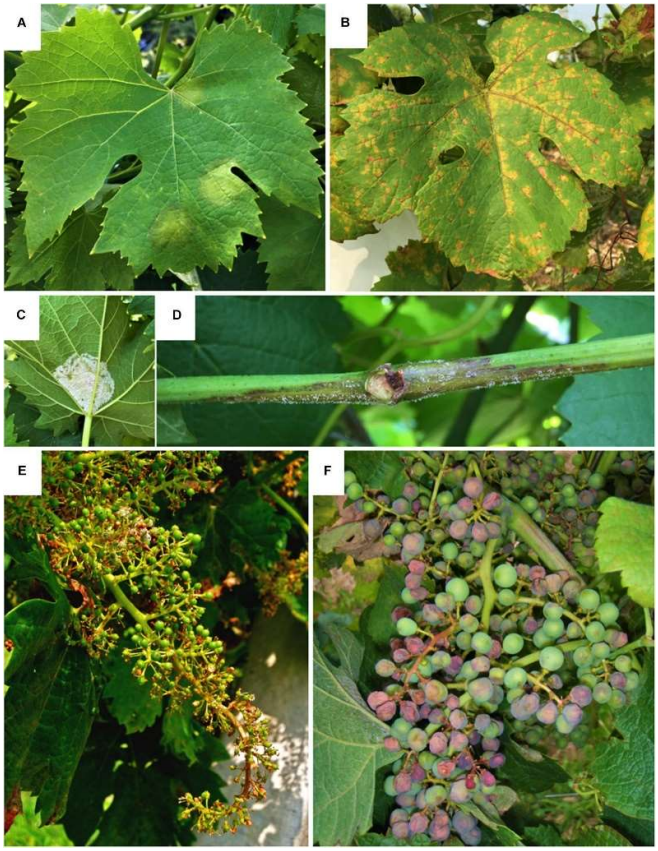

Figure 1.2 Downy mildew symptoms on grapevine plants (Sargolzaei *et al.*, 2020). Symptoms of grapevine downy mildew on leaves (**A-C**), shoot (**D**) and bunches (**E, F**). (**A**) Oilspot (yellow circular spots with an oily appearance) on the upper side of the leaf; (**B**) mosaic symptom (yellow spot restricted by veins to form yellow-to-brown small, angular spots in a mosaic pattern) on the upper side of the leaf; (**C**) sporulation (sporangiophores and sporangia appearing as a bright white, fluffy growth) on the undersides of leaves; (**D**) shoot covered by sporulation turning brown; (**E**) distorted bunch (U-shaped) turning necrotic; (**F**) shrinking berries turning violet.

Like *P. viticola*, *E. necator* is a pathogen that spread in Europe due to plant material exchanges with North America. It is an obligate parasite of *Vitaceae*, and the cultivated *V. vinifera* is highly susceptible to its infections (Gadoury *et al.*, 2012).

As in the case of the downy mildew agent, *E. necator* is able to infect all the green tissues of grapevine plants. In infected plants, first formed leaves show the presence of ascospores colonies on the abaxial surface, often accompanied by a similarly shaped chlorotic spot on the adaxial surface (Figure 1.3B). Young colonies appear whitish, while senescent ones are greyish, and may bear

cleistothecia in various developmental stages. In general, colonies are roughly circular, ranging in size from few millimetres to centimetres of diameter. They can occur singly or in groups that coalesce to cover much of the leaf. (Gadoury *et al.*, 2012). When leaves are severely affected, they develop necrotic blotches and fall prematurely, leading to qualitative losses in grape production. Inflorescences and berries are especially susceptible when young, and they can easily become completely covered in the whitish mildew (Figure 1.3A). This can lead to huge quantitative losses (Cadle-Davidson, Chicoine and Consolie, 2011). This explains why, since the pathogen arrived in Europe, its infections became very frequent and problematic. In France, after only six years from the first appearance, 2.5 million hectares of vineyards were routinely treated with Sulphur by 6 million of grape growers that were trying to suppress the disease (Gadoury *et al.*, 2007). Since then, the powdery mildew has remained a focus for disease management efforts (Gadoury *et al.*, 2012).

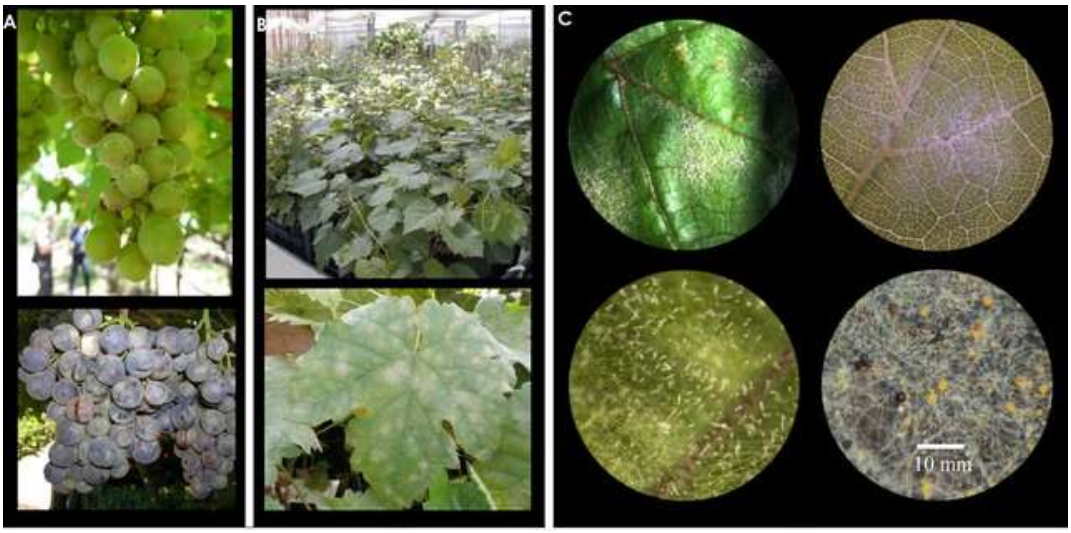

Figure 1.3 Symptoms of powdery mildew on grapevines plants (Pirrello *et al.,* 2019). Fungal morphological characteristics and symptoms of powdery mildew (**A-C**). (**A**) PM on grapes (field). (**B**) PM on leaves (greenhouse). (**C**) PM leaf disc infection under different magnification (above); conidiophores and conidia on a leaf surface (below-left); mature (black) and immature (yellow) chasmothecia (below-right).

Altogether, the massive use of fungicides against downy mildew and powdery mildew diseases has led to an intense use of chemicals in viticulture. In fact,

nowadays, viticulture is accountable for a big part of the total amount of fungicides used in EU agriculture (65%), a quantity that appear particularly disproportionate when considering viticulture arable land percentage, which happens to be comparably low (Eurostat 2007, http://ec.europa.eu/eurostat/de). This raises concerns about agriculture sustainability, given the stark contrast of this disease management strategy with current environmental and plant protection regulations (Directive 2009/128/CE; EU Regulation 1107/2009).

Furthermore, considering the future scenarios depicted by climate change, forecasting raises in temperatures and in CO_2, an increase in the disease incidence of downy mildew and powdery mildew has been predicted (Pugliese, Gullino and Garibaldi, 2011).

Therefore, it appears evident the necessity to develop different strategies for a better management of these huge viticulture threats. Among possible solutions, breeding programs appear to be certainly one of the most promising. A considerate cultivar selection usually results in the decrease of the input required for the plant management, and the increment of productions sustainability. Moreover, breeding of resistant varieties containing different sources of resistance will help to reduce the development of *P. viticola* and *E. necator* strains that lose their susceptibility to fungicides, a problem arising because of the frequent treatments (Buonassisi *et al.*, 2017; Salotti *et al.*, 2022).

1.4 Insights on downy mildew and powdery mildew resistance sources and mechanisms

DM and PM resistant grapevine varieties are usually obtained by crossing *V. vinifera* cultivars with wild non-*vinifera* species (typically American and Asian) that possess resistance to the pathogen because of their coevolution with it (Merdinoglu *et al.*, 2018). The resistance is based on different plant mechanism, involved in the detection of the pathogen, and the ability to initiate a proper defense response against it (Buonassisi *et al.*, 2017). The plant defense mechanism is organized on different consecutive levels (Figure 1.4): the first one is called Pathogen Associated Molecular Patterns (PAMP)-Triggered Immunity (PTI). PTI is characterized by a basal plant immune response activated by the

recognition of some conserved pathogen molecules. In this mechanism, specific Pattern Recognition Receptors (PRRs) on the plant cell plasma membrane are able to perceive the pathogen presence and the molecules it produces (Newman *et al.*, 2013). Nevertheless, some pathogens developed the ability to bypass this first defense level, by secreting specific proteins called effectors. Effectors can suppress the plant immune response and manipulate the physiology of the host cell to the pathogen advantage (Bozkurt *et al.*, 2012). During evolution, this ability of the pathogen led to the development of a second level of plants defence mechanism, called effector-triggered immunity (ETI). ETI relies on a second class of receptors, the resistance proteins (R), that can recognize effectors in a highly specific way. Finally, ETI activation leads to disease resistance and is often associated to a cell death response localized at the infection site, a process named hypersensitive response (HR) (Jones and Dangl, 2006).

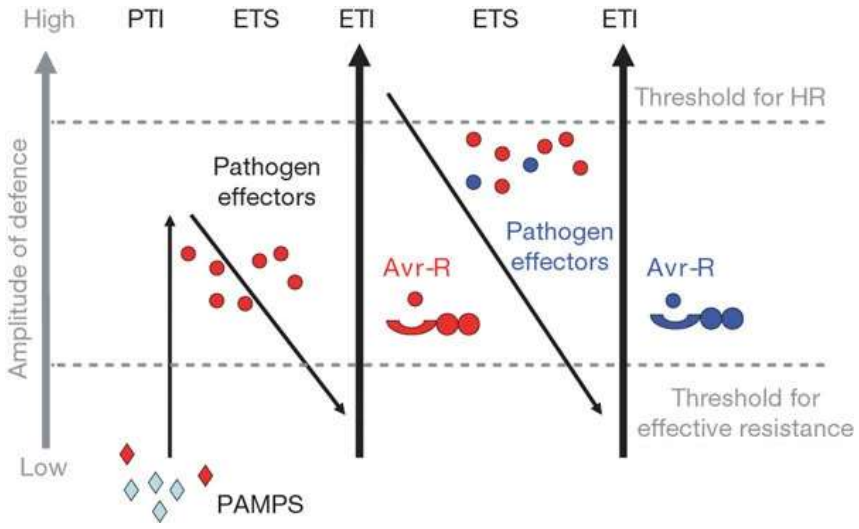

Figure 1.4 Zigzag model illustrating the quantitative output of the plant immune system (Jones and Dangl, 2006). Phase 1, plants detect microbial/pathogen-associated molecular patterns (MAMPs/PAMPs, red diamonds) via PRRs to trigger PAMP-triggered immunity (PTI). Phase 2, successful pathogens deliver effectors that interfere with PTI, or otherwise enable pathogen nutrition and dispersal, resulting in effector-triggered susceptibility (ETS). Phase 3, one effector (indicated in red) is recognized by an NB-LRR protein, activating effector-triggered immunity (ETI), that often passes a threshold for induction of hypersensitive cell death (HR). Phase 4, pathogen isolates are selected that have lost the red effector, and perhaps gained new effectors through horizontal gene flow (in blue)—these can help pathogens to suppress ETI. Selection favours new plant NB-LRR alleles that can recognize one of the newly acquired effectors, resulting again in ETI.

Effectors and receptors are codified by non-essential genes, usually dominant genes, and many R-genes encode for intracellular nucleotide-binding leucine-rich-repeat (NB-LRR) proteins. As a consequence, they are able to rapidly evolve. Because of the strong selective pressure on both the pathogen and the host plant, the first trying to avoid ETI by the diversification of its effectors and the second evolving new receptors so that ETI is able to properly function, this process becomes frequent (Buonassisi *et al.*, 2017). Unfortunately, this mechanism also implies that resistance acquired through R gene is readily overcome. To solve this inconvenient, it possible to use a different strategy to obtain resistant cultivars, one that employs both resistance genes pyramiding, and susceptibility genes (S-genes) (Van Schie and Takken, 2014).

S-genes are genes that critically facilitates the compatibility between plants and pathogens. They are essential for their interaction, especially in the case of biotrophic pathogens. Based on their role in the interaction between plant and pathogen during the different infection stages, S-genes are divided in three groups: a) plant genes involved with the pathogen colonization, b) genes related to the modulation of host defenses and c) plant genes that allow pathogen sustenance (Zhang *et al.*, 2022). Mutation or loss of an S-gene can limit the pathogen ability to cause the disease. Therefore, whereas R-genes are typically dominant, resistance conferred by loss or alteration of S-genes is generally recessive. Once mutated, S-genes can cause two different types of resistance: one more definite, pathogen-specific, based on the compatibility impairment caused by the absence of pre-penetration requirements or post-penetration requirements; the other one, a broad-spectrum resistance, where S-genes mutation leads to prolonged or constitutive defenses (Gorshkov and Tsers, 2022). Altogether, these types of resistance mechanisms, are difficult to overcome. For this reason, despite their frequent role in plants core metabolism, they could be useful resources for breeding of resistant varieties. Needless to say, after a careful assessment of their suitability for application (Figure 1.5) (Van Schie and Takken, 2014).

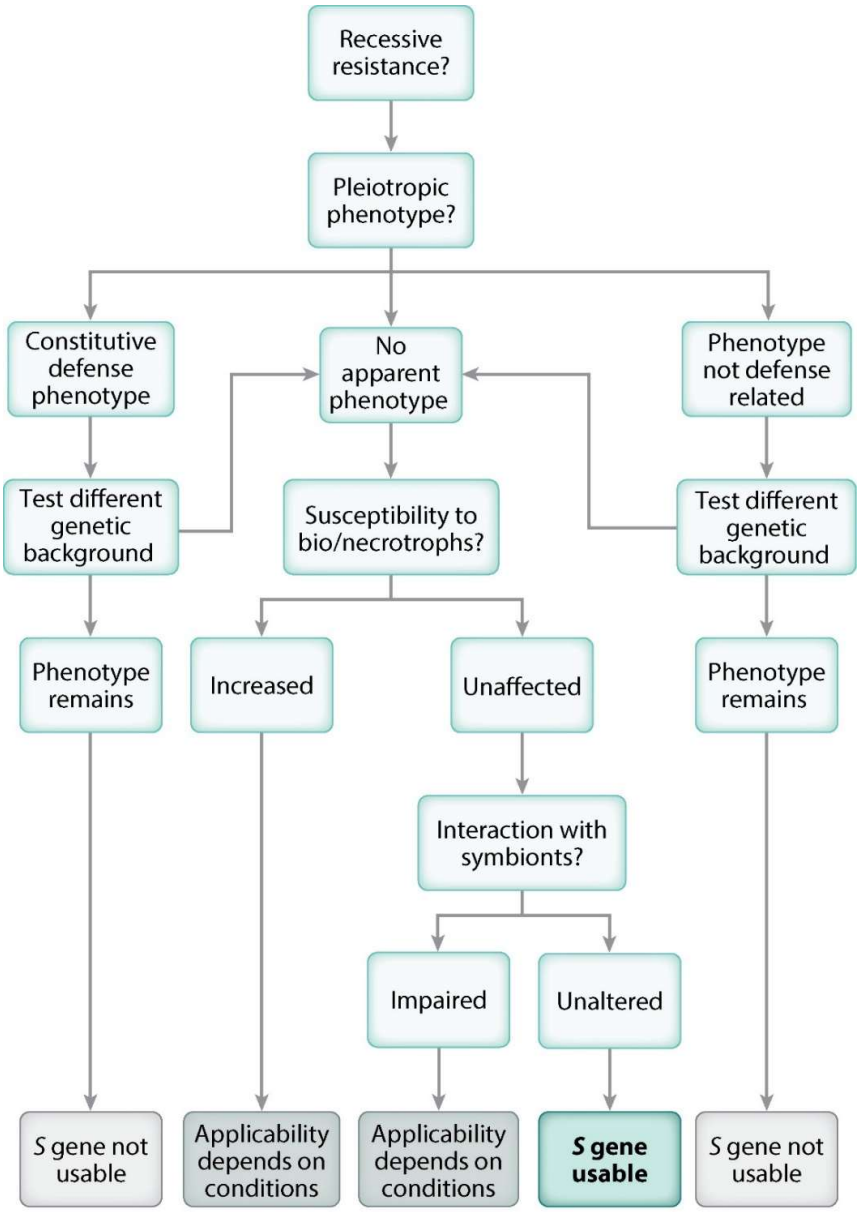

Figure 1.5 Classification scheme to determine the usability of a susceptibility (S) gene (Van Schie and Takken, 2014). First, recessive resistance is observed (mutant with reduced susceptibility). Second, pleiotropic effects should be monitored (growth, yield, fertility, senescence, and abiotic stress tolerance). If a deleterious phenotype is present, it is important to test whether it can be alleviated in a different genetic background. Third, the plant response to pathogens with a different lifestyle (biotroph *versus* necrotroph) should be evaluated. Lastly, plant performance should be tested in field conditions, as interactions with beneficial microbes, such as rhizobia and mycorrhiza, may be affected.

1.5 Resistance genes and susceptibility genes for durable resistant grape varieties

1.5.1 Grapevine DM and PM Resistance loci (R loci)

So far, 35 genomic regions are known to be associated with DM resistance (Table 1.1), and 13 with PM resistance (Table 1.2) (Zou *et al.*, 2023). However, their throughout characterization at candidate gene level has been achieved in few cases: *Rpv1* (Feechan *et al.*, 2013), *Rpv3* (Foria *et al.*, 2018) and *Rpv33* (Zou *et al.*, 2023)for DM; and a few more (*Ren2*, *Ren3*, *Ren4, Ren6, Ren11, Ren12* and *Run1*) (Massonnet *et al.*, 2022; Sapkota *et al.*, 2023) for PM. Most of DM and PM resistant sources confer varying levels of partial resistance, while the ones coming from *Muscadinia rotundifolia* and *V. piasezkii* are known to confer total resistance in the genetic context in which they are studied (Zini *et al.*, 2019).

All the work performed on R loci has revealed a striking degree of similarities between them. Often, they occur in complex loci that contain multiple copies of gene with a very high degree of similarity in their sequences. To describe this type of loci, the concept of haplotype is used to indicate the precise configuration of genes occurring in a particular complex locus variant. Nonetheless, same simple loci exist as well, and they usually encode for a single known resistance allele (Ellis, Dodds and Pryor, 2000).

The majority of R loci includes genes that encode proteins classified as NBS-LRR proteins (composed of a nucleotide binding site (NBS) domain and a leucine–rich repeat (LRR) domain), followed by Toll/Interleukin-1-receptors (TIR); proteins that include Coiled coil (CC) domain; Transmembrane domain (TrD); PEST aminoacid domain; Endocytosis cell signaling domain (ECS); Nuclear localization signal (NLS); WRKY amino acid domain (Gururani *et al.*, 2012). Some categories are more frequently associated with specific resistances (for example fungi or oomycetes), while others are related to broad spectrum resistance (Zini *et al.*, 2019).

Table 1.1 Table summarizing known downy mildew resistance loci. Per each locus, ID, disease resistance trait, origin, chromosome, position in the chromosome, and reference are shown (Source: VIVC database).

Locus ID	Resistance	Origin	Chr	Position (Mb)	Reference
Rpv1	*P. viticola*	*M. rotundifolia*	12	10.3	Merdinoglu et al., 2023
Rpv2	*P. viticola*	*M. rotundifolia*	18	n.a.	Wiedemann-Merdinoglu et al. (2006)
Rpv3	*P. viticola*	n.a.	18	26.9	Bellin et al., 2009
Rpv4	*P. viticola*	?	4	4.7-5.2	Welter et al., 2007
Rpv5	*P. viticola*	*V. riparia*	9	4	Marguerit et al., 2009
Rpv6	*P. viticola*	*V. riparia*	12	20.4	Marguerit et al., 2009
Rpv7	*P. viticola*	n.a.	7	11.4	Bellin et al., 2009
Rpv8	*P. viticola*	*V. amurensis*	14	6.6	Blasi et al., 2011
Rpv9	*P. viticola*	*V. riparia*	7	16.6	Moreira et al., 2011
Rpv10	*P. viticola*	*V. amurensis*	9	3.7	Schwander et al., 2012
Rpv11	*P. viticola*	n.a.	5	4.5	Fisher et al., 2004
Rpv12	*P. viticola*	*V. amurensis*	14	9.3	Venuti et al., 2013
Rpv13	*P. viticola*	*V. riparia*	12	10	Moreira et al., 2011
Rpv14	*P. viticola*	*V. cinerea*	5	20.2	Ochssner et al., 2016
Rpv15	*P. viticola*	*V. piasezkii*	18	n.a.	Pap et al., in preparation
Rpv16	*P. viticola*	n.a.	n.a.	n.a.	Pap et al., in preparation
Rpv17	*P. viticola*	n.a.	8	11.7	Divilov et al., 2018
Rpv18	*P. viticola*	n.a.	11	15.4	Divilov et al., 2018
Rpv19	*P. viticola*	*V. rupestris*	14	29.5	Divilov et al., 2018
Rpv20	*P. viticola*	n.a.	6	0.9	Divilov et al., 2018
Rpv21	*P. viticola*	n.a.	7	2.1	Divilov et al., 2018
Rpv22	*P. viticola*	*V. amurensis*	2	2.1-3.5	Fu et al., 2020
Rpv23	*P. viticola*	*V. amurensis*	15	9.9-139	Fu et al., 2020
Rpv24	*P. viticola*	*V. amurensis*	18	n.a.	Fu et al., 2020
Rpv25	*P. viticola*	*V. amurensis*	15	3.0-3.9	Lin et al., 2019
Rpv26	*P. viticola*	*V. amurensis*	15	14.7-15.0	Lin et al., 2019
Rpv27	*P. viticola*	*V. aestivalis*	18	24.6-26.0	Sapkota et al., 2019
Rpv28	*P. viticola*	*V. rupestris*	10	1.2-1.3	Bhattarai et al., 2020
Rpv29	*P. viticola*	*V. vinifera*	14	21.6	Sargolzaei et al., 2020
Rpv30	*P. viticola*	*V. vinifera*	3	16.2	Sargolzaei et al., 2020
Rpv31	*P. viticola*	*V. vinifera*	16	21.3	Sargolzaei et al., 2020
Rpv32	*P. viticola*	n.a.	n.a.	n.a.	Malagol et al., in preparation
Rpv33	*P. viticola*	V. × doaniana 'PI 588149'	9	0.8-1.3	Zhou et al., 2023
Rpv34	*P. viticola*	n.a.	n.a.	n.a.	Cadle-Davidson et al., in preparation
Rpv35	*P. viticola*	n.a.	n.a.	n.a.	Cadle-Davidson et al., in preparation

Table 1.2 Table summarizing known powdery mildew resistance loci. Per each locus, ID, disease resistance trait, origin, chromosome, position in the chromosome, and reference are shown (Source: VIVC database).

Locus ID	Resistance	Origin	Chr	Position (Mb)	Reference
Ren1	*E. necator*	*V. vinifera*	13	18.4	Hoffman et al., 2008
Ren1.2	*E. necator*	*V. vinifera*	13	17.9 -18.2	Possamai et al.2021
Ren2	*E. necator*	n.a.	*14*	26.9	Dalbo et al., 2001
Ren3	*E. necator*	n.a.	15	4.9-10.9	Zyprian et al., 2016; Zendler et al., 2017
Ren4	*E. necator*	*V. romanetii*	18	26.9	Riaz et al., 2012
Ren5	*E. necator*	*M. rotundifolia*	14	4.8	Blanc et al., 2012
Ren6	*E. necator*	*V. piasezskii*	9	8.6-9.1	Pap et al., 2016
Ren7	*E. necator*	*V. piasezskii*	19	0.2-0.9	Pap et al., 2016
Ren8	*E. necator*	n.a.	18	13.2	Zyprian et al., 2016
Ren9	*E. necator*	n.a.	15	1.4	Zendler et al., 2017
Ren10	*E. necator*	n.a.	2	17.9	Teh et al., 2017
Ren11	*E. necator*	*V. aestivalis*	15	13.7-15.3	Karn et al., 2021
Ren12	*E. necator*	*V. amurensis*	13	25.1-25.9	Sapkota et al., 2023
Ren13	*E. necator*	n.a.	n.a.	n.a.	Cadle-Davidson et al., in preparation
Run1	*E. necator*	*M. rotundifolia*	12	16.4-16.8	Feechan et al., 2013
Run2	*E. necator*	*M. rotundifolia*	18	26.9	Riaz et al., 2011

1.5.2 Grapevine DM and PM Susceptibility genes (S-genes)

Compared to R-genes, in grapevine only a couple of susceptibility genes have been identified and applied for the development of resistant plants. One is a gene of susceptibility to DM resistance and the other to PM resistance.

Well known and confirmed grapevine S-genes are *Downy mildew resistant 6 -1* (*DMR6-1*) and *Downy mildew resistant 6 -2 (DMR6-2)*. Different studies showed that mutation of *DMR6* genes leads to resistance to oomycetes and other pathogens, like fungi and bacteria, in many different species (Giacomelli *et al.*, 2023). The genes encodes for 2-oxogluatarate (2OG)-Fe(II) oxygenases, that acts as a negative regulators of plant immunity. *DMR6-1* and *DMR6-2* are part of the same family of *DLO* (*DMR6-like oxygenase*) genes, that function as a salicylic acid (SA)-hydroxylases. They convert, SA to 2,5- and 2,3-dihydroxybenzoic acid (DHBA), respectively. For this reason, the genes of this family are considered key-players in maintaining SA homeostasis during plant growth and response to biotrophic pathogens (Pirrello *et al.*, 2022). In grapevine,

the simultaneous knock-out by genome editing of *VviDMR6-1* and *VviDMR6-2* led to a significantly reduced susceptibility to downy mildew (Giacomelli *et al.*, 2023).

Nevertheless, the most notorious grapevine S-gene is *Mildew Locus O* (*MLO*), whose knock-down through RNA interference have been proved to confer resistance to powdery mildew, by reducing the severity of the disease up to 77% (Pessina *et al.*, 2016). *MLO* genes encode for membrane proteins involved in a variety of physiological processes, such as root morphogenesis and pollen tube reception by embryo (Acevedo-Garcia, Kusch and Panstruga, 2014). The S-genes of this family are thought to be involved in the negative regulation of vesicle-associated and actin-dependent defense pathways, at the site of *E. necator* penetration (Pessina *et al.*, 2016).

Their gene family is largely conserved across the plant kingdom and their loss of function resulted in PM resistance in many different species, from *Arabidopsis thaliana* (Consonni *et al.*, 2006) to wheat (Wang *et al.*, 2014). The gene family is divided into seven phylogenetic clades, of which only two includes S-genes. The S-genes can be identified in the clades by their increased expression in response to the pathogen, compared to the lack of response from the other members of the clade (Feechan *et al.*, 2013).

1.6 Caucasian *V. vinifera* cultivars are a unique germplasm source for DM resistance

As previously stated, until recently, resistance genes for grapevine breeding programs have been found in American and Asian species. From the cross of those species with productive varieties of interest, resistant hybrids have been obtained. However, the firsts generations of resistance hybrids where unsuitable for the production of high-quality wines, due to the lingering foxy aromas given to them by the plants source of resistance (Töpfer *et al.*, 2011).

Nowadays, the last generation varieties resulting from those crossings, like Regent in Germany and Bianca in Hungary, have no more the unpleasant defects of their parental. Nevertheless, the search of new resistance sources in *V. vinifera* varities could have a uniquely positive impact on breeding programs.

The use of resistance sources with the same genetic background of wine cultivars would simplify and shorten breeding programs, while being able to produce new resistant varieties with the quality levels required for wine production (Toffolatti *et al.*, 2016). To reach the aim, different studies were conducted in the past years and some of them have found in Southern Caucasus (Georgia) grapevine germplasm, a valuable source of resistance, in particular to downy mildew disease (Bitsadze *et al.*, 2015; Toffolatti *et al.*, 2016, 2018) and powdery mildew (Possamai *et al.*, 2021).

The uniqueness of Georgian germplasm lies in their origin, one of the two domestication centers of grapevine (Dong *et al.*, 2023). Because of this reason, Georgian germplasm has been proven to be a reach source of genetic diversity for a vast number of different traits, from eno-carpological ones, to phenology related ones and, finally, for abiotic and biotic resistance traits (Abashidze *et al.*, no date; Bitsadze *et al.*, 2015; Rustioni *et al.*, 2019; Sargolzaei *et al.*, 2021). For what concerns biotic resistance traits, in particular resistance to PM, a recent work identified two Caucasian cultivars, “Shavtsitska” and “Tskhvedianis tetra”, carrying a new resistant haplotype of *Ren1* (Possamai *et al.*, 2021).

In the same years, some studies focused on DM were able to identify a particularly interesting Georgian *V. vinifera* cultivar: Mgaloblishvili. The variety displays a unique mechanism of defense against *P. viticola*. The mechanism is founded on both growth and sporulation limitation of *P. viticola*, determined by the over-expression of genes related to pathogen recognition, the ethylene signaling pathway, the synthesis of antimicrobial compounds (such as VOCs) and enzymes, and the development of structural barriers (Figure 1.6) (Toffolatti *et al.*, 2018). In Toffolatti et al. (2018), among the Mgaloblishvili overexpressed genes related to defense mechanisms, some candidate genes were found to be particularly promising. The most interesting ones were some CC-NBS-LRR receptors, whose homologues seem to be involved in leaf rust resistance, and some transcription factors involved in ethylene signaling pathway, the probable network directing Mgaloblishvili defense response.

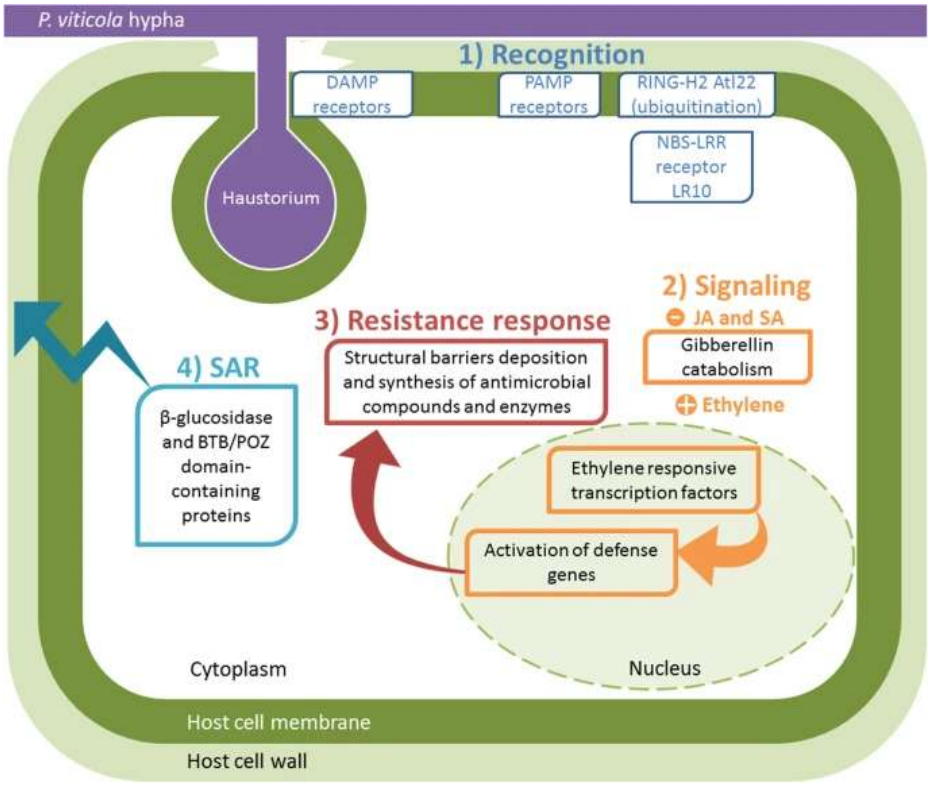

Figure 1.6 Schematic representation of the putative resistance mechanism of Mgaloblishvili (in green) against *P. viticola* (in purple) based on the overexpression of genes involved in the plant defense pathway at 1 dai (Toffolatti *et al.,* 2018). (**1**) Pathogen recognition through PAMP, DAMP and effector receptors, and ubiquitination. (**2**) Phytohormone signaling based on ethylene. (**3**) Resistance response based on synthesis of antimicrobial compounds and fungal wall degradating enzymes, and cell wall reinforcement. (**4**) Systemic signaling based on the indirect activation of the disease resistance protein PR1 that is involved in Systemic Acquired Resistance (SAR).

Furthermore, an in-depth transcriptomic study, was able to discover a putative candidate gene of susceptibility to DM (Toffolatti *et al*., 2020). The result was achieved by comparing Pinot noir (*V. vinifera* susceptible cultivar) and Mgaloblishvili transcriptomic responses to *P. viticola*. The gene, named *VvLBDIf7*, was found to be overexpressed in Pinot noir 24 hours after the inoculum with *P. viticola*. On the contrary, its expression was found to be decreased in the resistant Georgian cultivar. In literature, the *Arabidopsis thaliana* orthologue of *VviLBDIf7* is a confirmed gene of susceptibility to *Fusarium oxysporum* (Thatcher *et al*., 2012), and in Duncan grapefruit (*Citrus paradisi*) the gene was validated as susceptibility gene to *Xantomonas citri*, causal agent of

bacterial canker (Jia *et al.*, 2017). *A. thaliana* mutants suggests that the gene is involved in the jasmonate signaling, in particular as a repressor down-stream of *COI1* (*Corona insensitive 1*) and *MYC2* (*Jasmonate insensitive1*) that are required for full elicitation of *F. oxysporum*- and jasmonate-dependent responses (Thatcher *et al.*, 2012).

When working with perennial crops, finding new resources to be used in biotic stress resistance breeding programs is extremely important. Plants have to stay productive for years while maintaining thier resistance characteristics. To prevent the selection of pathogens strains able to overcome the plant resistance, the main strategy is the pyramiding of resistance loci (R loci) (Bourguet *et al.*, 2016). In this frame, the discovery of Mgaloblishvili new DM resistance resources introduced promising opportunities for breeding programs (Sargolzaei *et al.*, 2020). To be able to efficiently employ the cultivar for breeding purposes, a study to dissect the genetic architecture of Mgaloblishvili resistance mechanism against *P. viticola* was conducted. Using a Genome Wide Association Study (GWAS) approach, based on genotyping by Vitis18kSNP genotyping array, and the old version of grapevine reference genome (PN40024 12X v2), three new DM resistance loci were identified. The new loci were named Rpv29 (chromosome 14), Rpv30 (chromosome 3) and Rpv31 (chromosome 16) (Sargolzaei *et al.*, 2020).

Aim of the PhD project

In the frame of the described scenario, the aim of this PhD project was to contribute to eco-sustainable viticulture disease management with the identification and characterization of genetic resources to be used in breeding programs of resistant varieties. To do that, different studies were conducted to identify resistance and susceptibly genes to some of the most destructive grapevine disease, DM and PM.

To reach the scope, the project was divided into four work packages, whose results are reported in each one of the following chapters.

- **Chapter 2: Mgaloblishvili genome assembly and identification of its downy mildew resistance loci.**

  The aim of this study was to assembly and analyze the genome of the first identified downy mildew resistant *V. vinifera* variety, Mgaloblishvili. A whole genome comparison of this resistant variety with the genome of the susceptible reference accession PN40024 has been performed. Mgaloblishvili resistance loci were in-depth analysed in terms of structure, gene content, gene expression and impact of structural variants and SNPs.

- **Chapter 3: *VviLBDIf7* as a candidate gene of susceptibility to *Plasmopara viticola.***

  The aim of this work was to investigate the role of *VviLBDIf7* as a candidate gene of susceptibility to downy mildew, using RNA interference induced by exogenous application of dsRNA.

  After treatment with the target dsRNA, gene expression of *VviLBDIf7* was analysed in the plant tissues. Disease severity and sporangia production were evaluated on dsRNA-treated leaves inoculated with *P. viticola*. Furthermore, morphology of the pathogen vegetative and reproductive structures was studied in dsRNA-treated leaf tissues. Finally, a preliminary investigation of the putative systemic effect of dsRNA was performed, coupled with the evaluation of dsRNA treatment on off-target and jasmonic acid metabolism genes.

  The work was published in Frontiers in Plant Sciences – Volume 12 – 2021. DOI: 10.3389/fpls.2021.667319

- **Chapter 4: Mining grapevine nitrogen metabolism to identify candidate genes of susceptibility to downy mildew.**

  The aim of this study was to identify new candidate genes of susceptibility to downy mildew, to be exploited as new resources for the improvement of viticulture disease management. To do that, the work was divided in two parts.

Chapter 4.1 Influence of Nitrogen on Grapevine Susceptibility to Downy Mildew.

The role of nitrogen (N) metabolism and its effects on the interaction between grapevine and *P. viticola* interaction was explored in this study.

The effect of N on pathogen development and modulation of plant candidate genes of resistance and susceptibility was assessed on grapevine cuttings, subjected to different levels of nitrogen fertilization. After treatment, different parameters were evaluated: i) leaf nitrogen and chlorophyll content; ii) *P. viticola* development and disease severity; iii) expression of candidates R- and S-genes involved in N metabolism (*VviNRT3.1*, *VviGS*, *VviAS1*). As a result, a new candidate gene of susceptibility to *P. viticola*, *VviAS1* was identified.

This study was published in Plants – Volume 12 – 2023. DOI: 10.3390/plants12020263.

Chapter 4.2 *VviAS1* as a candidate gene of susceptibility to downy mildew: validation assay by transient RNAi interference.

In this work, the new candidate gene of susceptibility to downy mildew, *VviAS1*, was investigated for validation by transient RNAi approach (dsRNA assay), following the example reported in Chapter 3.

The candidate gene expression was evaluated after treatment with the target dsRNA. *P. viticola* infection was evaluated in the form of both disease severity and disease incidence, evaluated as Infection Frequency Rate (IFR). To gain new information about dsRNA dosage and plant age effect, the experiment was performed with some modifications compared to chapter 3. i) Grapevine plants more advanced in the vegetative growth stage were employed; ii) An increased dsRNA quantity was used (200 ug per plant instead of 100 ug per plant); iii) To prove the target-dsRNA specificity of action, an internal control gene (*VviUFGT*) was included in the experiment. Unfortunataly, unexpected outcomes were obtained and the experiment didn't proceed as intended.

- **Chapter 5: Identification of powdery mildew and downy mildew resistance loci in Caucasian germplasm.**

  In this study, a Genome Wide Association approach was used to identify new loci of resistance to both downy mildew and powdery mildew. To do that, a population of *V. vinifera* accessions originated in Caucasus and neighboring regions was anayzed. The accessions were genotyped with 13 SSR (Simple Sequence Repeat) loci for cultivar identification and six SSR loci associated with known resistance to DM and PM. The characterized population was genotypes with the *Vitis*18kSNP genotyping chip array and phenotyped for the resistance to DM and PM. Obtained data were used to perform a GWAS analysis. Finally, regions associated to positive GWAS signals were identified on PN40024 and Mgaloblishvili genome, and investigated for gene content.

Chapter 2: Mgaloblishvili genome assembly and identification of its downy mildew resistance loci

2.1 Introduction

Grapevine (*Vitis vinifera* L.) is one of the most important fruit crops worldwide. Nowadays, the world area dedicated to viticulture is 7.3 mha, with five Countries, respectively Spain, France, China, Italy and Turkey, representing 50% of this area. Grapes produced from these lands amount to about 77.8 mt, with 30% of this production coming from Europe (OIV V & International Organisation of Vine and Wine, 2019). One of the worst diseases affecting grapevine production is downy mildew. The disease is caused by the oomycete *Plasmopara viticola* [(Berk. & Curt.) Berl. & de Toni], a biotrophic pathogen able to infect all the green tissues of grapevine plants, including stems and bunches (Fröbel and Zyprian, 2019). This leads to huge losses both in terms of quantity and quality of grapes produced (Bellin *et al.*, 2009; Gessler, Pertot and Perazzolli, 2011). Usually, the disease is mainly treated with the regular and heavy application of fungicides, a solution that is considered no long sustainable, especially given current environmental regulations (Directive 2009/128/CE; EU Regulation 1107/2009). A considerable part of the solution could be the development of breeding programs of resistance varieties. Currently, these breeding programs are based on the introduction of resistance loci from American and Asian *Vitis* wild species into *V. vinifera* genetic backgrounds (the ones of wine production varieties) (Töpfer *et al.*, 2011). However, this leads to drawbacks in the breeding programs, due to issues related to linkage drag of undesirable traits (Eibach and Töpfer, 2015).

In recent years, some studies have highlighted a new interesting source of resistant germplasm, the *V. vinifera* varieties from Georgia (South Caucasus) (Bitsadze *et al.*, 2015; Toffolatti *et al.*, 2016). The uniqueness of Georgian germplasm lies in its origin, that is considered to be one of grapevine domestication centers (Dong *et al.*, 2023). Among those interesting varieties, some cultivars, such as Mgaloblishvili, were proven to possess a unique

mechanism of defense against *P. viticola* (Bitsadze *et al.*, 2015; Toffolatti *et al.*, 2016, 2018). Recently, the resistant mechanism of Mgaloblishvili against *P. viticola* infection has been proposed. Mgaloblishvili is able to limit *P. viticola* growth and sporulation and this defense mechanism is achieved by the overexpression of genes related to pathogen recognition, ethylene signaling pathway and the synthesis of antimicrobial compounds (VOCs) and enzymes, coupled with the deposition of structural barriers (Toffolatti *et al.*, 2018). In comparison to Pinot noir, a susceptible cultivar, Mgaloblishvili showed a faster response against the pathogen, regulating the resistance genes in the first 24 hours after inoculation (Toffolatti *et al.*, 2018). On top of it all, Mgaloblishvili allowed the discovery of a new candidate gene of susceptibility to downy mildew, *VviLBDIf7*, down-regulated by the cultivar during infection (Sargolzaei *et al.*, 2020). Using a transient RNA interference approach based on the exogenous application of dsRNA, the gene was validated as a successful way of decreasing downy mildew infection (Marcianò *et al.*, 2021).

In 2020, a study to define the genetic basis of Mgaloblishvili resistance was performed. A Genome Wide Association (GWAS) approach was used to study the resistant cultivar self-cross progeny and 48 genotypes of a Georgian germplasm collection (Sargolzaei *et al.*, 2020). As a result, three new loci of resistance to *P. viticola* where identified: i) *Rpv29* on chromosome 14; ii) *Rpv30* on chromosome 03; iii) *Rpv31* on chromosome 16. However, at that time, the study was performed using the grapevine reference genome PN40024 12X.v2 (Canaguier *et al.*, 2017) as a reference. PN40024 is a highly homozygous cultivar derived from selfing of cv. Helfensteiner, cross of cv. Pinot noir and Schiava grossa (Velt *et al.*, 2023) and as the majority of known *V. vinifera* varieties, it is susceptible to downy mildew. Nonetheless, PN40024 genome was used because of the limitations in the field of grapevine genomics, which made it hard to obtain easily and conveniently a good quality genome to use as a reference for this *vinifera* resistant variety. The difficulty in working with grape genomes is manly related to the fact that most grapevine cultivars represent crosses between distantly related parents. Due to this parentage, and the accumulation of somatic

mutations related to grapevine domestication history, grape cultivars are often highly heterozygous (Zhou *et al.*, 2019).

However, with the recent advent of third generation sequencing technologies, such as those of the Pacific Biosciences (PacBio) platform, things changed. Long reads sequencing technologies and the development of new tools able to properly process them, such as Falcon Unzip (Chin *et al.*, 2016), made the assembly of grapevine diploid genomes with a higher level of contiguity finally possible (Massonnet *et al.*, 2020; Minio *et al.*, 2022).

In this work, the use of these technologies made possible to obtain a chromosome-scale diploid genome assembly for the resistant cultivar Mgaloblishvili. To the best of our knowledge, this is the first genome of a *V. vinifera* downy mildew resistant variety ever assembled. By combining Mgaloblishvili genome information with data from the previous study based on the reference PN40024, it was possible to dissect the three resistant loci and here a comprehensive analysis of their content has been provided. For each locus, expression of the genes was analyzed using previously published RNA sequencing data (Toffolatti *et al.*, 2018). Furthermore, using DNA sequencing data of selected accessions of Mgaloblishvili self-cross progeny, resistance haplotypes were identified for *Rpv30* and *Rpv31*.

2.2 Materials and Methods

2.2.1 Plant material and DNA extraction

Young leaves of *V. vinifera* variety Mgaloblishvili were collected from plants grown in the ampelographic collection of the Department of Agricultural and Environmental Sciences, University of Milan, located in Torrazza Coste (Pavia, Lombardy, Italia).

High molecular weight (HMW) DNA isolation for the genome sequencing was performed by KeyGene Company (Wageningen, Netherlands), using KeyGene's proprietary uHMW protocol (version 3). HMW DNA was quality controlled using concentration measurements on Nanodrop (Thermo Fisher Scientific, Hanover

Park, IL) and Qubit (Thermo Fisher Scientific, Hanover Park, IL) and its length distribution was verified using the Femto Pulse (Agilent, Santa Clara, CA).
To identify resistant haplotypes and recombination events within the loci, DNA sequencing was performed. Two resistant accessions (97 – resistant, 124 – resistant) and two susceptible accessions (157M – susceptible, 145LIB – susceptible) were selected from the progeny of Mgaloblishvili self-cross. Plant DNA was extracted from young leaves of selected accessions using NucleoSpin Plant II Mini kit (Macherey-Nagel), according to manufacturer instructions. DNA quantity and quality were checked using Qubit (Thermo Fisher Scientific, Hanover Park, IL) and agarose gel electrophoresis.

2.2.2 Library preparation, genome sequencing and DNA sequencing

HMW DNA of Mgaloblishvili was used as input for the PacBio library preparation according to the Procedure and Checklist - Preparing HiFi SMRTbell® Libraries using SMRT bell Express Template Prep Kit 2.0 (PN 101-853-100 Version 05, August 2021). The Megaruptor 3 (Diagnode) was used to fragment the DNA to a mode size between ~15-20 Kb. A library was prepared and size-selected using the Blue Pippin prep (Sage Sciences). The size distribution of the library was verified using the Femto Pulse. The library was sequenced on one 8M ZMW Sequel IIe flow cell using adaptive loading and a 30 hrs data acquisition time. Raw data was processed using SMRT LINK version 10.1 following the CCS protocol with default settings to generate the HiFi data.
High quality genomic DNA was isolated from grape leaves Mgaloblishvili self-progeny selected accessions using the method described in Chin et al. (2016). DNA purity was evaluated with a Nanodrop 2000 spectrophotometer (Thermo Scientific, Hanover Park, IL), quantity with a Qubit 2.0 Fluorometer (Life Technologies, Carlsbad, CA) and integrity by gel electrophoresis.
Short-read sequencing genomic libraries were prepared from 1 mg of DNA extracted from young leaves using the Kapa LTP library prep kit (Kapa Biosystems, MA, USA). After quantity and quality evaluation with the High Sensitivity chip of a Bioanalyzer 2100 (Agilent Technologies, CA, USA), libraries

were sequenced in 150-bp-long paired-end reads on a HiSeq X Ten instrument (IDSeq, CA, USA).

2.2.3 Genome assembly and annotation

Mgaloblishvili HiFi reads were assembled using Hifiasm v.0.16.1-r374 (Cheng *et al.*, 2021) testing 136 different combinations of assembly parameters. The assembly showing, for both haplotypes, the least fragmentation and with the highest number of conserved full-length single copy BUSCO genes was selected (parameters: a=4, k=41, w=31, f=25, r=4, s=0.7, D=3, N=300, n=25). The draft genome assembly underwent quality control and scaffolding into a diploid set of chromosome-scale pseudomolecules using HaploSync (Minio *et al.*, 2022) and the *Vitis* consensus genetic map developed by (Zou et al., 2020). Two cycles of HaploFill were used to improve the completeness of the assembled pseudomolecules.

Mgaloblishvili genome was annotated following the procedure in (Minio, Massonnet, Figueroa-Balderas, Castro, *et al.*, 2019) and (Cochetel *et al.*, 2021). Briefly, repetitive sequences were identified with RepeatMasker ver. open-4.0.6 (Smith *et al.* (2013) http://www.repeatmasker.org) using a custom *V. vinifera* repeat library described in (Minio et al. 2018) and masked prior to gene prediction. Protein-coding genes were predicted with EVM ver. 1.1.1 (Haas *et al.*, 2008) using as input: (i) *ab initio* predictions from SNAP ver. 2006-07-28 (Korf, 2004), Augustus ver. 3.0.3 (Stanke *et al.*, 2006), and GeneMark-ES ver. 4.32 (Lomsadze *et al.*, 2005) trained on Cabernet Sauvignon; (ii) *ab initio* predictions of Augustus trained on BUSCO dataset; (iii) as experimental evidence: proteins from Swissprot viridiplantae, mapped with Exonerate ver. 2.2.0 (ftp://ftp.ncbi.nlm.nih.gov/, downloaded 2016.03.15) (Slater and Birney, 2005); (iv) as transcriptional evidence: Vitis ESTs and flcDNAs (ftp://ftp.ncbi.nlm.nih.gov/, downloaded on 2016.03.15), *Vitis vinifera* PN40024 V1 CDS (http://genomes.cribi.unipd.it/DATA/), Tannat (TSA GAKH01.1) (Da Silva *et al.*, 2013) and Corvina (TSA PRJNA169607) transcriptomes (Venturini *et al.*, 2013), and Cabernet Sauvignon corrected Iso-Seq reads (SRP132320)

(Minio, Massonnet, Figueroa-Balderas, Vondras, *et al.*, 2019); (v) PASA ver. 2.1.0 (Haas *et al.*, 2003, 2008; Campbell *et al.*, 2006) predicted gene models based on the transcriptional evidences in (iv). Functional annotations were assigned based on homology with proteins in the RefSeq plant protein database (ftp://ftp.ncbi.nlm.nih.gov/refseq, retrieved January 17th, 2017) and on functional domains identified with InterProScan ver. 5 (Jones *et al.*, 2014).

2.2.4 Loci identification through SNP probes and genome alignment

Rpv29, *Rpv30* and *Rpv31* where identified in Mgaloblishvili genome using the Vitis18KSNP genotyping array (Illumina Inc., San Diego, CA, United States) probes from the work of (Sargolzaei *et al.*, 2020). Loci regions were reconstructed starting from the probes that gave the positive signal in the GWAS. Probes defining the loci borders where then identified by looking for breaks in linkage disequilibrium between the loci signal's probes and the other probes of the SNP chip in the progeny accessions of Mgaloblishvili self-cross (data from Sargolzaei *et al.* 2020). Since the *Vitis*18k SNP chip was designed on PN40024 12X v2, the probes of interest where aligned against PN40024 v4 and Mgaloblishvili assemblies for validation, using BLASTn-short (Altschul *et al.*, 1990). For each locus, theregions identified in PN40024 v4 where then aligned to the first haplotype of Mgaloblishvili's genome using NUCmer from MUMmer 4.0.0beta5 tool suite (Marçais *et al.*, 2018). Afterwards, the regions of the first haplotype identified by homology with PN40024 loci were aligned against the haplotype 2 of Mgaloblishvili genome.

Finally, Integrative Genomics Viewer (IGV) v.2.16.2 (Robinson *et al.*, 2011) was used to characterize each locus gene content. For the purpose, genome annotation files where employed in combination with RNA-seq alignment files produced. Annotation was manually curated for eventual mistakes.

2.2.5 Refinement of resistance loci location and identification of the resistance-related haplotypes

From the crossings data reported in (Sargolzaei *et al.*, 2020), Mgaloblishvili was hypothesized to carry the resistance in heterozygous state. To identify the three loci resistance haplotypes and detect eventual recombination events inside their regions, we performed deep sequencing of two resistant accessions (97 – resistant, 124 – resistant) and two susceptible accessions (157M – susceptible, 145LIB – susceptible) of Mgaloblishvili self-cross progeny. Detection of recombination events data were analyzed to better refine the target loci boundaries.

Short-reads DNA reads of each accession underwent quality filtering and trimming with Trimmomatic (0.36, parameters "ILLUMINACLIP:2:30:10 LEADING:7 TRAILING:7 SLIDINGWINDOW:10:20 MINLEN:36", cit.). Filtered paired reads were mapped with BWA mem (unpublished) on the diploid genome assembly of Mgaloblishvili. Alignments were processed with Lumpy to identify the crossing over breakpoints and with and samtools depth (Danecek *et al.*, 2021) to evaluate the sequencing coverage and, therefore, the zygosity of each allele of the locus: for each sample, a locus with the same coverage distribution for the two parental haplotypes was considered as heterozygous, while unpaired coverage distribution toward one parental haplotype compared to the other (with almost null coverage) was considered homozygosity. After that, the loci regions of interest in windows of 10 Kb where checked for the same kind of differences, using Bedtools (Quinlan and Hall, 2010).

2.2.6 Genome comparisons for the detection of structural variants and SNPs

To identify existing differences between grapevine PN40024 v4 genome and Mgaloblishvili's haplotypes, a pairwise comparison between each pair of haplotypes was performed with NUCmer from MUMmer 4.0.0beta5 tool suite (Marçais *et al.*, 2018)with – mum option. Alignments where then filtered and used for variant calling of both SNPs and identification of long structural variants (SVs)

using show-snps and show-diff form MUMmer suite. Outputs files where converted in BED files to compare the called variants.
Finally, the same analyses were performed on the regions of the loci of interest. The locations of the identified variants were compared with the genes annotated in the loci of interest using Bedtools (Quinlan and Hall, 2010) to identify which gene features were affected.

2.2.7 RNA sequencing data analysis for loci genes expression

RNA-seq data from (Toffolatti *et al.*, 2018) (ENA project code: PRJEB24540) were used to analyse the loci gene expression. Mgaloblishvili leaves inoculated and not-inoculated with *P. viticola,* and collected at 24, 48, 72 hours after inoculation, where used for the purpose. After QC and preprocessing, reads where mapped on the diploid genome of Mgaloblishvili using HISAT2 (Kim *et al.*, 2019) with - - sensitive and - - k 50 parameters. Genome alignments where adjusted to transcriptome alignments using the genome's gene annotation employing Ubu 1.2 (https://github.com/mozack/ubu). Transcript abundance was evaluated with Salmon 1.5.2 (Patro *et al.*, 2017) and using the parameters - - seqBias and - - posBias.
Quantification files were imported using an R package, tximport v.1.20.0 (Soneson, Love and Robinson, 2015). DESeq2 v.1.16.1 (Love, Huber and Anders, 2014) was used to assess the gene-level expression and modulation of the annotated loci. Genes expression results were expressed in transcript per million (TPM).

2.3 Results

2.3.1 Genome sequencing, assembly and annotation

The genome of Mgaloblishvili was sequenced with PacBio HiFi long-reads technology. In total, ~32.5 Gb of HiFi data where generated, corresponding to a 60x X-Fold coverage of haploid genome. The high data quality along with the high sequencing depth allowed us to assemble a chromosome-scaled diploid

representation of the genome. The assembled sequences were two phased sets of 19 pseudochromosomes, ranging from 19.7 Mb to 37.9 Mb (Table S2.6) with only 1.12% of the assembled bases (11.0 Mb out of 985.6 Mb) remaining unplaced. The two alternative pseudomolecule sets show a very similar size of 491.4 Mb for the first haplotype and 483.3 Mb for the second encoding 29,235 and 29,139 protein coding gene loci respectively (Table 2.1). The assembly completeness was assessed using BUSCO analysis and by mapping the annotated genes of the closely related variety of *V. vinifera* PN40024. Each haplotype showed complete single-copy representant for 99.0% of the core plants genes and 99.1% of PN40024 genes confirming the completeness and the high quality of the assembly (Table 2.1).

Table 2.1 Summary of qualitative paramters of Mgaloblishvili genome. vMgal_v1.0 = diploid genome, vMgal_v1.0 hap1 = Mgaloblishvili haplotype 1, vMgal_v1.0 hap2 = Mgaloblishvili haplotype 2, vMgal_v1.0 unplaced = unplaced sequences (sequences that weren't possible to assign to the belonging haplotype.

Contigs	**vMgal_v1.0**	**vMgal_v1.0 hap1**	**vMgal_v1.0 hap2**	**vMgal_v1.0 unplaced**
Number of sequences	215	38	47	130
Average sequence length (bp)	4,584,189	12,930,565	10,282,442	84,341
Diploid genome	**vMgal_v1.0**	**vMgal_v1.0 hap1**	**vMgal_v1.0 hap2**	**vMgal_v1.0 unplaced**
Cumulative length (Mb)	985.6	491.4	483.3	11.0
Number of sequences	168	19	19	130
Average sequence length (bp)	5,866,950	25,862,130	25,436,988	84,341
Minimum sequence length (bp)	14,966	19,696,782	19,962,441	14,966
Maximum sequence length (bp)	37,861,983	37,861,983	37,048,420	795,768
N50 Length (bp)	25,855,461	25,885,461	25,245,956	270,052
BUSCO (v5.1.1) Viridiplantae_odb10	-	99.2%	99.0%	1.1%
Number of protein coding loci	-	29,235	29,139	-
Number of CDSs	-	43,363	43,121	628
% of PN40024 mapping genes	-	99.1%	99.1%	-

2.3.2 Identification of *Rpv29*, *Rpv30* and *Rpv31* in the genome of Mgaloblishvili

The location of resistance loci *Rpv29*, *Rpv30* and *Rpv31* were identified on chr 14, 03, and 16, respectively, by GWAS analysis (Sargolzaei *et al.*, 2020)based on genotyping data that were generated with the Vitis18KSNP genotyping array (Laucou *et al.*, 2018). The array probes were designed on PN40024 12X v2 version of the genome. To assess the transferability of loci-location information on Mgaloblishvili genome, the array SNP probes were mapped first on PN40024 v4 genome (Velt *et al.*, 2023) and then on Mgaloblishvili haplotypes. The probes revealed to be fully specific in the case of *Rpv29* and *Rpv31*, guiding to locate their position on both haplotypes of Mgaloblishvili genome assembly. Issues were found in the case of *Rpv30*, as for this locus the probes mapped multiple times, an ambiguity that can be attributed to the presence of repetitive sequences (Table S2.1). Alignment of whole genomic regions between PN40024 v4 genome and Mgaloblishvili genome assembly clarified the Vitis18KSNP genotyping array data (Table S2.2), revealing the presence in Mgaloblishvili of a novel region in correspondence of *Rpv30* locus. *Rpv30* SNP probe showed the same ambiguity in Mgaloblishvili genome, particularly in the case of haplotype 2. With respect to PN40024, where the locus extends for a length of 6.5 Mb in chr03, in Mgaloblishvili the *Rpv30* locus extends for 9.2 Mb and 9.8 Mb in haplotype 1 and haplotype 2 respectively (Figure 2.1, Table S2.2). Similarly, *Rpv29* and *Rpv31* loci showed to follow the same trend extending over a wider region of Mgaloblishvili genome rather than what observed in PN40024 (Figure 2.1). In the context of Mgaloblishvili genome, the loci showed to be more extended in the haplotype 1 compared to haplotype 2, with *Rpv29* haplotype 1 equal to 140.0 Kb and *Rvp29* haplotype 2 equal to 129.4 Kb, *Rpv31* haplotype 1 equal to 206.6 Kb and *Rpv31* amounting to 199.4 Kb (Figure 2.1).

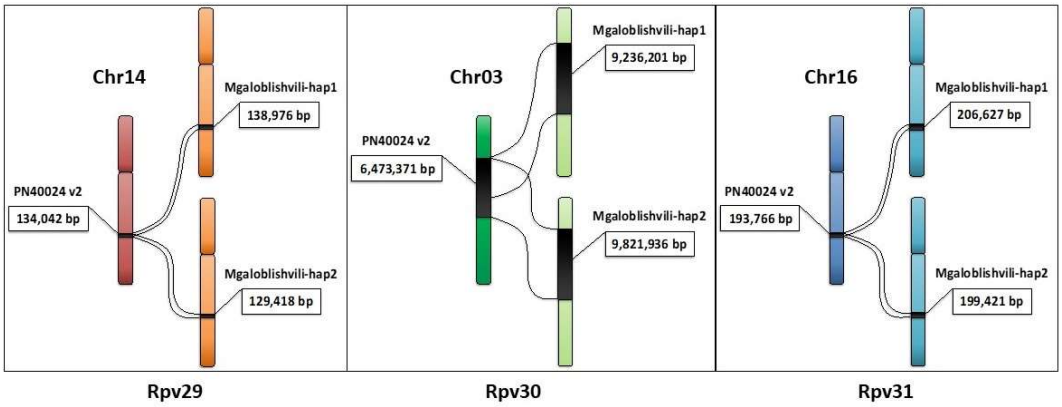

Figure 2.1 *Rpv29*, *Rpv30*, and *Rpv31* loci position on the different chromosomes of Mgaloblishvili genome. Per each locus, a comparison of the region between PN40024 v2 and Mgaloblishvili genome haplotypes is shown. Per each region the length is indicated in base pairs (bp).

2.3.3 Detection of recombination events and identification of *Rpv29*, *Rpv30* and *Rpv31* resistance haplotypes

To further define the dimension of the loci of interest, and in particular of *Rpv30*, the genomes of four progeny accessions of Mgaloblishvili obtained through self-cross have been sequenced. Two accessions (97, 124) showed to have inherited the resistant traits, while the other two accessions (145LIB, 157M) showed to be susceptible. Acquired susceptibility in part of the selfing progeny suggests that the resistance traits are present in heterozygous state in Mgaloblishvili. The presence of recombination events would allow to better describe the location of the resistance loci, while the inherited haplotypes allow to identify the resistance-related allelic forms.

Different recombination events were detected on all the chromosomes (chr) of the loci of interest (Figure S2.1). Short-reads sequencing data of resistant accession 97 revealed the major number of recombination events, affecting all the chromosomes of interest. On chromosome 03, a recombination event was found ~ 2.5 Mb upstream of *Rpv30* (Figure S2.1A). In the case of chromosome 14, two recombination events where detected, one ~ 16 Mb upstream of *Rpv29*, while the other was ~ 7 Mb downstream of the locus (Figure S2.1B). Finally, on chromosome 16 one single recombination event was found ~ 5 Mb upstream of *Rpv31* (Figure S2.1C). Genomic data of 124 accession (resistant) revealed a

recombination event on chromosome 30, ~ 700 Kb upstream of *Rpv30* (Figure S2.1D) and two events on chromosome 16, one at ~5 Mb and the other around ~3.5 Mb upstream of *Rpv31* (Figure S2.1F). Of all the detected recombination events, none of them was located within the target loci regions. For this reason, it was not possible to refine the target loci boundaries defined by the Vitis18KSNP genotyping array data.

DNA sequencing data were also utilized to genotype Mgaloblishvili self-cross progeny accessions. In this way, per each target locus, the haplotypes allelic forms associated to the resistance traits were investigated. Figure 2.2 shows an heatmap summarizing the genotyping results. In the analyzed accessions, *Rpv29* was present either in heterozygous allelic state or in combination with other loci genotypes that did not make possible to gain any definitive information. For this reason, in the case of *Rpv29*, no meaningful information could be collected. On the contrary, the study of 157M accession (susceptible), allowed to associate the resistance to the allelic form present in haplotype 2 of *Rpv30*. In this susceptible accession, *Rpv29* and *Rpv31* were present in heterozygous allelic form and *Rpv30* in homozygous allelic form for Mgaloblishvili haplotype 1. Coupling this data with the phenotype, *Rpv30* resistance haplotype was inferred. On top of that, we were able to define this locus as a fundamental contributor to the resistant phenotype. Unfortunately, given the size of the locus and the impossibility to break it down and identifying which genes were actually involved in the resistance, this locus wasn't further analyzed. Similarly, *Rpv31* resistant form was associated with allelic form of the locus in haplotype 2 thanks to 124 accession (resistant). In this accession, both *Rpv29* and *Rpv30* were present in heterozygous allelic form, while *Rpv31* presented homozygous allelic form for Mgaloblishvili haplotype 2. This information linked to the phenotype data allowed us to identify *Rpv31* resistance haplotype. However, in the case of this locus, the result is less definitive, since at the moment no certain information about the single loci effect on the resistant phenotype is available (Sargolzaei et al., 2020).

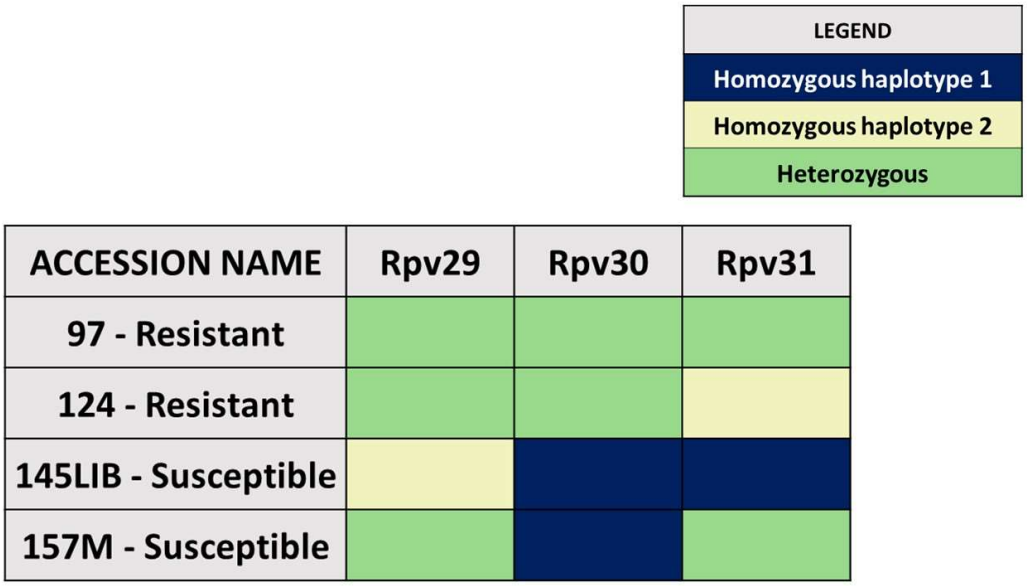

Figure 2.2 Heatmap reporting the results of the genotyping for the identification of *Rpv29*, *Rpv30* and *Rpv31* resistance haplotypes. Results were obtained by analysing DNA sequencing data, and by using Mgaloblishvili genome haplotypes as references. In the first column are reported the analysed accessions of Mgaloblishvili self-cross progeny. Name of the accession is indicated as ID number – phenotype (resistant or susceptible to *P. viticola*). The other columns show each one the results of the genotyping for the loci of interest. Per each locus, results are reported by color code: homozygosity for haplotype 1 (blue), homozygosity for haplotype 2 (yellow), and heterozygosity for both haplotypes (green).

2.3.4 Genome comparison between PN40024 v4 and Mgaloblishvili haplotypes

To detect existing differences between grapevine reference genome PN40024v4 and both haplotypes of Mgaloblishvili genome, a whole genome comparison analysis was carried out. The genomes were aligned to each other and variant calling for SNPs and long SVs was performed on the resulting data. In terms of SVs counts (Figure 2.3), the variants having the major impact on the differences between the genomes were insertions and deletions. In general, as expected, there were less SVs between the haplotypes of Mgaloblishvili than between Mgaloblishvili and PN40024 genomes (Figure 2.3A). Regarding the chromosomes of interest, the trend of the whole genome comparison was confirmed. This can be appreciated in Table 2.2, where the percentage of the target chromosomes sequences affected by SVs is reported. The percentage of

SVs affecting the chromosomes was between 26% (Chr14) and 40% (Chr16) and in this case, duplications appeared as the highest number of SVs present between the compared targets, probably due to the activity of repetitive elements.

Table 2.2 Summary of the structural variants (SVs) identified on the chromosomes where *Rpv29*, *Rpv30* and *Rpv31* are located. SVs rapresents differences in the sequences of Mgaloblishvili haplotypes (Mgalo-hap1 and Mgalo-hap2) aligned to grapevine reference genome PN40024 v4. The alignments pairs are specified in the first column. Results are indicated as percentage of structural variats between the compared chromosomes sequences (% of SVs). SVs evaluated where: **CID** (Complex insertion-deletions), **DEL** (Deletions), **DUP** (Duplications), **INV** (Inversions), **TRA** (Translocations), **INS** (Insertions). The total percentages of chromosome sequences affected by SVs is reported in the last column (**Total**).

Chr03	**% of SVs**						
COMPARISON	**CID**	**DEL**	**DUP**	**INV**	**TRA**	**INS**	**Total**
PN40024 *vs* Mgalo-Hap1	0.2	0.5	24.9	0.1	2.6	7.0	35.5
PN40024 *vs* Mgalo-Hap2	0.6	0.5	27.7	0.1	2.2	6.5	37.8
Mgalo-Hap2 *vs* Mgalo-Hap1	0.3	0.4	21.6	0.1	2.4	5.4	30.3
Chr14	**% of SVs**						
COMPARISON	**CID**	**DEL**	**DUP**	**INV**	**TRA**	**INS**	**Total**
PN40024 *vs* Mgalo-Hap1	0.3	0.6	18.7	0.1	1.7	6.8	28.2
PN40024 *vs* Mgalo-Hap2	0.3	0.6	22.8	0.1	2.3	6.4	32.4
Mgalo-Hap2 *vs* Mgalo-Hap1	0.2	0.5	17.8	0.1	1.7	5.7	26.0
Chr16	**% of SVs**						
COMPARISON	**CID**	**DEL**	**DUP**	**INV**	**TRA**	**INS**	**Total**
PN40024 *vs* Mgalo-Hap1	0.4	0.5	31.2	0.3	4.0	7.1	43.6
PN40024 *vs* Mgalo-Hap2	0.4	0.9	24.8	0.2	2.8	5.4	34.5
Mgalo-Hap2 *vs* Mgalo-Hap1	0.4	0.5	29.3	0.1	4.0	6.4	40.6

On the target loci, interesting results emerged. In Figure 2.3B, a plot displaying *Rpv29* SVs count differences between PN40024v4 and Mgaloblishvili haplotypes is shown. Mgaloblishvili haplotype 1 showed a lower number of structural differences with PN40024 v4, than with Mgaloblishvili haplotype 2. On top of that, Mgaloblishvili haplotype 1 SVs showed a tendency to be shorter than the ones

of Mgaloblishvili haplotype 2, when compared with PN40024 v4 (Figure S2.3A). Around 50% of the locus was found to be affected by SVs (Table S2.3), a value that is equal to two times the chromosome level value (Table 2.2).

Regarding *Rpv31*, the trend in the SVs count between PN40024 v4 and Mgaloblishvili haplotypes was found to be the same as the one of whole genome comparison, with fewer SVs between Mgaloblishvili haplotypes than compared to PN40024 v4 (Figure 2.3C). In this case, ~20 % of the locus was affected by SVs, a value equal to half of what happened at chromosome level (Table 2.2, Table S2.3). In this case, the majority of SVs impacted genes (Table S2.4).

Due to the impossibility of adequately define *Rpv30* locus region, SVs and SNPs data weren't analyzed for the locus.

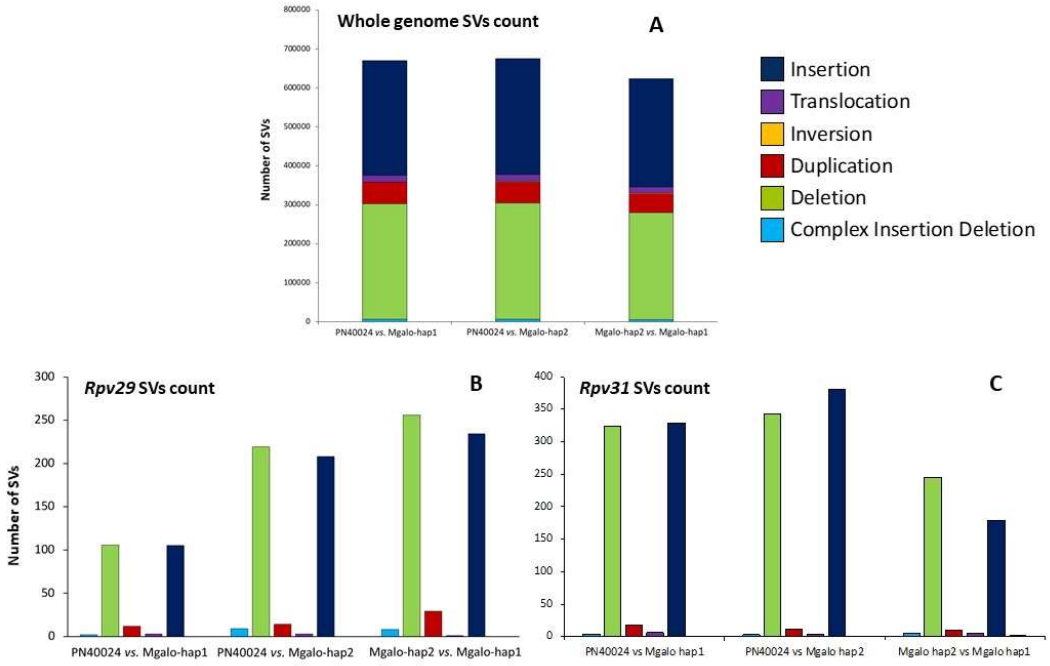

Figure 2.3 Barplots rapresenting the number of structural variants (SVs count) indentified comparing Mgaloblishvili haplotypes against grapevine reference genome PN40024 v4. SVs count at whole genome level (**A**), SVs count of the locus *Rpv29* (**B**), SVs count for locus *Rpv31* (**C**). Each SV is shown in a different color.

2.3.5 *Rpv29* and *Rpv31* gene content and gene expression

The loci of interest were characterized for gene content, impact of variants onto the genes and gene expression. Loci content was analyzed comparing Mgaloblishvili haplotypes to grapevine reference genome PN40024 v4. Further investigation of *Rpv30* locus was hindered by the impossibility of clearly defining the locus region and which of the present genes were actually related to the resistance. For *Rpv29*, seven genes were identified into PN40024 v4 genome, among them a NADPH – dependent diflavin oxidoreductase (*VviNDOR1*) (VITVvi_vMgal_v1.0.hap1.chr14.ver1.0.g208030; VITVvi_vMgal_v1.0.hap2.chr14.ver1.0.g500550), three uncharacterized proteins, a cellulose synthase gene (*VviCESA9*) (VITVvi_vMgal_v1.0.hap1.chr14.ver1.1.g208032; VITVvi_vMgal_v1.0.hap2.chr14.ver1.0.g500551), an acyl-CoA-binding protein gene (*VviACBP*) (VITVvi_vMgal_v1.0.hap1.chr14.ver1.0.g208040) and a HEAT repeat – containing protein gene (*VviHEATR*) (VITVvi_vMgal_v1.0.hap1.chr14.ver1.0.g208050; VITVvi_vMgal_v1.0.hap2.chr14.ver1.1.g500560), probably part of the SWEETIE family (Figure 2.4). With the exception of the uncharacterized proteins, all the genes were found to be involved in biotic stress resistance mechanisms (Iqbal *et al.*, 2021). Nevertheless, Mgaloblishvili haplotypes revealed to be missing some of those genes. In particular, Mgaloblishvili *Rpv29* haplotype 2 (3 genes) was missing more genes than haplotype 1 (5 genes), lacking the three uncharacterized proteins and the *VviACBP* gene present in haplotype 1 (Figure 2.4).

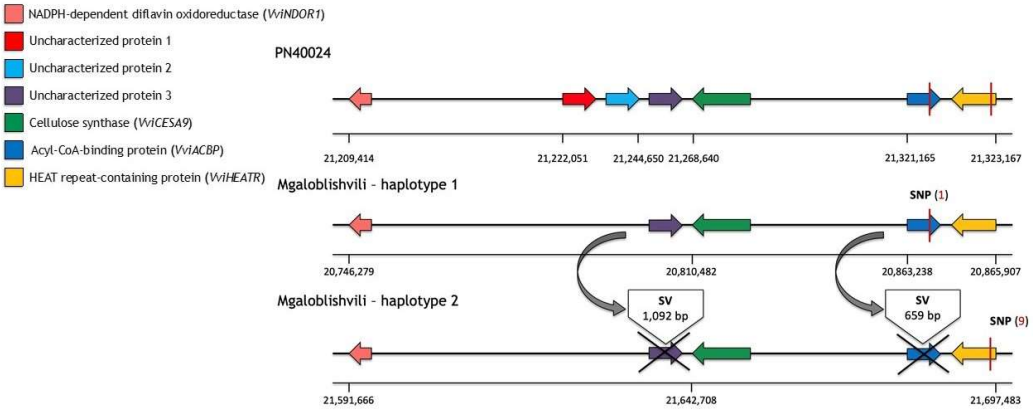

Figure 2.4 Rapresentation of *Rpv29* locus gene content in grapevine reference genome PN40024 v4 (*P. viticola* susceptible variety) and Mgaloblishvili genome haplotypes (*P. viticola* resistant variety). Genes are shown as colored arrows. Red bars indicated the position of SNPs indentified in the genes sequences, between parenthesis is indicated their number. White shapes indicate structural variants (SVs) interrupting genes sequences and their length expressed in base pairs (bp).

Looking at SVs impacting the genes, two relatively big variants, were identified. The first one 1092 bp long and the second one 659 bp long, accounting for the absence of the uncharacterized protein 3 and *VviACBP* genes missing in Mgaloblishvili *Rpv29* haplotype 2 (Figure 2.4, Table S2.4). One SNP was identified between PN40024 v4 and Mgaloblishvili haplotype 1 *VviACBP* gene, and nine SNPs were identified between PN40024 v4 and Mgaloblishvili haplotype 2 *VviHEATR* gene. None of the SNPs were found to be cause of nonsense mutations nor deleterious ones (Table S2.4).

Expression of the genes was studied during infection with *P. viticola* at 24, 48 and 72 hours after inoculation, revealing a pattern of constitutively low expression of the genes throughout all the timepoints (5 ± 2 TPM). (Table S2.5). Compared to *Rpv29*, locus *Rpv31* displayed a denser gene content, in both PN40024 v4 (30 genes) and Mgaloblishvili haplotypes (31 genes and 32 genes, respectively for haplotype 1 and 2) (Figure 2.5). Mgaloblishvili *Rpv31* revealed to possess more genes compared to the reference genome, due to the presence of an expansion in the subtilase family protein genes (VITVvi_vMgal_v1.0.hap1.chr16.ver1.1.g241360; VITVvi_vMgal_v1.0.hap2.chr16.ver1.1.g533110) at the beginning of the locus. On top of that, Mgaloblishvili haplotype 2 had one more gene (unknown gene - VITVvi_vMgal_v1.0.hap2.chr16.ver1.1.g533221), missing in both PN40024 v4

and Mgaloblishvili haplotype 1(Figure 2.5). As in the case of *Rpv29*, the genes were found to be involved in response to biotic stress direct or indirect responses (Iqbal *et al.*, 2021). All these genes were impacted by small variants, mainly small indels and SNPs, with none of them causing nonsense mutations (Figure 2.5, Table S2.4).

The study of Mgaloblishvili *Rpv31* gene expression through RNA-seq data revealed more variability in the regulation of the genes compared to *Rpv29* (Table S2.5). Among them, one member of the subtilase family protein (VITVvi_vMgal_v1.0.hap1.chr16.ver1.1.g241550; VITVvi_vMgal_v1.0.hap2.chr16.ver1.1.g533300) was strongly up-regulated during infection with *P. viticola*, starting from a value of 30.8 TMP in non-inoculated samples, and reaching a pique of 110 TPM at 2 day after inoculation with *P. viticola* (dai). Another up-regulated gene was cytochrome b5 – like heme/steroid – binding domain protein gene (VITVvi_vMgal_v1.0.hap1.chr16.ver1.0.g241620; VITVvi_vMgal_v1.0.hap2.chr16.ver1.0.g533380). The gene showed an expression increase from 55.6 TPM (0 dai) to 82.2 TPM (1 dai) in haplotype 1, and from 53.5 TPM (0 dai) to 77.7 TPM (1 dai) in haplotype 2. From 2 dai the gene expression remained constitutively up-regulated when compared to 0 dai, with values ranging between 69.0 – 66.3 TPM in haplotype one, and 67.2 – 65.5 TPM in haplotype 2 (Table S2.5). A probable receptor gene (VITVvi_vMgal_v1.0.hap1.chr16.ver1.0.g241500; VITVvi_vMgal_v1.0.hap2.chr16.ver1.0.g533250) was constitutively strongly up-regulated during the infection (369 – 447 TPM in both haplotypes) and other were down-regulated during infection. The ubiquitin – 60S ribosomal protein L40 gene (VITVvi_vMgal_v1.0.hap1.chr16.ver1.0.g241400; VITVvi_vMgal_v1.0.hap2.chr16.ver1.0.g533340), showed an expression decrease from 254. 8 TPM (0 dai) to 155.4 TPM (3 dai) in haplotype 1 and from 250.8 TPM (0 dai) to 169.2 TPM (3 dai) in haplotype 2. Similarly, the auxin responsive family protein gene (VITVvi_vMgal_v1.0.hap1.chr16.ver1.0.g241540; VITVvi_vMgal_v1.0.hap2.chr16.ver1.0.g533290) was down-regulated from 49.6

TPM (0 dai) to 35.0 TPM (dai) in haplotype 1, and from 12.8 TPM (0 dai) to 8.7 TPM (3 dai). Interestingly, also the unknown gene (VITVvi_vMgal_v1.0.hap2.chr16.ver1.1.g533221) present in Mgaloblishvili *Rpv31* haplotype 2 was consistently down-regulated during infection with the pathogen. Its expression decreased from 36.4 TPM (0 dai) to 12.3 TPM (3 dai) (Table S2.5).

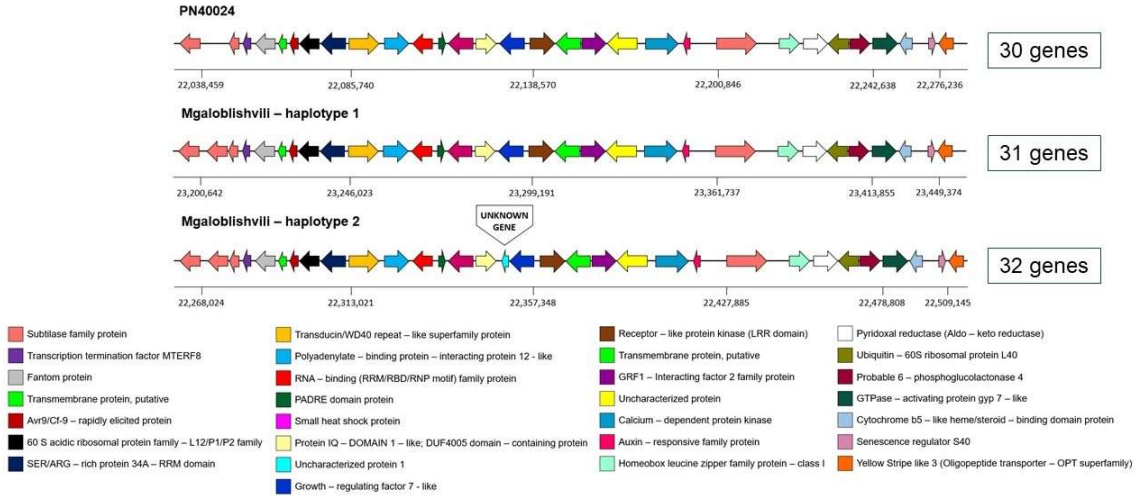

Figure 2.5 Rapresentation of *Rpv31* locus gene content in grapevine reference genome PN40024 v4 (*P. viticola* susceptible variety) and Mgaloblishvili genome haplotypes (*P. viticola* resistant variety). Genes are shown as colored arrows. On the right side, gene number per each genome/haplotype are shown. Position are indicated in base pairs (bp).

2.4 Discussion

Breeding programs for resistant varieties could be a good solution to decrease the devastating effects of downy mildew on grapevine production. To reach the scope, research of new resistance sources in *V. vinifera* could bring a great advantage. Breeding programs would be simplified and shortened, while being able to produce new resistant varieties with the quality levels required for wine production. Recently, a *V. vinifera* variety resistant to downy mildew, Mgaloblishvili, was identified. A GWAS study was able to identify the resistances bases, the loci *Rpv29*, *Rpv30* and *Rpv31*. The loci were located and analyzed for their gene content in PN40024 12X v2 genome. Given the downy mildew

susceptible phenotype of PN40024 accession, the genome of Mgaloblishvili was sequenced and is presented in this work. Understanding what distinguishes Mgaloblishvili from the other *V. vinifera* susceptible varieties could make available new resources for breeding programs, facilitating them as a consequence of the closer genetic background shared by the resources.

The obtainment of a chromosome-level diploid genome with few unplaced sequences (~11 Mb) allowed us to study in detail the Mgaloblishvili downy mildew resistance loci: *Rpv29*, *Rpv30* and *Rpv31*. The loci were successfully identified in Mgaloblishvili with the data from the Vitis18KSNP genotyping array (Laucou *et al.*, 2018). PN40024 based data were transferred without issue of compatibility to Mgaloblishvili genome, confirming once again the validity and versatility of this instrument across grapevine germplasm (Bianchi, Brancadoro and De Lorenzis, 2020; D'Onofrio *et al.*, 2021). The comparison between PN40024 v4 genome and Mgaloblishvili haplotypes revealed that the loci are more extended in the resistant variety (Figure 2.1). Nevertheless, this extension translates into a higher gene content only in the case of *Rpv31*, and poorly (Figure 2.5). For *Rpv29*, on the contrary, Mgaloblishvili haplotypes revealed a lower gene content, particularly in case of haplotype 2 (Figure 2.4).

2.4.1 Non-host and basal resistance coupled with loss of disease susceptibility are part of Mgaloblishvili resistance mechanism

Non-host resistance (NHR) is the ability of all the genotypes of a plant species to confer resistance against all genotypes of a pathogen species. NHR can be conditional; it can depend on environmental conditions and plant age, be organ or tissue specific, or only effective against certain developmental stages of pathogens (Panstruga and Moscou, 2020). It is inherited polygenically, and exhibits strong similarity and association with the basal resistance of plants to adapted pathogens (Niks and Marcel, 2009). Basal resistance is a qualitative definition referring to completely effective non-host resistance against a potential pathogen. It is a defense that inhibits pathogen spread after successful infection

and onset of the disease (Dangl and Jones, 2001). As a consequence, given their broad range of action, these mechanisms could be potentially exploited as a source of novel disease resistance strategies (Delventhal *et al.*, 2017).

In this study, all the loci displayed a gene content consisting of genes strictly related to biotic stress resistance mechanism. Focusing on *Rpv29*, the genes that seem to gain more attention are *VviACBP* and *VviHEATR.* The first one is an acyl – CoA – binding protein gene, whose family members are involved in cuticle deposition, a developmental process related also to biotic stress responses (Lai and Chye, 2021). The genes affect both basal and resistance protein-mediated defense against bacterial and fungal pathogens (Xia *et al.*, 2012). Moreover, these genes are shown to be involved in the plant ability to reach full systemic acquired resistance (SAR). SAR is a mechanism of induced defense that confers long-lasting protection against a broad spectrum of pathogens. The mechanism involves salicylic acid (SA) or its derivative, methyl salicylate, as key signals, that are able to induce the up-regulation of genes encoding pathogenesis-related (PR) proteins (Conrath, 2006). Loss of function mutants of the genes involved in SAR leads to plants being unable to reach it (Xia *et al.*, 2012; Panthapulakkal Narayanan *et al.*, 2020). Interestingly, Mgaloblishvili haplotype 2 is missing the copy of this gene. Furthermore, the gene in haplotype 1 presents one SNP compared to PN40024. The other gene, *VviHEATR,* is part of the HEAT repeat – containing proteins, and in this case is probably part of the SWEETIE family. This gene has nine SNPs when compared to PN40024. Some proteins carrying the HEAT repeat domain are involved in non-host and basal resistance against bacterial pathogens (Monaghan and Li, 2010). Moreover, this specific protein could be involved in sugars transport and flux (Veyres *et al.*, 2008), a process that is known to be involved in biotic stress responses (Chong *et al.*, 2014). RNA-seq data analysis about Mgaloblishvili *Rpv29* genes, showed that these genes are constitutively lowly expressed, a pattern maintained during infection with *P. viticola* (Table S2.5). This could indicate that, among the resistance mechanisms used by Mgaloblishvili, one of them could be the down-regulation of susceptibility factors toward the pathogen. Plant susceptibility to pathogens is usually considered from the perspective of

the loss of resistance. However, susceptibility doesn't translate to plant passivity, since active host cooperation is usually required for the pathogen to colonize and cause the disease. This cooperation consists of the induction of susceptible responses, that transform a plant from an autonomous biological unit into a component of a patho-system. Compared to induced resistance, susceptibility is less frequently discussed in the literature, regardless of the fundamental impact it has on plant–pathogen interactions and disease progression (Gorshkov and Tsers, 2022). Nevertheless, plant resistance can also be achieved through loss-of-function of so-called susceptibility (S)-genes. S-genes can act as providers of signals attracting pathogens and increasing their aggressiveness, or contribute to the in-planta accommodation of pathogens (Van Schie and Takken, 2014). Therefore, loss-of-function mutation of these genes can be considered a promising strategy to improve agriculture disease management.

2.4.2 *Rpv31* reveals the key to Mgaloblishvili unique resistance mechanism

Mgaloblishvili is a unique *V. vinifera* resistant variety, from one of grapevine domestication centers. This cultivar possesses a unique mechanism of defense against *P. viticola*. The mechanism was theorized to be based on *P. viticola* growth and sporulation limitation, determined by the over-expression of genes related to pathogen recognition, the ethylene signaling pathway, the synthesis of antimicrobial compounds (such as VOCs) and enzymes, and the development of structural barriers (Toffolatti *et al.*, 2018).

In this work, Mgaloblishvili *Rpv29* data suggested that the key difference between Mgaloblishvili and the other *V. vinifera* susceptible PN40024 could lay in a different regulation of present genes. The subsequent analysis of *Rpv31* strongly supported the hypothesis. The region is denser in gene content compared to *Rpv29*. However, even though this locus is larger in Mgaloblishvili compared to PN40024 (Figure 2.1), its gene content is relatively conserved, with only one gene of Mgaloblishvili haplotype 1 missing in PN40024 and two from Mgaloblishvili haplotype 2 (Figure 2.5). Interestingly, the analysis of the progeny of Mgaloblishvili self-cross revealed that the haplotype carrying the resistance in

Mgaloblishvili is indeed *Rpv31* haplotype 2 (Figure 2.2, Figure S2.1). One of the genes present in Mgaloblishvili and absent in PN40024 is part of a probable expansion of the subtilase (Subtilisin-like proteases) family proteins. These genes are confirmed players in the response to biotic stresses (Schaller, Stintzi and Graff, 2012) and in particular in the response against both downy mildew and powdery mildew in grapevine (Figueiredo, Monteiro and Sebastiana, 2014). They are serine proteases, and recently it was hypothesized that part of grapevine resistance mechanism against *P. viticola* could rely on them. Resistant varieties probably possess proteases that are not recognized by the secretome of the pathogen, that on the contrary, is able to recognize and inhibit proteases of susceptible varieties (Figueiredo, Monteiro and Sebastiana, 2014). In this work, the role of these genes in the interaction between grapevine and *P. viticola* is confirmed by the strong up-regulation of the genes found in *Rpv31* coupled with constitutively high expression of a putative membrane receptor (Table S2.5). Another interesting pattern of expression involves the "unknown gene" in Mgaloblishvili haplotype 2 (VITVvi_vMgal_v1.0.hap2.chr16.ver1.1.g533221). The gene is absent in haplotype 1, and is strongly and consistently down-regulated during the infection with the pathogen (Table S2.5). Unfortunately, we weren't able to retrieve any information regarding its function.

All *Rpv31* genes except one (subtilase family protein, missing in PN40024), showed a presence of small indels and SNPs in their gene sequences. As for *Rpv29*, none of these variants causes nonsense mutations. Therefore, what these variants could probably indicate is a difference in the binding affinity with regulative elements (Hill, Vande Zande and Wittkopp, 2021).

Transcriptomic analysis of Mgaloblishvili gene expression during downy mildew infection revealed that the majority of the genes involved in the defense mechanism were regulated within the first 24 hours after the inoculation with *P. viticola*. The interesting fact, emerges when this response has been compared with the one of a susceptible variety. A previous work where Mgaloblishvili response to *P. viticola* infection was compared with the one of susceptible variety Pinot noir, did that. In that experiment, they observed that the varieties regulated almost the same genes, however Mgaloblishvili was able to regulate them during

the first 24 hours after infection, while Pinot noir was able to do so only after 72 hours, when it is too late to successfully fight the infection (Toffolatti *et al.*, 2018). These findings support the hypothesis that the key difference between Mgaloblishvili and PN40024 relies exactly in this ability of regulating more efficiently the genes present in the R loci.

2.5 Conclusions

The employment of *V. vinifera* germplasm for the development of downy mildew resistant varieties could greatly benefit breeding programs.

This study was able to reveal the resistance mechanisms of the first identified downy mildew resistant *V. vinifera* variety, Mgaloblishvili. The mechanism, based on non-host and basal resistance and early onset response against the pathogen, could be employed with success in breeding programs of resistance varieties. In particular, these resources could be useful in programs based on pyramiding with other stronger but late onset *Rpv* loci, in order to be able to decrease selective pressure on them. This could help making possible to achieve the development of resistant varieties with durable resistance.

Chapter 3: *VviLBDIf7* as a candidate gene of susceptibility to *Plasmopara viticola*

3.1 RNAi of a Putative Grapevine Susceptibility Gene as a Possible Downy Mildew Control Strategy

Demetrio Marcianò†, Valentina Ricciardi†, Elena Marone Fassolo, Alessandro Passera, Piero Attilio Bianco, Osvaldo Failla, Paola Casati, Giuliana Maddalena, Gabriella De Lorenzis* and Silvia Laura Toffolatti*

Dipartimento di Scienze Agrarie ed Ambientali, Università degli Studi di Milano, Milan, Italy

Downy mildew, caused by the oomycete *Plasmopara viticola*, is one of the diseases causing the most severe economic losses to grapevine (*Vitis vinifera*) production. To date, the application of fungicides is the most efficient method to control the pathogen and the implementation of novel and sustainable disease control methods is a major challenge. RNA interference (RNAi) represents a novel biotechnological tool with a great potential for controlling fungal pathogens. Recently, a candidate susceptibility gene (*VviLBDIf7*) to downy mildew has been identified in *V. vinifera*. In this work, the efficacy of RNAi triggered by exogenous double-stranded RNA (dsRNA) in controlling *P. viticola* infections has been assessed in a highly susceptible grapevine cultivar (Pinot noir) by knocking down *VviLBDIf7* gene. The effects of dsRNA treatment on this target gene were assessed by evaluating gene expression, disease severity, and development of vegetative and reproductive structures of *P. viticola* in the leaf tissues. Furthermore, the effects of dsRNA treatment on off-target (EF1a, GAPDH, PEPC, and PEPCK) and jasmonic acid metabolism (COI1) genes have been evaluated. Exogenous application of dsRNA led to significant reductions both in *VviLBDIf7* gene expression, 5 days after the treatment, and in the disease severity when artificial inoculation was carried out 7 days after dsRNA treatments. The pathogen showed clear alterations to both vegetative (hyphae and haustoria) and reproductive structures (sporangiophores) that resulted in stunted growth and reduced sporulation. Treatment with dsRNA showed

signatures of systemic activity and no deleterious off-target effects. These results demonstrated the potential of RNAi for silencing susceptibility factors in grapevine as a sustainable strategy for pathogen control, underlying the possibility to adopt this promising biotechnological tool in disease management strategies.

Keywords: susceptibility gene, gene silencing, dsRNA, obligate parasite, disease resistance, *Vitis vinifera*

3.1.1 Introduction

Since the late 1800s, *Vitis vinifera* has suffered damage from downy mildew, a disease caused by the oomycete *Plasmopara viticola*, originating from Northern America. This biotrophic, obligate parasite can infect all the green parts of grapevine plants, causing quantitative and qualitative damage and leading to extensive yield losses (Yu *et al.*, 2012). Non-*vinifera* species, such as those with center of origin in North America and Asia, are resistant to *P. viticola* due to coevolution with the pathogen. This resistance is mediated by different mechanisms that at first detect the pathogen and then initiate a proper defense response (Gessler, Pertot and Perazzolli, 2011). The first level of defense is called Pathogen - Associated Molecular Pattern (PAMP) - Triggered Immunity (PTI), a plant basal immune response activated by the recognition of conserved molecules of the pathogen (Newman *et al.*, 2013). A second, more selective, plant defense mechanism is called Effector-Triggered Immunity (ETI). ETI relies on a class of

highly specific receptors, the resistance proteins (R-proteins), that recognize pathogen effectors. Activation of ETI leads to disease resistance and is often associated with localized apoptosis at the infection site (hypersensitive response) (Jones and Dangl, 2006). Since effectors and receptors are codified by non-essential genes, resistance genes (R-genes) undergo rapid evolution, due to the strong selective pressure on both pathogen and plant (Buonassisi *et al.*, 2017). This phenomenon implies a short duration of the resistance triggered

by R-genes. For a durable resistance, targeting susceptibility genes (S-genes) can be a winning strategy in breeding (Zaidi, Mukhtar and Mansoor, 2018). S-genes facilitate the compatibility between plant and pathogen and are essential for their interaction, especially for biotrophic pathogens. Therefore, mutation or loss of S-genes can limit pathogenicity toward the plant (Van Schie and Takken, 2014). MLO (Mildew Locus O) genes are a striking example of S-gene usefulness in breeding programs: their knockdown confers resistance to powdery mildew in grapevine, reducing the disease severity by up to 77% (Pessina *et al.*, 2016). MLO-based resistance to powdery mildew is, indeed, widely employed in barley breeding since few decades even if the function encoded protein is not yet completely established (Kusch and Panstruga, 2017). To date, downy mildew-resistant grapevine varieties are obtained by crossing *V. vinifera* cultivars with non-*vinifera*

species or hybrids. Nevertheless, to reduce the background of non-*vinifera* species, several cycles of backcrossing with susceptible cultivars are needed, which makes the breeding process very lengthy. The identification of grapevine S-genes against *P. viticola* opens new possibilities to breed for downy mildew resistance because usually S-gene-mediated resistance is durable and broad spectrum. The research of S-genes in grapevine is still pioneering. Pessina *et al.* (2016) identified two MLO genes responsible for *V. vinifera* susceptibility to powdery mildew and some others were proposed for downy mildew (Toffolatti *et al.*, 2020; Pirrello *et al.*, 2022). Recently, resistance to *P. viticola* has been identified in Mgaloblishvili (Toffolatti *et al.*, 2016), a *V. vinifera* cultivar from Georgia (Southern Caucasus). Studying its unique resistance mechanism, different R-genes and an interesting candidate S-gene have been identified (Toffolatti *et al.*, 2018, 2020). The S-gene *VvLBDp1* [from here on called *VviLBDIf7* based on Grimplet et al., (2017), encoding for a LOB (LATERAL ORGAN BOUNDARIES) domain-containing (LBD) protein, belongs to plant LOB family of transcription factors. This family has been comprehensively analyzed in many species, such as *Arabidopsis thaliana* (Liu *et al.*, 2005), *Malus domestica* (Wang *et al.*, 2013), *Glycine max* (Yang et al., 2017), *Eucalyptus grandis* (Lu et al., 2018), *Brassica rapa* (Huang et al., 2018), *Camellia sinensis* (Teng et al.,

2018), *Gossypium spp.* (Yu et al., 2020), and *Pyrus bretschneideri* (Song et al., 2020). LBD genes show a key role in the regulation of plant organ development and in the response to abiotic and biotic stresses (Xu et al., 2016). They are involved in the establishment of organ boundaries (Rast and Simon, 2012), leaf formation (Semiarti et al., 2001), pulvinus differentiation and petiole development (Chen et al., 2012), regulation of lateral root organogenesis (Okushima et al., 2007), root and stem development (Yu et al., 2020), development of sepal and petal primordia of flowers (Xu et al., 2008), pollen development (Kim et al., 2015), regulation of light/dark-dependent hypocotyl elongation (Mangeon et al., 2011), and secondary phloem growth (Yordanov et al., 2010). Moreover, LOB genes are also involved in pathogen and abiotic response (Thatcher et al., 2012; Grimplet

et al., 2017; Yu et al., 2020), and they can act as repressor of anthocyanin biosynthesis and affect nitrogen response (Rubin et al., 2009). Biological processes where LBD genes are involved have been extensively reviewed by Zhang et al. (2020). A genome-wide characterization has been performed in grapevine as well, and up to 50 LBD genes have been identified (Grimplet et al., 2017). Expression patterns across different tissues, including both mature/woody and vegetative/green tissues, indicate roles of LBD genes in organ differentiation, in berry development and ripening (Fasoli et al., 2012), and in response to abiotic (such as salt, cold and drought) and biotic stresses (such as *Botrytis cinerea* attack and Bois noir disease) (Albertazzi et al., 2009; Agudelo-Romero et al., 2015).

The S-gene VviLBDIf7 is the putative ortholog of an LBD transcriptional factor acting as repressor of jasmonate-mediated defense mechanisms during infection of *A. thaliana* roots with *Fusarium oxysporum*. In this system, LBD disruption resulted in an increased resistance to the pathogen (Thatcher et al., 2012).

Silencing plant S-genes represents a promising way to achieve disease resistance as an alternative or in addition to breeding for R-genes. However, gene silencing is usually obtained via stable plant transformation, and the use of genetically modified plants in Europe is strictly regulated, and in several countries, they are not authorized for cultivation. A novel emerging approach,

which allows to overcome procedures for a stable genome modification, is represented by RNA interference (RNAi) triggered by the application of exogenous double-stranded RNA (dsRNA) molecules (Dubrovina et al., 2019). The effect of dsRNA treatment has been recently studied and proposed as a new environmentally-friendly crop protection tool from viruses, fungi, and insects (Konakalla et al., 2016; Luo et al., 2017; Wang et al., 2017; Cagliari et al., 2019; Dubrovina and Kiselev, 2019; Morozov et al., 2019; Vadlamudi et al., 2020).

RNAi has emerged as a technique with the ability to selectively knock down target genes (Kerschen et al., 2004). RNAi is a natural mechanism used by various organisms, including plants, to regulate specific gene activities or to defend their genome from invasions of exogenous nucleic acids. In the first case, the plant specifically produces molecules called microRNAs (miRNAs) serving as guides to selectively degrade the mRNA of target genes. In the second case, the plant recognizes dsRNAs introduced into the cytoplasm and produces short interfering RNA (siRNA) molecules that defend the plant from exogenous nucleic acids (Meister et al., 2004). As a consequence, RNAi mediated by post-transcriptional gene silencing can be stimulated also by the addition of ad hoc designed dsRNA molecules. This technique, although not yet regulated at European level, will likely fall outside the strict GMO regulation, being transgenefree. The exogenous application of polynucleotides that can affect mRNA levels of important virulence-related plants genes without modifying the host genome opens new opportunities for the development of new scientific techniques and crop improvement strategies (Dubrovina et al., 2019). This study evaluated the efficacy of a dsRNA treatment in silencing, through RNAi, *VviLBDIf7*, the candidate S-gene responsible for susceptibility toward *P. viticola* in *V. vinifera*. For this purpose, Pinot noir leaves were treated with synthetized dsRNA targeting *VviLBDIf7* gene and then inoculated with the pathogen, to evaluate (i) *VviLBDIf7* gene expression in the plant tissues after dsRNA treatment, (ii) disease severity and sporangia production on dsRNA-treated leaves inoculated with *P. viticola*, and (iii) the morphology of both vegetative and reproductive *P. viticola* structures in the dsRNA-treated leaf tissues. Finally, a preliminary investigation of the systemic effect of dsRNA and the evaluation of

dsRNA treatment on off-target and jasmonic acid metabolism genes have been performed.

3.1.2 Material and Methods

3.1.2.1 Basal Expression of *VviLBDIf7*

The basal expression level of *VviLBDIf7* (LOC100246173), candidate S-gene, was evaluated on leaves collected from three 6-year-old *V. vinifera* L. cv. Pinot noir plants, grown in a greenhouse, as reported in Toffolatti et al. (2018), via RT-qPCR. The first two well-developed leaves were collected in June 2020 twice at 1-day intervals. Leaves were ground with liquid nitrogen into a fine powder using mortar and pestle. RNA was extracted using the Spectrum™ Plant Total RNA Kit (Sigma-Aldrich, Germany) and then digested with Amplification Grade DNase I (Sigma-Aldrich), according to the manufacturer's instructions. Quantity and quality of RNA were checked by NanoDrop 1000 Spectrophotometer (Thermo Scientific, United Kingdom) and 1% agarose gel electrophoresis stained with Midori Green Advance ® (Nippon Genetics, Japan). *VviLBDIf7* real-time PCR primers (VvLBD_F and VvLBD_R; Table 3.1) were designed on the available sequence [VIT_13s0019g03750 according to Canaguier et al. (2017)] using the Primer3 Plus software (Untergasser et al., 2007) and NCBI Primer-BLAST (Ye et al., 2012). To avoid amplification of eventual genomic DNA carried over, one of the primers was designed to span across the exon–exon junction of the gene. Ubiquitin (Fujita et al., 2007) and actin (Reid et al., 2006) genes were used as references for data normalization. Total RNA (500 ng) was reverse transcribed with SuperScript® IV Reverse Transcriptase (Invitrogen, United Kingdom), using a 1:1 mix of random primers and oligo(dT), following manufacturer's instructions. Real-time PCR reaction was carried out using 4 µl of cDNA diluted 1:10, 10 µl of PowerUp™ SYBR™ Green Master Mix (Applied Biosystems, United Kingdom), 500 nM of primer forward and reverse and water up to 20 µl. Each reaction was performed in triplicate on QuantStudio 3 Real-Time PCR Systems (Thermo Fisher, United Kingdom) using the following cycling conditions: 50°C for 2 min, 95°C for 10 min, 50 cycles at 95°C for 20 s, 60°C for 45 s, and 72°C for 30 s.

Each thermal cycle was followed by a melting curve stage, with temperatures ranging from 60°C to 95°C. The *VviLBDIf7* gene expression at the two time points was calculated by comparing $2^{-\Delta\Delta Ct}$ (Ct = cycle threshold) values (Livak and Schmittgen, 2001). Geometric average of Ubiquitin and Actin was used to normalize the Ct values.

Table 3.1 List of primers used in this work to synthetize the dsRNA. VvLBD_F and VvLBD_R primers were used to detect the basal gene expression of *VviLBDIf7* in leaves of Pinot noir. VvLBD_RNAi_F and VvLBD_RNAi_R primers were used to amplify partially the target gene to synthetize the dsRNA. VvLBD_RNAiT7_F and VvLBD_RNAiT7_R were used to perform MEGAscript RNAi Kit protocol. VvLBD_2_F and VvLBD_2_R primers were used to evaluate the expression of VvLBD gene on dsRNA- and water-treated leaves. The primer position refers to the start of the sequence (LOC100246173) annotated in NCBI (https://www.ncbi.nlm.nih.gov/).

Name	Sequence (5'-3')	Tm (°C)	GC %	Primer position (bp)
VvLBD_F	GCCTGCAAAATCCTTCGTCG	60.18	55.0	196 - 215
VvLBD_R	GACTCGGGAAGTTCCTGCAA	59.97	55.0	322 - 341
VvLBD_RNAi_F	TATGGTTGTGCTGGTGCAAT	60.00	45.0	406 - 425
VvLBD_RNAi_R	CACACGGCTCTCCTTTTTCT	59.50	50.0	798 - 817
VvLBD_RNAiT7_F	TAATACGACTCACTATAGGGAG ATATGGTTGTGCTGGTGCAAT	71.30	41.9	406 - 425
VvLBD_RNAiT7_R	TAATACGACTCACTATAGGGAG ACACACGGCTCTCCTTTTTCT	72.30	44.2	798 - 817
VvLBD_2_F	CTTGCAGGAACTTCCCGAGTC	60.94	57.0	321 - 341
VvLBD_2_R	GCCAAGAAGGCTCCAAGACGG	63.56	62.0	566 - 586

3.1.2.2 *VviLBDIf7* dsRNA Design and Synthesis

In order to synthesize the dsRNA molecules, *VviLBDIf7* was partially amplified. To allow the synthesis of dsRNA template of proper dimension (400–500 bp) through PCR, new primers of *VviLBDIf7* (VvLBD_RNAi_F and VvLBD_RNAi_R; Table 3.1) were designed on the available sequence (LOC100246173) using the Primer3 Plus software and NCBI Primer-BLAST. In order to reduce the probability of off-target amplicons, the partial *VviLBDIf7* sequence was amplified starting from cDNA samples obtained in the Basal expression of *VviLBDIf7* subsection. PCR reaction was carried out using 4 µl of cDNA diluted 1:10, 5 µl of 5X Colorless GoTaq Reaction Buffer (Promega, Wisconsin, United States), PCR Nucleotide Mix 0.2 mM each dNTP (Promega), 0.6 mM of primer forward

and reverse, 0.125 µl of GoTaq G2 (5 U/µl) (Promega), and water up to 25 µl. To ensure the production of enough DNA template for the next steps, the reaction was performed in five replicates using the following thermal cycling conditions: 95°C for 2 min, 35 cycles at 95°C for 30 s, 60°C for 1 min, 72°C for 1 min, and a last step at 72°C for 5 min. PCR fragments were visualized on 1% agarose gel electrophoresis stained with Midori Green Advance. The amplification products were used as a template in another PCR reaction using RNAi primers 5' attached with T7 RNA polymerase promoter sequences (VvLBD_RNAiT7_F and VvLBD_RNAiT7_R; Table 3.1), as requested by MEGAscript RNAi Kit protocol (Thermo Fisher Scientific, United Kingdom). PCR reaction was carried out using 1 µl of amplification product, 5 µl of 5X Colorless GoTaq Reaction Buffer, PCR Nucleotide Mix 0.2 mM each dNTP, 0.6 mM of primer forward and reverse, 0.125 µl of GoTaq G2 (5 U/µl), and water up to 25 µl. To guarantee a sufficient amount of dsRNA DNA template, the reaction was performed in 50 replicates using the following thermal cycling conditions: 94°C for 5 min, 5 cycles at 94°C for 45 s, 62°C for 1 min, 72°C for 1 min, 30 cycles at 94°C for 45 s, 65°C for 1 min, 72°C for 1 min, and a last step at 72°C for 5 min. PCR products were solved on 1% agarose gel electrophoresis stained with Midori Green Advance. Replicates of PCR product were pooled and purified through Wizard SV Gel and PCR Clean-Up System (Promega). Purified samples were quantified using Qubit™ 3.0 fluorometer (Thermo Fisher Scientific), using the Qubit™ dsDNA HS Assay Kit (Thermo Fisher Scientific), and Sanger sequenced by Macrogen Europe B.V. in two replicates, using RNAiT7 primers. Sequences were aligned to reference sequence using ClustalW (Thompson et al., 1994). The obtained template was used in the dsRNA synthesis reaction using MEGAscript RNAi Kit, according to the manufacturer's instructions. Synthetized dsRNA was solved on 1% agarose gel electrophoresis stained with Midori Green Advance and quantified by NanoDrop 1000 Spectrophotometer.

3.1.2.3 *VviLBDIf7* dsRNA Treatment

Treatments with *VviLBDIf7* dsRNA were carried out on 6 – year – old Pinot noir plants grafted onto SO4, maintained in a glasshouse in 5 - L pots filled with sand – peat mixture (7:3 v/v), regularly watered via a drip system and fertilized twice a year with Osmocote Topdress fertilizer (ICL Specialty Fertilizers, Italy), as reported in Toffolatti et al. (2018). The plants, grown in a greenhouse, never came in contact with *P. viticola* structures and were regularly inspected for disease symptoms to be sure to work with healthy tissues. Three plants were treated with 100 mg/plant of dsRNA dissolved in 1 ml of sterilized water, and three were treated with only sterilized water (1 ml per plant), as suggested by Nerva et al. (2020). Treatments were performed with an airbrush on both sides of the first five fully developed leaves of a single vine shoot (from the second to the sixth leaf from the apex of the shoot) per plant (Figure S3.1). One sprayed leaf per plant was randomly collected at 3, 5, 7, and 15 days after
treatment (dat) (Figure 3.1A). To validate the dsRNA treatment data, the experiment was repeated, as previously described, on self-rooted cuttings of Pinot noir grown in the same conditions, to remove any possible effect of rootstock on scion behavior. In this second experiment, leaves were collected at 5 and 7 dat (Figure 3.1B), corresponding to the time points when, according to the first experiment, downregulation of S – gene and response to the pathogen occurred. In the second experiment, the possible systemic effect of dsRNA treatment was investigated on the untreated leaf immediately above the treated one at 7 dat (leaf S7, Figure 3.1B). From each leaf (biological replication), three 1.5 – cm – diameter disks (technical replication) were excised and inoculated with the pathogen.
The remaining leaf tissue was frozen in liquid nitrogen and stored at – 80°C until gene expression analysis and assessment of *P. viticola* presence.

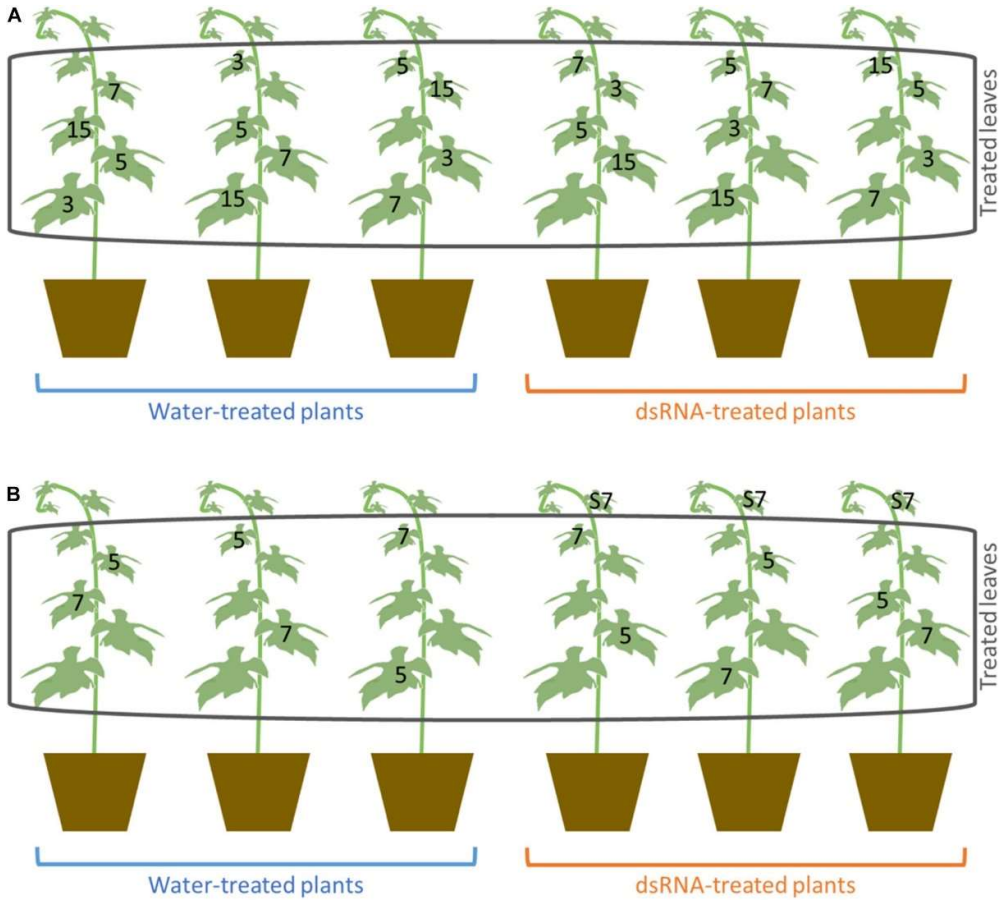

Figure 3.1 Scheme of the treatment and sampling carried out in the first (**A**) and second experiment (**B**). Numbers indicate the number of days after treatments (dat) at which the leaves were collected. S7 indicates the untreated leaves that were sampled at 7 dat for the evaluation of systemic activity of dsRNA in the second experiment.

3.1.2.4 *VviLBDlf7* Gene Expression Analysis on dsRNA - and Water - Treated Leaves

Expression of the candidate S – gene on dsRNA – and water – treated samples was evaluated through RT-qPCR. RNA extraction, RT-qPCR, and comparison of Ct values were carried out following the procedures described in the Basal expression of *VviLBDlf7* subsection, with some modifications: (i) to ensure the specific retrotranscription of only functional mRNAs, oligo(dT) primers were used in RT-PCR; (ii) qPCR was performed on 8 µl of cDNA; and (iii) to avoid possible amplification of incomplete cDNA sequences due to amplification of small RNAs resulting from degradation of the target gene mRNA following dsRNA treatment,

qPCR primers (VvLBD_2_F and VvLBD_2_R; Table 3.1) were specifically designed, using Primer3 Plus software and NCBI Primer-BLAST. The forward primer was designed to match the target gene sequence in the middle of the region amplified by the first qPCR primer pair (see the Basal expression of *VviLBDIf7* subsection), and the reverse primer was designed to match the same sequence region targeted by the dsRNA fragment.

3.1.2.5 Inoculation of *Plasmopara viticola* on Treated Leaves and Phenotypic Characterization of the Plant–Pathogen Interaction

Experimental inoculation of the leaf disks with the pathogen were carried out by mixing *P. viticola* sporangia coming from Western (S. Maria della Versa, Pavia) and Eastern (Casarsa della Delizia, Pordenone) Italian field populations (Maddalena et al., 2020; Sargolzaei et al., 2020). To verify that the leaf tissues used for the experimental activities were not previously contaminated by *P. viticola*, a PCR assay with primers specific for the ITS region of *P. viticola* (Toffolatti et al., 2012) was carried out on all leaf samples. Leaf tissues were collected from each sample (dsRNA – and water – treated) at all time points. DNA was extracted using the DNeasy Plant Mini kit (Qiagen Italia, Milano) and checked by NanoDrop for quantity and quality. PCR reactions were performed using 2 µl of DNA template, 12.5 µl of DreamTaq Green PCR Master Mix (2X) (Thermo Fisher Scientific), 0.5 mM of forward (AF_2F: 5' – TCCTGCAATTCGCATTACGT – 3') and reverse (AF_2R: 5' – GGTTGCAGCTAATGGATTCCTA – 3') primers (Toffolatti et al., 2012), and water up to 25 µl.

The thermal cycling conditions were as follows: 94°C for 3 min, 30 cycles at 94°C for 30 s, 57°C for 30 s, 72°C for 1 min, and a last step at 72°C for 5 min. PCR products were solved on 2.5% agarose gel electrophoresis and stained with Realsafe nucleic acid staining solution (Real, Valencia).

Positive control consisted of DNA extracted from sporangia and infected leaf disks and negative controls consisted of water and *B. cinerea* DNA.

Leaf disks, sampled at each time point, were placed, lower surface upward, in a Petri dish (9 cm diameter) containing moistened filter paper. The leaf disks were

airbrushed with 0.2 ml of a sporangia suspension (5 x 10^4 sporangia ml^{-1}) obtained by collecting sporangia in sterile distilled water, and incubated in a growth chamber at 22°C with a 12-h photoperiod (Toffolatti et al., 2018). The effect of dsRNA treatment on the pathogen's ability to infect the leaf tissues was evaluated at 7 days after inoculation by combining quantitative (disease severity and the production of sporangia) and qualitative traits, related to the morphology of vegetative and reproductive structures of the pathogen.

Disease severity was evaluated in both experiments, while sporangia production and microscopy were performed in the first experiment only. The disease severity of each biological replicate was estimated from the percentage of leaf disk area covered by sporulation (PSA) (Toffolatti et al., 2012). The number of sporangia produced by the pathogen per leaf unit (sporangia cm^{-2}) was determined as described by Toffolatti et al. (2016) by collecting the sporangia from each leaf disk in 1 ml of 20% glycerol:water (v:v) and counting them in Kova chambers.

Microscopy observations were performed by aniline blue staining (Wick, 2009) on leaf disks fixed in absolute ethanol and cleared as described by Alexander et al. (2005) with some modifications: samples were boiled in 85% ethanol:water (v:v) for 10 min, and incubated in pre-warmed lactic acid at 70°C for 30 min, following the procedure reported by Ricciardi et al. (2021). Reagents were purchased from Sigma-Aldrich. Samples were observed under an EasyLab CX40 (Olympus) bright-field optical microscope equipped with Primo Cam HD5 camera (Tiesselab, Milano, Italy). Pictures were taken as Z sections and overlapped by using ImageJ software (https://imagej.nih.gov/ij/index.html).

3.1.2.6 Evaluation of dsRNA Treatment on Off-Target and Jasmonic Acid Metabolism Genes

In order to evaluate the effect of dsRNA treatment on off-target genes, the following genes were evaluated via RT-qPCR: *EF1a* (*elongation factor 1a*; EF1a_F: 5' – GAACTGGGTGCTTGATAGGC – 3'; EF1a_R: 5' - ACCAAAATA TCCGGAGTAAAAGA – 3') and *GAPHD* (*glyceraldehyde – 3 – phosphate dehydrogenase*; GAPHD_F: 5' – TCAAGGTCAAGGACTCTAACACC – 3';

GAPHD_R: 5' – CCAACAACGAACATAGGAGCA – 3') (Figueiredo et al., 2015); *PEPC* (*phosphoenolpyruvate carboxylases*; PEPC_F: 5' – CATGAAGGGTATTGCTGCTG – 3'; PEPC_R: 5' – AGAGGATTTGATTTTGGTACGG – 3') and *PEPCK* (*PEP carboxykinases*; PEPCK_F: 5' – TGGCTGGTCAACACTGGTTG – 3'; PEPCK_R: 5' – CTTCAGAAGGCTTCCAGAGTG – 3') (Sweetman et al., 2012).

Gene expression analysis was performed on dsRNA – and water – treated leaves at 3, 5, 7, and 15 dat (first experiment).

On the same samples, the *COI1* (*coronatine insensitive 1*; COI1_F: 5' – ATGCCCATAGTATTCCCTTTT – 3'; COI1_R: 5' – GAACTTCTAATCCTCTGTCTC – 3') and *JAR1* (*jasmonate resistant 1*; JAR1_F: 5' – GAGAATTGCGGATGGTGATA – 3'; JAR1_R: 5' – CTAAAGGCGAAAGAGGTT – 3') (Figueiredo et al., 2015) genes, involved in the jasmonic acid metabolism and modulated by *P. viticola* infection, were investigated via RT – qPCR.

For more details about the reaction conditions, please refer to the Basal expression of *VviLBDIf7* subsection.

Annealing temperature was set to 58°C.

3.1.2.7 Statistical Analysis

The $2^{-\Delta\Delta Ct}$ values were subjected to Levene's test to assess homogeneity of variance in R software. LSD (least significant difference) test was performed in R to evaluate (i) *VviLBDIf7* basal expression in leaves, (ii) differences among dsRNA – and water – treated leaves in *VviLBDIf7* gene expression values, and (iii) differences among dsRNA – and water – treated leaves in expression values of off – target and jasmonic acid metabolism genes.

ANOVA was carried out with IBM SPSS v.25 software on (i) transformed PSA values $asin\frac{\sqrt{PSA}}{100}$ to establish the existence of significant differences among dsRNA – and water – treated samples at each sampling time, and (ii) sporangia cm^{-2} values to establish the existence of significant differences between dsRNA – and water – treated samples at each dat.

All the results were plotted in bar plots generated by SPSS v.25 software.

3.1.3 Results

3.1.3.1 dsRNA Treatment Decreases *VviLBDIf7* Gene Expression

To assess the basal expression level of *VviLBDIf7* gene, RT-qPCR was performed on Pinot noir leaves collected at 1 - day intervals.

Results highlighted that the *VviLBDIf7* gene is constitutively expressed in leaves of Pinot noir plants grown in the glasshouse: there was no significant variation in basal expression level in the examined time points (0.45 ± 0.11 versus 0.83 ± 0.23, for first and second sampling, respectively, p value > 0.05), suggesting a relatively constant expression of the candidate S-gene. A dsRNA 412 - bp long has been synthesized on the *VviLBDIf7* gene sequence of Pinot noir to be applied in the RNAi experiment (File S3.1). Pinot noir plants grafted onto SO4 were treated with the dsRNA and the knocking down of the target gene was assessed at 3, 5, 7, and 15 days after dsRNA treatment (dat). A decrease in *VviLBDIf7* expression, even if not statistically significant, was observed between dsRNA and water – treated leaves at 3 dat, and a statistically significant expression reduction was observed at 5 dat (Figure 3.2A). At 7 and 15 dat, no significant differences were detected between samples, indicating a progressive end of the transient dsRNA effect (Figure 3.2A). The experiment was repeated treating selfrooted cuttings of Pinot noir and collecting leaves at 5 and 7 dat. Statistically significant differences in the expression levels of *VviLBDIf7* gene were observed between dsRNA – and water – treated leaves at 5 dat also in the second trial (Figure 3.2B). No significant difference was observed at 7 dat (Figure 3.2B).

The dsRNA treatment induced no visible negative effects on grapevine plants, which kept their normal phenotypic traits and vigor.

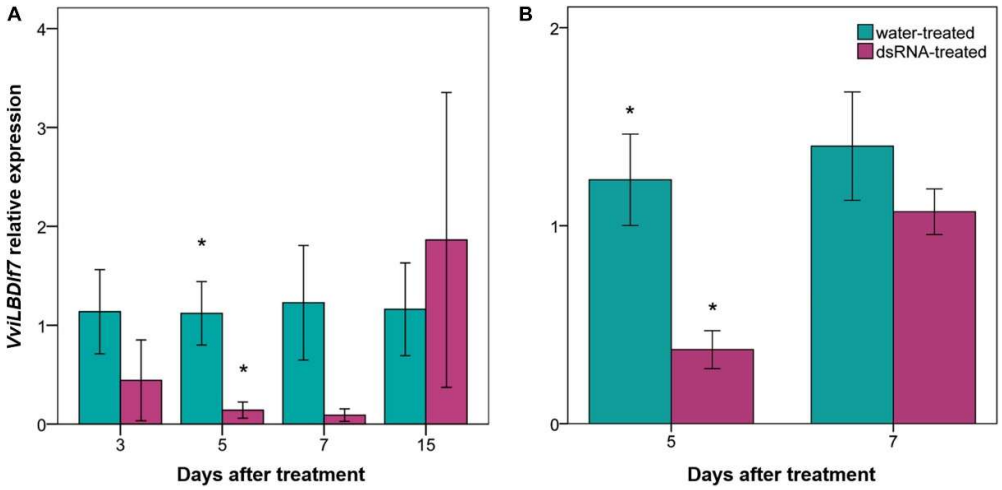

Figure 3.2 Effect of dsRNA treatment on *VviLBDIf7* gene expression. *VviLBDIf7* gene expression analysis determined based on the $2^{-\Delta\Delta Ct}$ method at 3, 5, 7, and 15 days after treatment (dat) on Pinot noir plants grafted onto SO4 (**A**), and at 5 and 7 dat on self-rooted Pinot noir plants (**B**). Bars represent standard errors. Asterisks indicate statistically significant differences among the dsRNA- and water-treated conditions at each time point (*p value = 0.05).

3.1.3.2 dsRNA Treatment Reduces Pathogen Infection and Sporulation

The complete absence of pathogen DNA was observed in the analysis of the leaves used for the experimental inoculations with *P. viticola*, confirming that the samples were healthy before inoculation. An example of the results obtained is reported in Figure S3.2. To investigate whether the dsRNA treatment induced changes in the downy mildew disease extent, dsRNA – and water – treated leaf tissues were experimentally inoculated with *P. viticola* to evaluate phenotypic traits such as disease severity, estimated through PSA, sporangia production, and morphology of pathogen structures. In the first experiment, phenotyping was carried out at 3, 5, 7, and 15 dat; in the second, at 5 and 7 dat.

Percentage of leaf disk area covered by sporulation values of water – treated samples ranged from 41 to 52% (Figure 3.3A) and from 70 to 73% (Figure 3.3B) in the first and second experiment, respectively. No significant differences ($0.8 < F < 2.5$; df = 1– 4; $p > 0.22$) were found among PSA values of dsRNA – and water – treated samples inoculated at 3, 5, and 15 dat (Figure 3.3A).

Instead, the PSA values of the water-treated leaves inoculated at 7 dat were four times higher, with statistical significance ($9.7 < F < 29.6$; df = 1–4; $p < 0.036$),

than those recorded on dsRNA-treated samples inoculated at 7 dat in both experiments (Figures 3.3A, B).

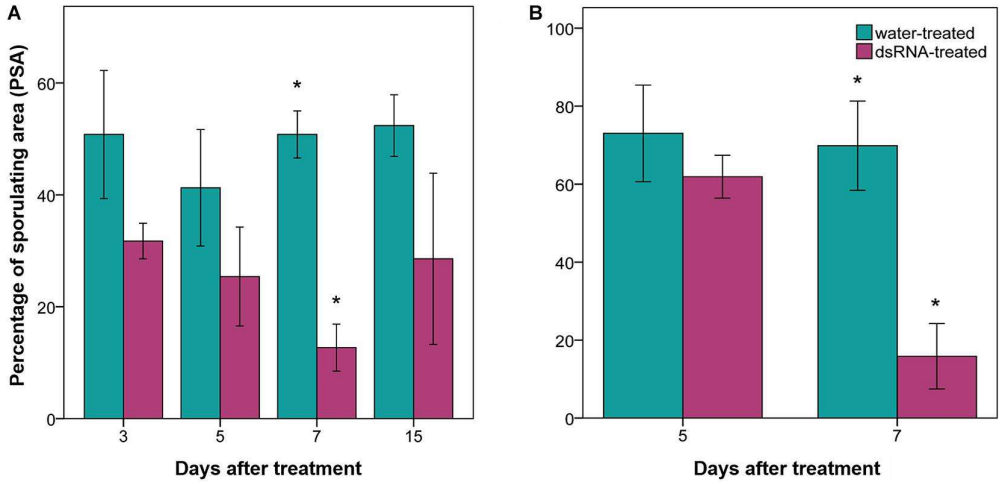

Figure 3.3 Effect of dsRNA treatment on percentage of sporulating area (PSA) evaluated 7 days after *Plasmopara viticola* inoculation. PSA evaluated on Pinot noir plants grafted onto SO4 at 3, 5, 7, and 15 days after treatment (dat) (**A**), and on self-rooted Pinot noir plants at 5 and 7 dat (**B**). Bars represent standard error. Asterisks indicate statistically significant differences among the dsRNA- and water-treated conditions at each time point (*p value < 0.036).

Sporangia production in the water-treated leaf disks ranged from 13,683 ± 2959 (average ± standard error) to 36,801 ± 17,849 sporangia cm^{-2} and did not significantly differ from those of the dsRNA – treated samples at any time from treatment ($F < 4.9$; $df = 1 – 4$; $p > 0.09$) apart from 7 dat ($F = 31$; $df = 1 – 4$; $p = 0.005$), when sporangia production was significantly reduced to 1,486 ± 316 sporangia cm^{-2} in the dsRNA – treated samples (Figure 3.4).

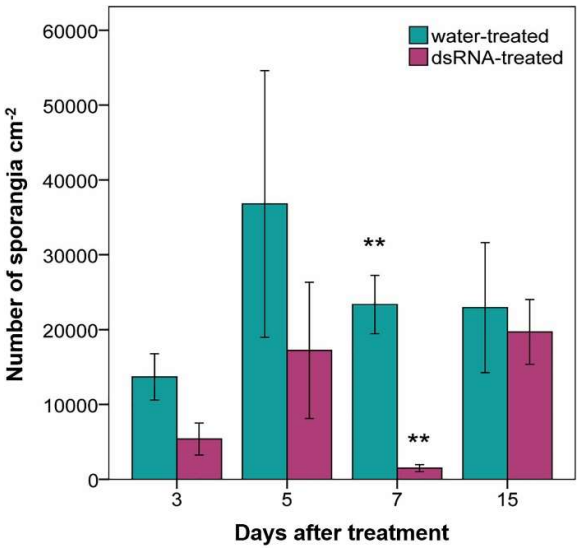

Figure 3.4 Production of sporangia (number of sporangia cm^{-2}) evaluated 7 days after *Plasmopara viticola* inoculation on dsRNA- and water-treated leaves at 3, 5, 7, and 15 days after treatment of Pinot noir plants grafted onto SO4. Bars represent standard error. Asterisks indicate statistically significant differences among the dsRNA- and water-treated conditions at each time point (***p* value 0.005).

The development of vegetative and reproductive structures of *P. viticola* in the leaf tissues was observed at the microscope by using a staining procedure with aniline blue dye, which allowed us to observe the pathogen structures in bright field. Hyphae with numerous haustoria, also clearly visible at low magnification (Figures 3.5A, B), regularly developed in the intercellular spaces of the lacunose space of the water – treated leaf tissues (Figures 3.5A – C). Sporangiophores emerged from the stomata (Figure 3.5C) and numerous sporangia could be observed on the leaf surface (Figure 3.5A). Alterations in the pathogen structures were clearly visible in the dsRNA – treated leaves only at 7 dat (Figures 3.5D – G): hyphae had a reduced diffusion (Figure 3.5G) and appeared lightly colored and highly vacuolated (Figure 3.5D); haustoria were lightly colored and visible only at high magnification (Figure 3.5F); short, hyperbranched, and sterile sporangiophores emerged from the stomata (Figure 3.5E). The same alterations were seen in all the points where the pathogen attempted penetration, indicating a uniform response of the leaf tissues to dsRNA treatment and pathogen inoculation.

The PSA values of the untreated leaves sampled immediately above the dsRNA – treated leaves (leaf sample S7; Figure 3.1B) at 7 dat in the second experiment (PSA = 21.4% ± 7.1 SD) did not significantly differ (F = 5.3; df = 1 – 4; *P* = 0.08) from the PSA values recorded in the dsRNA-treated leaves (PSA = 14.6% ± 8.4 SD) and significantly differed (F = 15.8; df = 1 – 4; *P* = 0.016) from the PSA values of the water-treated leaves (PSA = 69.8% ± 11.4 SD) sampled at the same time point.

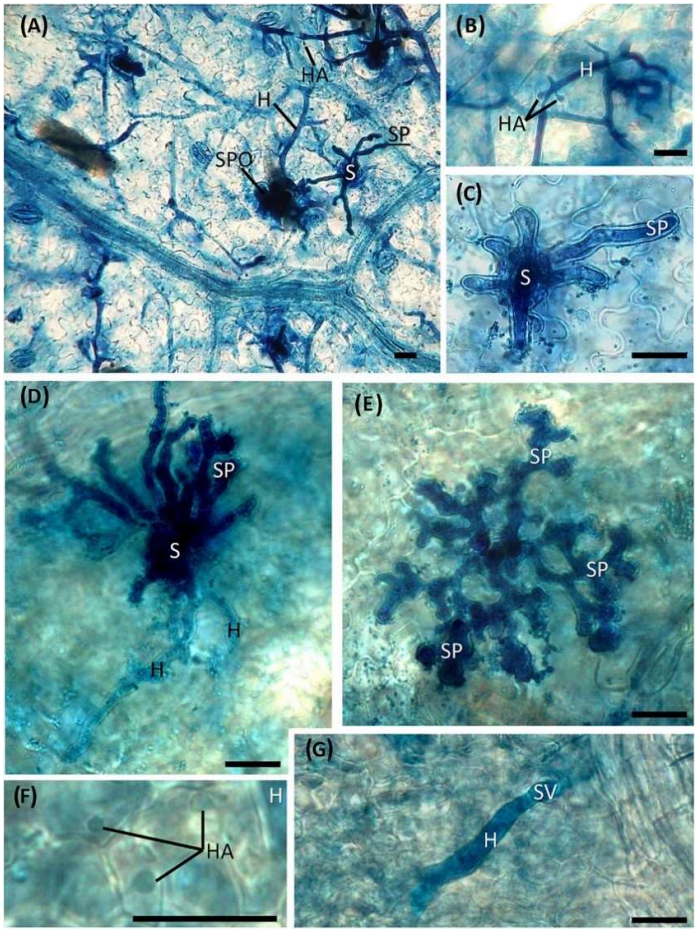

Figure 3.5 Development of *Plasmopara viticola* structures inside untreated (**A–C**) and treated (**D–G**) leaf tissues inoculated at 7 dat. (**A**) Hyphae with haustoria developing in the mesophyll cells and sporangiophores emerging from the stomata. (**B**) Mycelium with haustoria; (**C**) detail of sporangiophores emerging from a stoma; (**D**) degenerating hyphae, slightly colored and vacuolized, with no visible haustoria, and hyperbranched sporangiophores emerging from the stoma; (**E**) short, hyperbranched and sterile sporangiophores; (**F**) light-colored haustoria; (**G**) hypha developing from the substomatal vesicle with no visible haustoria. S = stoma; H = hypha; HA = haustorium; SP = sporangiophore; SPO = sporangium; SV = substomatal vesicle. Scale bar, 20 μm.

3.1.3.3 Treatment With dsRNA Does Not Reduce Expression of Off-Target Genes

The effect of dsRNA treatment has been evaluated in the gene expression of some off-target genes: *EF1a*, *GAPHD*, *PEPC*, and *PEPCK* (Figure 3.6). Relative gene expression of *PEPC* and *PEPCK* genes did not show statistical significant differences between dsRNA – and water – treated leaves at any time points (Figures 3.6C, D). Statistical significant differences between dsRNA – and water – treated leaves have been detected at 3 and 7 dat for *EF1a* gene (Figure 3.6A) and at 5 and 7 dat for *GAPHD* gene (Figure 3.6B), with expression values of dsRNA – treated leaves higher than the water – treated ones.

Regarding the effect of dsRNA treatment on jasmonic acid metabolism genes, the relative gene expression of two genes (*COI1* and *JAR1*) has been investigated. *JAR1* primers did not amplify any fragments at our amplification conditions (annealing temperature = 58°C), while aspecific fragments have been amplified at lower annealing temperature (data not shown).

Amplification of *COI1* gene showed statistically significant differences between dsRNA – and water – treated leaves only at 5 dat, with expression values of dsRNA-treated leaves lower than the water-treated ones (Figure 3.6E).

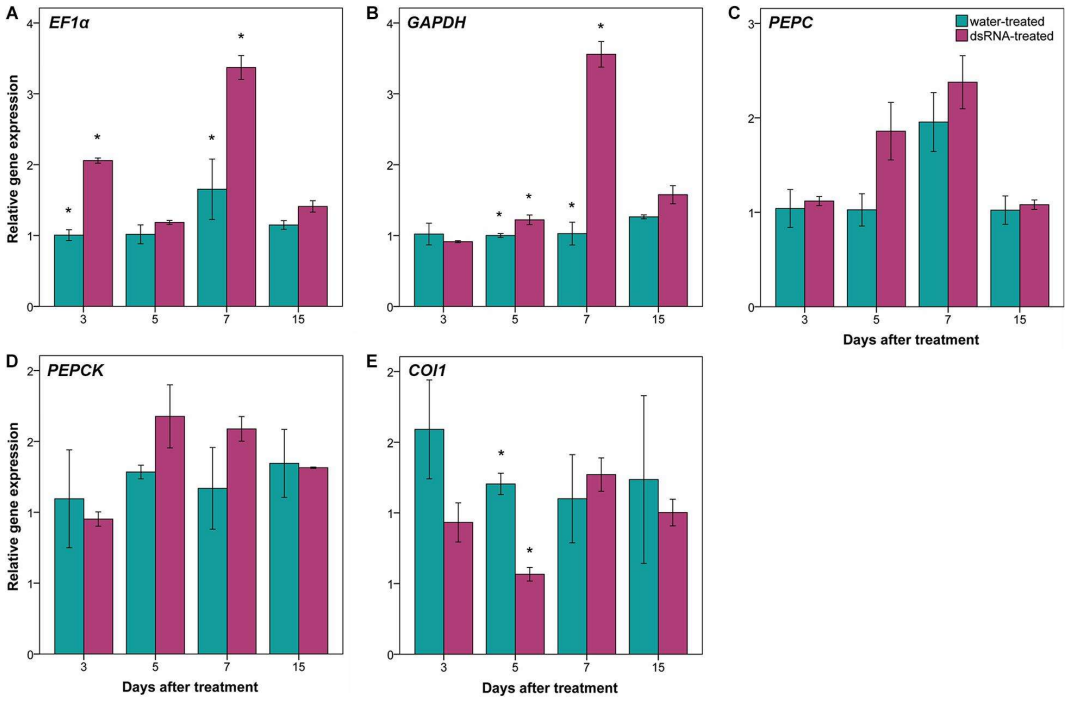

Figure 3.6 Effect of dsRNA treatment on *VviEF1α* [elongation factor 1α; (**A**)], *VviGAPHD* (glyceraldehyde-3-phosphate dehydrogenase; **B**), *VviPEPC* [phosphoenolpyruvate carboxylases; (**C**)], *VviPEPCK* [PEP carboxykinases; (**D**)], and *VviCOI1* [coronatine insensitive 1; (**E**)] gene expression at 3, 5, 7, and 15 days after treatment (dat) on Pinot noir plants grafted onto SO4. Gene expression analysis determined based on the $2^{-\Delta\Delta Ct}$ method. Bars represent standard errors. Asterisks indicate statistically significant differences among the dsRNA- and water-treated conditions at each time point (*p value = 0.05).

3.1.4 Discussion

3.1.4.1 Foliar-Applied dsRNA Reduces Expression of *VviLBDlf7* Gene

All plant genes involved in facilitating pathogen infection and supporting a compatible plant–pathogen interaction are considered S – genes (Van Schie and Takken, 2014); therefore, silenced S – genes no longer support a compatible plant–pathogen interaction and can cause pathogen-specific resistance (Pavan et al., 2010; Thatcher et al., 2012).

RNAi is a post – transcriptional gene silencing mechanism triggered by dsRNA molecules to prevent the expression of target genes (Kim and Rossi, 2007). The exogenous application of dsRNAs targeting essential interaction genes in plants (S genes) or plant pathogens and pests has been successfully used to both

control diseases and induce gene silencing as a valid alternative to genetic transformation (Mitter et al., 2017; Ghosh et al., 2018; Rosa et al., 2018; Dubrovina and Kiselev, 2019; Gu et al., 2019; Dalakouras et al., 2020).

In this work, the efficacy of RNAi approach in knocking down the putative grapevine S – gene (*VviLBDIf7*) identified by Toffolatti et al. (2020) in grapevine-*P. viticola* interaction has been investigated. A prerequisite for setting up a successful foliar RNAi experiment to knock down the target gene is the expression of the target gene in leaves at any stages, regardless of environmental conditions.

Therefore, the first step of this study was the evaluation of S – gene basal expression. RT-qPCR data showed that the expression of *VviLBDIf7* in Pinot noir leaves did not change significantly over time in the absence of perturbing conditions, confirming that S – genes can show a constitutive expression (Eichmann et al., 2004).

Foliar – applied dsRNA molecules targeting plant *VviLBDIf7* gene proved to knock down *VviLBDIf7* gene expression in Pinot noir, a grapevine cultivar susceptible to *P. viticola* infection, at 5 dat. The RNAi triggered by exogenous dsRNA is known to be transient, lasting from a few days up to a couple of weeks (Dalakouras et al., 2016, 2020; Niehl et al., 2018; Dubrovina and Kiselev, 2019; Nerva et al., 2020). In this interval, the efficiency peak of the dsRNA treatment is affected by several factors, determining the absorption rate of the exogenous molecules by plant cells, including dsRNA concentration, dose and length, application method, delivery technique, plant organ-specific activities, and stability of the molecule under unfitting environmental conditions (Das and Sherif, 2020).

In our experimental conditions, evaluations performed at 7 (both experiments) and 15 (first experiment) dat indicated a progressive reduction of the transient dsRNA effect in knocking down the expression of *VviLBDIf7* gene. Instead, knockdown at 5 dat has been confirmed by the second experiment as well, when self-rooted plants were used. This second approach was used to validate the results, avoiding any rootstock interference.

Rootstock can affect the scion behavior at different levels, such as plant development, biomass accumulation and phenology (Ollat et al., 2015). These results demonstrated that the transient effect of dsRNA was not affected by rootstock and that in our conditions, the RNAi is terminated by 15 dat.

Fifty LBD genes have been identified in grapevine genome (Grimplet et al., 2017), expressed in different tissues (such as young leaves, developed tendril, and inflorescences), in berry development and ripening and in response to abiotic and biotic stresses (Albertazzi et al., 2009; Fasoli et al., 2012; Agudelo-Romero et al., 2015). *VviLBDIf7* seems to be expressed at low levels in all mature/woody and vegetative/green tissues, while it appears to be up - regulated in berries upon *B. cinerea* attack (Agudelo-Romero et al., 2015). In our experimental conditions, no negative effects could be observed in grapevine plants treated with dsRNA: this could be due to the transient effect of RNAi.

The presence of pleiotropic effects on biological processes and in response to abiotic and biotic stresses (not yet investigated) associated with *VviLBDIf7* silencing should be better investigated in future studies on stable grapevine transformants.

3.1.4.2 Reduction of *VviLBDIf7* Expression Is Followed by Reduced Susceptibility to *Plasmopara viticola*

The developed staining protocol has two main advantages: firstly, the staining is stable and does not fade away rapidly, as normally occurs when using aniline blue staining techniques for fluorescence microscopy (Díez-Navajas et al., 2007), allowing the operator to perform a more thorough investigation of the pathogen structures; secondly, the observations can be performed with a microscope that is normally present in a basic mycology laboratory, without the need for a fluorescence microscope.

Aniline blue binds to b-glucans (b-1,3-glucans in particular) located in the *P. viticola* cell wall, staining the pathogen structures in blue. However, also plant cell walls can be stained, especially callose depositions (Hood and Shew, 1996) that are frequently found as a defense reaction to the invading pathogen

(Trouvelot et al., 2008), causing some faint blue staining also in plant tissues. No differences could be observed between treatments in pathogen growth and sporulation at all time point except at 7 dat (2 days after downregulation of *VviLBDIf7)*, when Pinot noir leaves treated with dsRNA showed a significant reduction in disease severity as well as impairment in *P. viticola* growth and sporulation, compared to the water-treated leaves.

In the dsRNA – treated samples, the alterations in the vegetative structures of the pathogen were evident. The hyphae did not freely diffuse inside the leaf tissues but developed only in the area immediately surrounding the infection point and led to the differentiation of hyperbranched, partly sterile, sporangiophores.

Analogous alterations were observed as a consequence of resistance response in Mgaloblishvili (Toffolatti et al., 2018) and in response to environmental (Rumbolz et al., 2002) and chemical (Ricciardi et al., 2021) stresses. The vacuolation of the hyphae underneath the sporangiophore could be associated with the necessity of the mycelium to provide material to support sporulation, as occurs in true fungi (Thrane et al., 2004), or to a degradation of the mycelium. Abnormal hyphal vacuolation has been observed in hyphae of the oomycete *Saprolegnia ferax* following the application of growth inhibitors (Bachewich and Heath, 1999). Moreover, the vegetative structures of the pathogen in the dsRNA – treated samples appeared more lightly colored compared to the water – treated samples. Since aniline blue binds to b-glucans, this discoloration could indicate an alteration in the cell wall composition. While this altered mycelium was clearly visible following aniline blue staining, haustoria were less colored and hardly recognizable. This could indicate that the dsRNA treatment primarily affected the haustoria, which are the only structures of the pathogen that actively interact with the host cell (Toffolatti et al., 2011). *P. viticola* is an obligate parasite of grapevine and does not directly damage the host cell, the activity of which must be preserved to allow the absorption of nutrients. Alterations at haustoria level can induce a reduced pathogen growth not only because they have a role in nutrient uptake, but also because they represent a specialized interface for delivering effectors to plants that are associated with resistance (Judelson and

Ah-Fong, 2019). More accurate investigation on the haustoria ultrastructure is needed to confirm these preliminary results. The alteration in the differentiation of sporangiophores was associated with a significant reduction in the sporangia production.

The analogous disease severity of the pathogen observed in the second experiment both on the leaves that were directly treated with dsRNA and those directly above the treated leaves (systemic diffusion), which was significantly lower than that achieved in the water – treated samples, indicates the presence of a systemic effect of the treatment that should be more deeply investigated in future studies. Systemic RNAi has been observed in other plants, such as *A. thaliana* (Melnyk et al., 2011), *Hordeum vulgare* (Biedenkopf et al., 2020), and *Nicotiana benthamiana* (Chen et al., 2018), but to the best of our knowledge, no information is reported for grapevine.

3.1.4.3 *VviLBDIf7* Is a Candidate Gene to Be Silenced to Reduce Downy Mildew Susceptibility

A potential limitation of RNAi approach can be the possible effect on off-target genes. Off-target effects occur when a siRNA downregulates unintended targets. For this reason, it is useful to assess off-target potential in order to avoid undesirable phenotypes (Rosa et al., 2018). In this work, dsRNA treatment did not reduce the expression of *EF1a*, *GAPHD*, *PEPC*, and *PEPCK* off-target genes. The up-regulation of *EF1a* and *GAPHD* genes in dsRNAtreated leaves at some time points can be a consequence of the knockdown of the *VviLBDIf7* gene (the plant reacts to the gene silencing by improving its basal metabolism).

In *A. thaliana*, the *lbd20* mutant showed a reduced disease severity after *F. oxysporum* infection and a modulation of jasmonic acid-mediated defense genes (Thatcher et al., 2012).

In grapevine, some evidences of jasmonic acid involvement in resistant cultivar in response to *P. viticola* infection have been described (Figueiredo et al., 2015; Li et al., 2015). After *P. viticola* inoculation, Figueiredo et al. (2015) observed an up - regulation of jasmonic acid biosynthesis - related genes (*LOXO*, *AOS*, *AOC*,

and *OPR3*) at 6 and 12 hpi (hours post-infection), and an up - regulation of genes involved in the jasmonic acid activation and signaling (*JAR1* and *COI1*, respectively) at 18 and 24 hpi. In this work, due to the sampling times (3, 5, 7, and 15 dat), only the gene expression profile of *JAR1* and *COI1* genes has been investigated.

Although we have to refer to only *COI1* gene expression data (no amplification fragments were detected for *JAR1* gene), the jasmonic acid pathway appears to be down - regulated, as *COI1* gene expression values at 5 dat in dsRNA – treated leaves were lower than in the water – treated ones. These data confirm what has been observed for *LBD20* gene in *A. thaliana,* where *coi1* mutants did not induce *LBD20* gene expression, and support the role of *LBD* genes in jasmonic acid signaling (Thatcher et al., 2012).

3.1.5 Conclusion

The results reported in this work highlight the great potential of RNAi – based strategies in sustainable defense management. In the current scenario, the treatment with fungicides still represents the most effective agronomical practice to defend vineyards by *P. viticola* attack. Nevertheless, Directive 2009/128/EC and Regulation (EC) No. 1107/2009 of the European Parliament and of the Council concerning the placing and use of plant protection products on the market impose to the farmers the reduction of fungicide applications, due to their negative impact on human health and environment. In this view, the development of novel and sustainable disease management strategies is essential. Numerous efforts are ongoing with the aim to obtain resistant varieties, exploiting alternative strategies to classical biotechnological tools, such as GMOs (genetically modified organisms), which are currently subjected to strict regulation (Capriotti et al., 2020). For this purpose, the use of RNAi for silencing plant susceptibility genes, which facilitate infection and support compatibility (Van Schie and Takken, 2014), represents a promising alternative to traditional means, such as fungicides, for disease control. Indeed, the phenotypic characterization of quantitative and qualitative *P. viticola* traits allowed us to establish the efficacy

of exogenous dsRNA application in silencing the *VviLBDIf7* gene, which led to a reduced pathogen growth and sporulation rate in Pinot noir, a cultivar that is normally highly susceptible to the pathogen. Based on gene expression and PSA values, the RNAi effect is concluded by 15 dat indicating that further treatments are needed for the subsequent disease control.

The signatures of systemic activity shown in the present study suggest that the dsRNA treatment could also reach untreated parts of the plant, a feature that is highly desirable since grapevine has an important growth in open field and systemic properties of RNAi could allow the protection of the newly formed vegetation not covered by the treatment. Further investigation is, however needed to clarify the movement inside the plant as well as the duration and the efficacy of dsRNA on untreated parts of the plant. Moreover, considering the high heterozygosity and the varietal rigidity imposed by registered designations of origin that affect development and cultivation of resistant varieties obtained by crossing non – *vinifera* species with *V. vinifera*, the use of RNAi approach in grapevine could represent a valid tool for specifically targeting a known gene. Further implementation of the method is, however, needed to improve the delivery of the dsRNA and achieve a more rapid silencing of the gene that could be compatible with a field use, although an appropriated regulation of topical RNAi applications is still missing (Mezzetti et al., 2020). For an effective field application of dsRNAs as a disease management tool, the following aspects need to be optimized: (i) the concentration and length of dsRNA molecules, (ii) the formulation that should prevent dsRNA degradation (encapsulation could solve this issue) and allow the uptake of dsRNAs into cells, (iii) the delivery strategy (high – pressure spraying or brush – mediated leaf applications), and (iv) the efficacy of dsRNA recognition by the RNAi pathway of the target organism. Furthermore, this approach that uses dsRNA to silence the susceptibility gene of the plant instead of targeting an essential gene of the pathogen should reduce the possible cross-species effect of the dsRNA (e.g., on beneficial microorganisms) and the development of resistances in the pathogen population. Overall, RNAi – mediated silencing could make a great contribution toward integrated pest management, which, taking a holistic approach that

exploits all the available disease management tools (i.e., resistant varieties, agronomic practices, and chemical and nonchemical pathogen control), represents the most effective way to manage diseases.

Chapter 4: Mining grapevine nitrogen metabolism to identify candidate genes of susceptibility to downy mildew

4.1 Influence of Nitrogen on Grapevine Susceptibility to Downy Mildew

Demetrio Marcianò[1, †], Valentina Ricciardi[1, †], Giuliana Maddalena[1,2], Annamaria Massafra[2], Elena Marone Fassolo[2], Simona Masiero[2], Piero Attilio Bianco[1], Osvaldo Failla[1], Gabriella De Lorenzis[1,*] and Silvia Laura Toffolatti[1,*]

[1] Department of Agricultural and Environmental Sciences, University of Milan, 20133 Milano, Italy

[2] Department of Biosciences, University of Milan, 20133 Milano, Italy

* Correspondence: gabriella.delorenzis@unimi.it (GDL); silvia.toffolatti@unimi.it (SLT)

† These authors contributed equally to this work.

Abstract

Downy mildew, caused by the obligate parasite *Plasmopara viticola*, is one of the most important threats to viticulture. The exploitation of resistant and susceptibility traits of grapevine is one of the most promising ways to increase the sustainability of disease management. Nitrogen (N) fertilization is known for influencing disease severity in the open field, but no information is available on its effect on plant-pathogen interaction. A previous RNA-seq study showed that several genes of N metabolism are differentially regulated in grapevine upon *P. viticola* inoculation, and could be involved in susceptibility or resistance to the pathogen. The aim of this study was to evaluate if N fertilization influences: (i) the foliar leaf content and photosynthetic activity of the plant, (ii) *P. viticola* infectivity, and (iii) the expression of the candidate susceptibility/resistance

genes. Results showed that N level positively correlated with *P. viticola* infectivity, confirming that particular attention should be taken in vineyard to the fertilization, but did not influence the expression of the candidate genes. Therefore, these genes are manipulated by the pathogen and can be exploited for developing new, environmentally friendly disease management tools, such as dsRNAs, to silence the susceptibility genes or breeding for resistance.

Keywords: oomycete; *Vitis vinifera*; nitrogen fertilization; plant pathogen interaction; susceptibility genes; resistance genes

4.1.1 Introduction

Nitrogen (N) is the nutrient element applied in the largest quantity in cultivated soils (Conklin et al., 2007; Huber and Thompson, 2007). In plants, the production of amino acids, nucleic acids, chlorophylls, and hormones, among other cellular components, requires nitrogen (Huber and Thompson, 2007). Nitrogen promotes plant growth, delays maturity, and affects cell size and cell wall thickness. It is also involved in plant resistance to pathogens, since it is essential for the production of antimicrobial compounds, such as phytoalexins and phenolics. Nitrogen stimulates vegetative growth, vine productivity, and grape quality (Verdenal et al., 2021). In viticultural soils, the availability of nitrogen is usually insufficient to optimize the growth and productivity of crop. To overcome this, farmers use a huge number of fertilizers. However, the increase in nitrogen availability may have consequences on the susceptibility of the vine to fungal diseases, including downy mildew (caused by the oomycete *Plasmopara viticola*), for indirect effects related to the modification of canopy microclimate and to the persistence in the growth of main and lateral shoots, whilst the possible direct effects of the nitrogen nutritional status on the interaction mechanisms of parasite host are controversial (Sun et al., 2020).

The management of grapevine downy mildew is based on the integration of all available tools (cultivation of resistant cultivars, adoption of agronomic practices, and the use of resistance inducers and/or plant protection products with

antifungal activity) finalized to reduce yield losses. Agronomic practices have an important role in supporting the cultivation of resistant grapes and chemical control. They aim to reduce the conditions that favor pathogen infections, such as excessive canopy growth induced by vigorous rootstocks and excessive fertilization (https://www.agric.wa.gov.au/table-grapes/downy-mildew-grapevines?nopaging=1, accessed on 20 November 2022). Moderate N fertilization is always recommended (Keller, 2005), since excessive nitrogen fertilization triggers uncontrolled shoot growth and dense canopies, favoring high humidity as well as fungal infections (Wheeler and Pickering, 2005). Moreover, cells exposed to nitrogen over-fertilization develop thinner and weakened cell walls, increasing disease risk (Thomidis et al., 2016). A multifactor analysis highlighted that, among the others, leaf nitrogen content has an influence on the downy mildew severity in grapevine (*Vitis vinifera*) (De Oliveira et al., 2021). Even if nitrogen fertilization is known for influencing the disease severity of *P. viticola* in the open field, no information is available on the specific mechanisms underlying its role in the plant-pathogen interaction. This is because the disease severity is commonly evaluated in vineyard where climatic conditions, pathogen genetics, and host phenology vary greatly (Simón et al., 2020). Furthermore, studies on P. viticola are difficult, since it is a biotrophic obligate plant pathogen (Fröbel and Zyprian, 2019).

Metabolic reprogramming is a general feature of plant–pathogen interactions (Fagard et al., 2014): it is necessary for the plant to synthesize defense metabolites and for the pathogen to acquire nutrients (C and N) from its host. The expression of N genes, in particular, is commonly affected by pathogen infection. A recent comparative transcriptome analysis, where the transcriptome of inoculated and non-inoculated grapevine cultivars (cv) with different resistance levels towards *P. viticola* where compared, showed that different plant genes involved in N metabolism are differentially modulated by the pathogen (Toffolatti et al., 2018). In detail, genes encoding a glutamine synthetase (*VviGS*) and a high-affinity nitrate transporter (*VviNRT3.1*) were upregulated in the resistant cv Bianca and not differentially expressed or downregulated in the susceptible cv Pinot noir, while an asparagine synthetase (*VviAS1*) was highly upregulated in

the susceptible cv Pinot noir and downregulated in the resistant cv Bianca. These genes are potentially involved in the mechanisms of grapevine resistance (*VviGS* and *VviNRT3.1*) or susceptibility (*VviAS1*) to *P. viticola*, and could be exploited to control the disease. The silencing of susceptibility genes through stable or transient transformation via genome editing or RNA interference (RNAi) is gaining importance (Zaidi et al., 2018; Pirrello et al., 2021). For instance, RNAi has been successfully applied against *P. viticola* in greenhouse conditions, by targeting the *VviLBDIf7* gene encoding a LOB (LATERAL ORGAN BOUNDARIES) domain-containing (LBD) protein that belongs to plant LOB family of transcription factors (Marcianò et al., 2021). To establish if the candidate resistance/susceptibility genes involved in N metabolism are truly modulated by the plant upon pathogen interaction and not by a differential presence of nitrogen in the plants, it is necessary to evaluate their basal expression under different N conditions and in absence of the pathogen.

In this study, performed under controlled conditions, we aimed to assess the effect of N on both the pathogen development and the modulation of plant candidate resistance/susceptibility genes. To this purpose, we subjected grapevine cuttings to different levels of nitrogen fertilization for evaluating: (i) leaf nitrogen and chlorophyll content; (ii) *P. viticola* development and downy mildew severity; and (iii) the expression of the candidate resistance/susceptibility plant genes (*VviNRT3.1*, *VviGS* and *VviAS1*).

4.1.2 Material and Methods

4.1.2.1 Plant material, Growth Conditions and Sampling

The experimental activities were conducted in the greenhouse of Department of Agricultural and Environmental Sciences (University of Milan, Milan, Italy), with a 12 h-photoperiod and 24 °C. Thirty vine cuttings of cv Pinot noir grafted onto SO4 were put in 25 - L aerated tanks filled with a hydroponic nutrient solution for shooting and growing. The tanks were initially filled with 20 L of Hoagland solution for hydroponic culture: 2 mM $Ca(NO_3)_2$, 0.75 mM K_2SO_4, 0.65 mM

$MgSO_4$, 0.5 mM KH_2PO_4, 0.1 mM FeNaEDTA, 0.005 mM H_3BO_3, 0.001 mM $MnSO_4$, 0.0005 mM $CuSO_4$, 0.0005 mM $ZnSO_4$, 0.00005 mM $(NH_4)_6Mo_7O_{24}$, pH 6.1 (Brancadoro et al., 1995). After 30 days, the developed plants were grown in N starvation (Hoagland solution without N) for 15 days and then divided into five groups. Each group was exposed to Hoagland nutrient solutions containing different $Ca(NO_3)_2$ concentrations: 0, 0.05, 1, 2 (standard reference concentration) and 5 mM. All of the solutions, prepared with distilled water, were changed weekly with fresh ones. The starvation period was necessary to deplete the N reserves that are located in grapevine roots (Verdenal et al., 2021) and make the treatments with different N concentrations effective. Starting from T0 (the first day of exposure to the five different Hoagland solutions), three leaf samplings (T1, T2 and T3) were performed: T1 leaves were collected 7 days after the treatment, while T2 and T3 at 17 and 27 days after treatment, respectively. Leaves were used to: (i) quantify N amount; (ii) evaluate photosynthetic performance (only on T3 samples); (iii) inoculate *P. viticola* and determine disease severity; (iv) evaluate expression of genes related to N metabolism. Five leaves were randomly collected from three different plants per treatment at each sampling time (Figure 4.1.6). From these leaves, 12 leaf discs were immediately collected with a cork borer (Ø 1.5 cm) and used for pathogen inoculation and photosynthetic performance evaluation (Figure 4.1.6 A,B). The remaining leaf tissues of three leaves were stored at room temperature until N quantification (Figure 4.1.6C), while the tissues of the other two leaves were then immediately frozen with liquid nitrogen and kept at −80 °C until RNA extraction (Figure 4.1.6D).

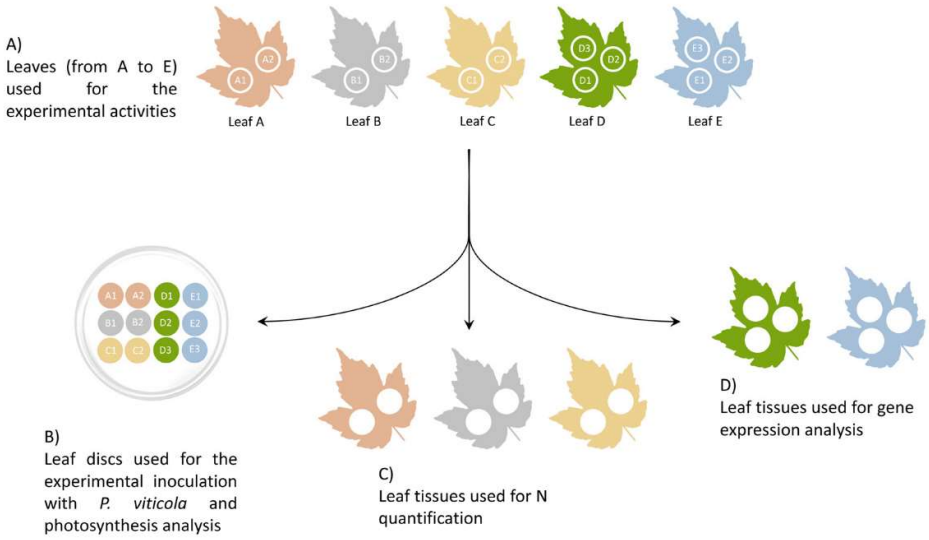

Figure 4.1.6. Scheme of the utilization of the leaves. (**A**) Five leaves (A, B, C, D, and E) were sampled for each treatment. Two leaf discs (A1-2, B1-2 and C1-2) were cut from leaves A–C, while three leaf discs (D1-3 and E1-3) were sampled from leaves D and E. (**B**) The leaf discs were placed, lower surface upwards, in a Petri dish for experimental inoculation with *P. viticola*. The leaf tissues remaining from leaves A–C were used for N quantification (**C**) while those remaining from leaves D and E were used for gene expression analysis (**D**).

4.1.2.2 Nitrogen quantification

After sampling, leaves were dried (60 °C, 2 days) to a stable dry weight. Dried leaves were ground using the Retsch MM300 tissuelyser (Gemini B.V., Apeldoom The Netherlands). Levels of leaf N were estimated using an elemental analyzer NA 1500 series 2 NC (Carlo Erba, Italy), starting from 3 mg of each ground leaf sample (Bianchi and Brancadoro, 2021).

4.1.2.3 Photosynthetic Performance Analysis

At T3, chlorophyll fluorescence was measured to evaluate the photosynthetic performance associated with excised leaf discs through an imaging chlorophyll fluorometer Imaging PAM (Walz, Effeltrich, Germany). Maximum quantum yield (MQY) and effective quantum yield of photosystem II were measured and imaging data analyzed using the ImagingWinGigE (Walz, Germany) software to

retrieve the MQY mean value associated with each leaf disc (Colombo et al., 2020; Perrault et al., 2010; Schreiber et al., 2007). Two measurements per sample were performed: the first measure (t1) was done without acclimatization to darkness, while the second (t15) was performed after 15 min of acclimatization to darkness.

4.1.2.4 Pathogen Infection

The leaf discs were placed with their abaxial surface up in a Petri dish (9 cm diameter) containing moistened filter paper underneath. Each leaf disc was inoculated with five drops (5 μL) of a *P. viticola* sporangia suspension (5 × 105 sporangia mL−1) obtained by washing previously infected leaves with sterile distilled water. The *P. viticola* inoculum used was a mix of three different populations with different geographical origins (Oltrepò Pavese, Franciacorta and Friuli-Venezia Giulia) (Ricciardi et al. 2021). After the inoculation, plates were incubated for seven days in a growth chamber at 22 °C (18:06 h photoperiod) and dried with filter paper for 24 h post-inoculation. After 7 days, a picture was taken with a digital camera (Fujifilm Digital camera A160) for each plate, and the sporulated area (SA) of each leaf disc (mm2) was determined by manual segmentation of pixels (Mattos et al., 2020; Bock et al., 2020) corresponding to sporulation using the GIMP 2.10 software (https://docs.gimp.org/2.10/en/, accessed on 5 June 2022). The disease severity was expressed as the percentage of sporulated area (PSA) over the total leaf disc area. For T3 samples only, sporangia were collected from the leaf discs in 1 mL of sterile distilled water-glycerol solution (80:20 v/v) and counted in KOVA chambers (KOVA International Inc., Garden Grove, CA, USA) to calculate the number of sporangia (S) produced by the pathogen per leaf unit (sporangia mm–2) (Ricciardi et al. 2021). The inoculated leaf discs were then fixed in Carnoy's solution (1:3 glacial acetic acid:absolute ethanol), and stored at 4 °C until use, then the discs were cleared and stained with aniline blue (Ricciardi et al. 2021). The pathogen structures, visible in the blue inside the stained leaf discs, were observed at Zeiss Primo Vert optical microscope equipped with Primo Cam HD5

camera (Tiesselab, Milano, Italy). For maintaining continuity with the inoculum over time, the artificial *P. viticola* population used for infecting T1 leaves was propagated on fresh detached leaves obtained from potted plants of cv Pinot noir following the above described protocol.

4.1.2.5 Gene Expression Analysis

Total RNA was isolated from leaves, frozen in liquid nitrogen after sampling, and stored at −80 °C until their use. Leaves were ground in liquid nitrogen and 100 mg of ground tissue were used to perform RNA extraction, using Spectrum™ Plant Total RNA Kit (Sigma-Aldrich, Darmstadt, Germany), according to manufacturer's instructions. Qubit® 3.0 Fluorometer (Life Technologies, Carlsbad, CA, USA) was used for RNA quantification, using Qubit® RNA HS Assay Kit (Life Technologies), while NanoDrop 8000 Spectrophotometer (Thermo Fisher Scientific, Waltham, MA, USA) was used to check RNA quality (260/230 and 260/280 ratios). Lithium-chloride treatment was not required, as no samples showed a 260/230 ratio lower than 1.8. Five hundred ng of total RNA were reverse transcribed with SuperScript®IV Reverse Transcriptase (Thermo Fisher Scientific), according to manufacturer's instructions. Semi-quantitative real-time RT-PCR was carried out on QuantStudio® 3 Real-Time PCR Systems (Thermo Fisher). Each reaction was carried out in a volume of 20 µL, using 10 µL of PowerUp™ SYBR™ Green Master Mix (Applied Biosystems Waltham, MA, USA), 500 nM of each primer, 4 µL of cDNA diluted 1:10 and water up to the final volume. Each reaction was performed in triplicate. The expression of three genes was evaluated: nitrate transporter (*VviNRT3.1*), glutamine synthetase (*VviGS*) and asparagine synthetase (*VviAS1*) (Table 4.1.3). Primers were designed on the available sequences using the Primer3 Plus software (Untergasser et al. 2007). Sequence primers are reported in Table 4.1.3. Ubiquitin (Fujita et al. 2007) and glyceraldehyde-3-phosphate dehydrogenase (Figueiredo et al. 2015) genes were used as references for data normalization. The expression of each gene was calculated following the $2^{-\Delta\Delta Ct}$ method (Livak and Schmittgen, 2001).

Table 4.1.3. List of genes analyzed in this work. Gene ID, protein name and primers are reported.

Gene	Gene ID	Protein Name	Primers (5' – 3')
VviNRT3.1	XM_002279825.3	high-affinity nitrate transporter 3.1	F: TTCCAACAATTCCGTAGAGTGG R: AGTTACGGTTTCTCTAATCACC
VviGS	XM_002274103.2	glutamine synthetase leaf isozyme	F: GCTGATCTCCAGAACATCAACC R: CGGCAGTTGCGCTGGGCCAGTG
VviAS1	NM_001281237.1	asparagine synthetase	F: GCAATGGATATTGACCCTGAGTG R: AAAAGCCCTCCTGAGAACCC

4.1.2.6 Statistical analysis

Statistical analyses of nitrogen quantification were performed using the R package agricolae (version 3.6.0; De Mendiburu and Simon, 2015) via ANOVA test and Fisher's least significant difference (LSD) post-hoc test with Bonferroni's correction. Statistical analysis of photosynthetic performances was performed using the R package agricolae via Kruskal-Wallis H test and Fisher's least significant difference (LSD) post-hoc test with Bonferroni's correction.

The continuous outcome provided by the leaf disc surface covered by sporulation (mm^2) can be assumed as a sample of gamma distribution (Segarra et al., 2001; Thom, 1958; Van den Bosch et al., 1988). For this reason, a gamma family multiple generalized linear model (GLM) was fitted [$gy = \beta_0 + \beta_{ij}X_{ij} + \beta_1 X_i X_j$ where: β_0 is the model intercept; β_{ij} the parameter's intercept and β_1 the interaction term's intercept, whereas g(•) represent the link function (log)] by using glm function in R stats. In detail, the disease severity data (y) were transformed as y + 1 to include null values, whereas the X_{ij} parameter was represented by two categorical factors: the i-th experimental timepoint (T1, T2 and T3) and the j-th nitrogen concentration (0, 0.05, 1, 2 and 5 mM $Ca(NO_3)_2$), respectively. The $X_i X_j$ parameter represented the interaction term. Estimated Marginal Means (EMMs) were retrieved from the fitted model via emmeans and multiple pairwise comparisons (with Sidak's correction) among estimated EMMs were calculated through pairs function. In addition, to account for the overall effect of independent variables, an ANOVA-like type III test was performed through joint_test in

emmeans package (https://CRAN.R-project.org/package=emmeans, accessed on 5 June 2022).

A Spearman's Rho correlation test (cor.test in R stats) was employed to measure the strength of association between the disease severity (PSA), and the number of sporangia per leaf unit (sporangia mm^{-2}). The distribution of SA values at T1, T2 and T3 was represented with violin plots, i.e., a combination of a box plot and a density plot which shows peaks in the data (Hintze and Nelson, 1998). In detail, violin plots show inside the box-plot distribution of the data, with the median, quartile, and outside the distribution shape of the data, where the width of the box is proportional to the estimated density: wider and skinnier sections of the violin plot represent, respectively, higher and lower estimated densities.

To account for differences in the MQY values recorded at different $Ca(NO_3)_2$ concentrations, a Kruskal Wallis test followed by a Fisher's least significant difference post-hoc test using kruskal in agricolae package was performed (De Mendiburu and Simon, 2015). All of the statistical analyses were performed using R (https://www.r-project.org/, accessed on 5 June 2022) in R studio 9.1 (http://www.rstudio.com, accessed on 5 June 2022).

The $2^{-\Delta\Delta Ct}$ values were subjected to Levene's test to assess the homogeneity of variance in R software. LSD test was performed in R to evaluate differences in the expression of *VviNRT3.1*, *VviGS* and *VviAS1* genes across all the different N conditions.

4.1.3 Results

Grapevine plants were grown in hydroponic conditions in a greenhouse and treated with different $Ca(NO_3)_2$ concentrations (0, 0.05, 1, 2, and 5 mM) after a period of N starvation. The optimal (control) concentration is 2 mM $Ca(NO_3)_2$. Leaf samples were collected at three timepoints (T1 = 7 days after the treatment; T2 = 17 days after the treatment; and T3 = 27 days after the treatment) for evaluating the N and chlorophyll content, the pathogen infection, and the expression of the target genes.

4.1.3.1 Nitrogen Content

Nitrogen quantification (N%) was evaluated at each timepoint (T1, T2 and T3) and for every $Ca(NO_3)_2$ treatment (0, 0.05, 1, 2 and 5 mM). The samples of control treatment (2 mM) showed the highest N percentage (3.45% ± 0.18) at all timepoints, while the samples treated with 0 (N = 2.9% ± 0.18) and 0.05 (N = 2.9% ± 0.23) mM $Ca(NO_3)_2$ showed the lowest concentrations (Figure 4.1.1A). Statistically significant differences with 2 mM samples ($3.5 < F < 7.1$; df = 4–10; $p < 0.048$) were found at T1 for 0.05 mM samples, at T2 for 0 mM and at T3 for 0 and 0.05 $Ca(NO_3)_2$ samples (Figure 4.1.1A). The leaves collected from the plants treated with 1 and 5 mM $Ca(NO_3)_2$) did not differ from the 2 mM leaves for the N content. Timing did not influence leaf N content apart from the unfertilized treatment, where N percentage significantly decreased from T1 to T2 and T3 ($F = 8.84$; df = 2–6; $p = 0.016$).

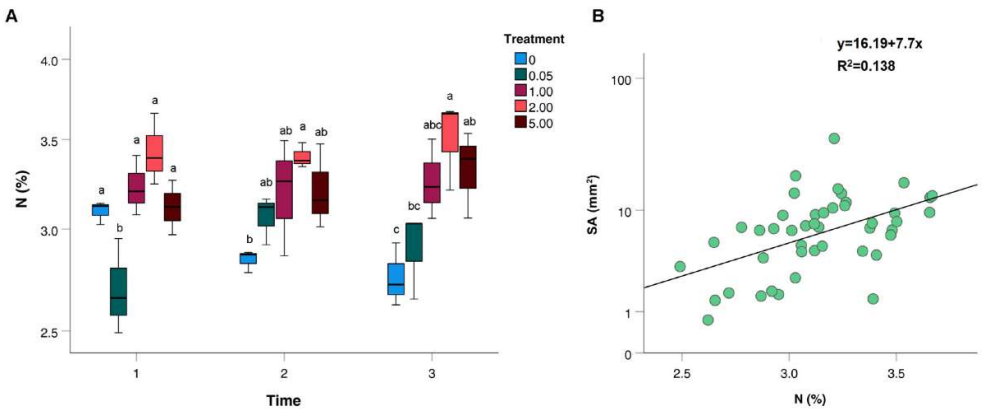

Figure 4.1.1 (A) Box-plot distribution of nitrogen (N) content (%) at different $Ca(NO_3)_2$ concentrations. Different letters indicate significant differences ($p < 0.05$) in N (%) among treatments within timepoint. (**B**) Scatter plot showing the positive linear correlation existing between N content (%) and sporulated area (SA; mm^2).

4.1.3.2 Photosynthetic Activity of the Plants

Leaf photosynthetic performance was evaluated by using an imaging chlorophyll fluorometer on the samples collected at T3 from the plants treated with the

different $Ca(NO_3)_2$ concentrations. The average maximum quantum yield (MQY) values are reported in Table 4.1.1. Compared to the 2 mM treatment, the leaves collected from plants treated with lower or higher nitrogen concentrations showed a wider distribution towards lower MQY values (Figure 4.1.2A). The effect was particularly marked for the absence of fertilization. Significant differences among the different concentrations were found (KW = 43.276, df = 4, $p < 0.001$). Without acclimatization to darkness (t1), the highest average photosynthetic performance (0.75) was detected for the 2 mM treatment (Table 4.1.1). Fluorescence significantly decreased at increasing (5 mM) and decreasing (0.05 mM) N concentrations, reaching the lowest values (0.68) at 0 mM treatment. The 2 mM concentration statistically differed for MQY values from 0, 0.5 and 5 mM but not from 1 mM.

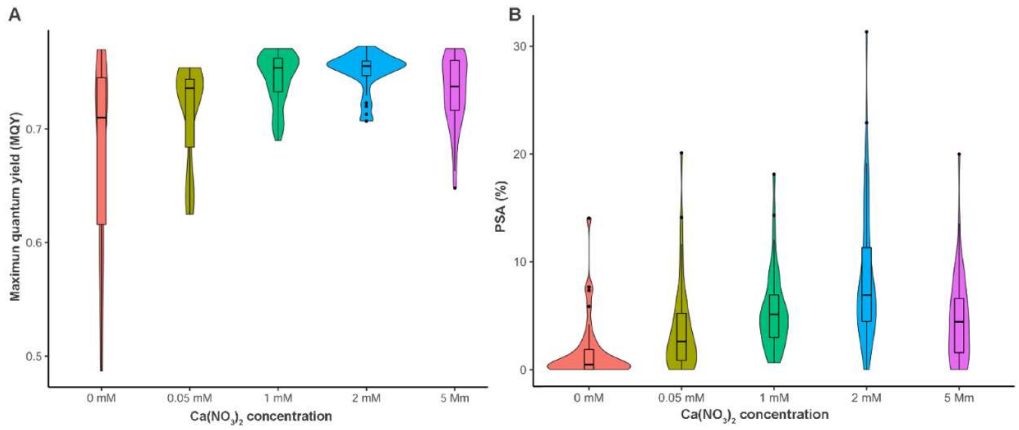

Figura 4.1.2 Violin plot distribution of (**A**) maximum quantum yield (MQY) without acclimatization and (**B**) disease severity (PSA) recorded at T3 in the leaf discs sampled from plants treated with different $Ca(NO_3)_2$ concentrations (0, 0.05, 1, 2 and 5 mM). The width of the plot is proportional to the estimated density.

Table 4.1.1 Mean measured MQY (maximum quantum yield) values ± standard deviations at each $Ca(NO_3)_2$ concentration before (t1) and after 15 min of dark acclimatization (t15) at T3. Means sharing a letter are not significantly different.

$Ca(NO_3)_2$ Concentration (mM)	t1	t15
0	0.68 ± 0.08 a	0.30 ± 0.08 a
0.05	0.71 ± 0.04 ab	0.38 ± 0.07 b
1	0.74 ± 0.02 cd	0.37 ± 0.05 b
2	0.75 ± 0.02 d	0.38 ± 0.04 b
5	0.73 ± 0.03 bc	0.39 ± 0.05 b

After 15 min of darkness acclimatization (t15), photosynthetic performance did not show statistically significant differences between samples at 0.05, 1, 2, and 5 mM treatments (2 mM mean value = 0.39). Photosynthetic performance decreased at 0 mM treatment, showing statistically significant values (mean value = 0.3) compared to the 2 mM treatment (Table 4.1.1). The three highest $Ca(NO_3)_2$ concentrations (1, 2 and 5 mM) showed the highest chlorophyll content at both timepoints (Table 4.1.1).

4.1.3.3 Pathogen Development and Disease Severity

Leaf discs were cut from the sampled leaves and experimentally inoculated with *P. viticola* to quantify the sporulated area (SA, expressed in mm^2), the percentage of sporulated area (PSA, expressed in percentage of sporulated leaf disc), and the sporangia produced by the pathogen (S, expressed as sporangia mm^{-2}).

A significant positive correlation was found between N (%) and SA (mm^2) (Kendall tau = 0.39; N = 45; $p < 0.001$; Spearman rho = 0.52; N = 45; $p < 0.001$) (Figure 4.1.1B).

The gamma regression model provided a comprehensive picture (McFadden's pseudo $R^2 = 0.18$) of the sporulated area (SA) outcome under different nitrogen concentrations while considering the different experimental inoculations. The ANOVA like test found significant differences in the interaction of predictors (F-value = 34.51; df = 8; $p < 0.001$) and in different $Ca(NO_3)_2$ concentrations (F-

value = 42.01; df = 4; $p < 0.001$), whereas no differences among timepoints (F-value = 1.05; df = 2; $p < 0.35$) were found. For this reason, multiple comparisons on EMMs were restricted to the interaction term, to simultaneously visualize differences in disease severity among $Ca(NO_3)_2$ concentrations. The mean SA values showed little or no differences among $Ca(NO_3)_2$ concentrations at T1 and T2 (Table 4.1.2). The only slight difference among SA values was found at T1, when the 0.05 mM concentration showed a significant 2-fold reduction compared to the reference concentration (2 mM). The most important differences among SA values were found at the last timepoint (T3): the SA recorded in absence of nitrogen fertilization showed a significant 4-fold reduction compared with 2 mM $Ca(NO_3)_2$, with the other $Ca(NO_3)_2$ concentrations ranging in between these two. T3 was therefore chosen for further investigating the plant-pathogen interaction and collecting quantitative (disease severity and secondary inoculum quantification) and qualitative (microscopy) information of the infection process.

Table 4.1.2 Mean sporulated area (SA, mm^2) and sporangia production (S = sporangia mm^{-2}) ± standard deviation at each $Ca(NO_3)_2$ concentrations and timepoint. Different letters indicate significant differences among estimated marginal means (EMMs) of SA or mean S values ($p < 0.05$).

$Ca(NO_3)_2$ Concentration (mM)	SA (mm^2)			S (Sporangia mm^{-2})
	T1	T2	T3	T3
0	9.90 ± 6.37 cd	5.01 ± 4.96 abc	2.99 ± 5.14 a	56.97 ± 54.02 a
0.05	3.94 ± 3.35 ab	8.84 ± 6.58 c	6.60 ± 7.83 abc	128.84 ± 121.99 ab
1	7.59 ± 3.76 bc	7.93 ± 6.08 bc	9.64 ± 6.68 cd	168.55 ± 160.54 bc
2	9.00 ± 6.03 cd	7.48 ± 5.3 bc	15.37 ± 11.73 d	244.04 ± 230.84 c
5	8.12 ± 5.28 bc	7.61 ± 5.71 bc	8.42 ± 7.62 bcd	103.58 ± 127.62 ab

The distribution of disease severity values (PSA) showed a progressively positive skewing distribution at decreasing N concentrations (starting from 2 mM) (Figure 4.1.2B). In total absence of fertilization, the SA values were in most of the cases close to 0%. On the opposite, moving from 2 to 5 mM a tendency towards a negative skew can be noticed.

Compared to the reference, significantly low sporulation (KW = 35.02; df = 4; $p < 0.0001$) was found in absence of N fertilization (Table 4.1.2). The other $Ca(NO_3)_2$ ranged in between. According to Spearman's Rho test (Rho: 0.70, $p <$

0.001), the sporangia production (S, expressed as sporangia mm^{-2}) followed a positive and significant correlation with the sporulated area (mm^2) (Figure 4.1.3).

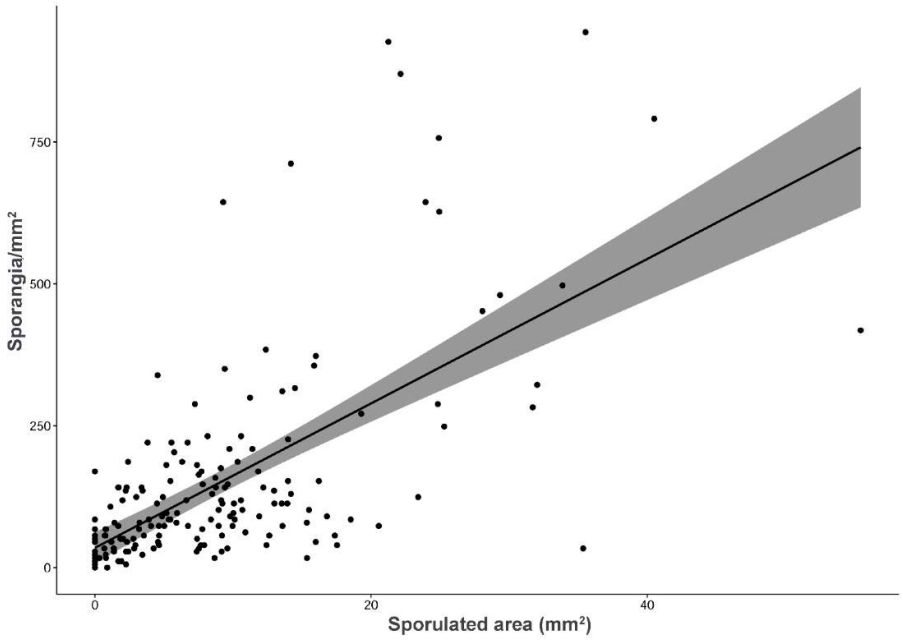

Figura 4.1.3 Scatter plot showing the positive linear correlation existing between sporangia production (sporangia mm^{-2}) and sporulated area (mm^2). Grey shade represents confidence interval.

The T3 inoculated leaf discs were stained with aniline blue to observe *P. viticola* structures (hyphae with haustoria developing in the intercellular spaces and sporangiophores emerging from the stomata) under an optical bright-field microscope (Ricciardi et al., 2021). Microscopy observations highlighted the greatest differences in *P. viticola* colonization between the reference nitrogen fertilization level (2 mM) and the absence of fertilization (0 mM). In detail, the pathogen development in leaves collected from plants treated with 2 mM $Ca(NO_3)_2$ followed a regular pattern, with the hyphae departing from the infected stomata, freely developing within the intercellular spaces and producing numerous haustoria for feeding (Figure 4.1.4A). On the opposite end, a total absence of nitrogen fertilization associated with a limited diffusion of the pathogen in the leaf tissues: the hyphae did not move far from the infected

stomata and produced few haustoria (Figure 4.1.4B–D). Sporangiophores emerging from the stomata were sporadically seen (Figure 4.1.4B).

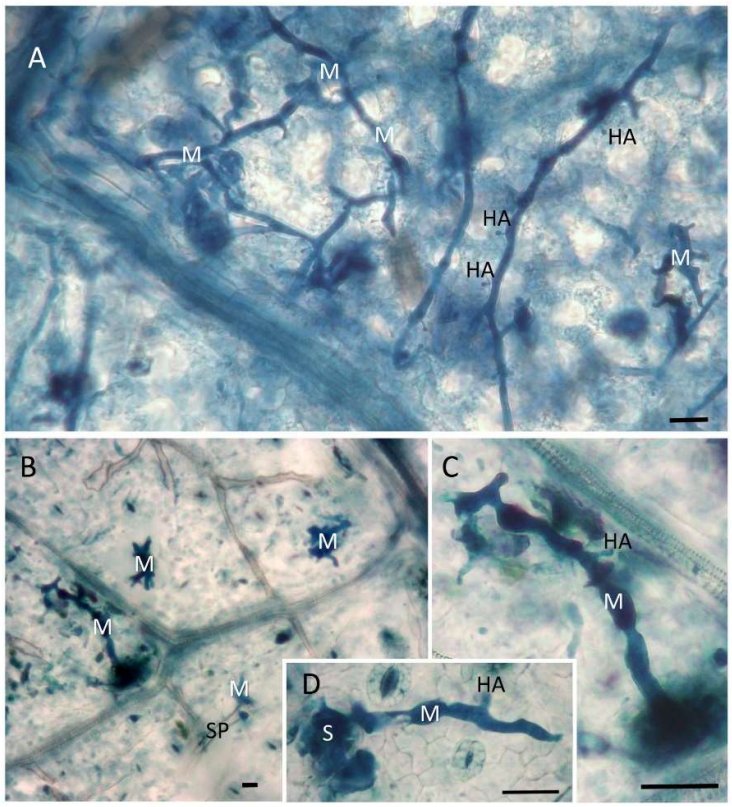

Figure 4.1.4 *P. viticola* structures inside leaves sampled at T3 from plants that were fertilized with 2 mM nitrogen (**A**) or not fertilized (**B–D**) and observed at 7 dpi (day post inoculation). (**A**) Mycelium with haustoria regularly elongating and branching in the mesophyll cells. (**B**) Short portions of mycelium departing from infected stomata with a sporangiophore. (**C,D**) Short hypha with a clearly visible haustorium. S = stoma; M = mycelium; HA = haustorium; SP = sporangiophore. Scale bar = 50 µm.

4.1.3.4 Expression of the Candidate Susceptibility/Resistance Genes

The relative gene expression of three genes (*VviNRT3.1*, *VviGS* and *VviAS1*) involved in N metabolism was determined per treatment (0, 0.05, 1, 2, and 5 mM $Ca(NO_3)_2$) and timepoint (T1, T2 and T3). Statistical analysis showed that a significantly higher abundance of *VviNRT3.1* transcripts was recorded in Pinot noir leaves treated with 1 mM $Ca(NO_3)_2$ at T3 (Figure 4.1.5A). This value was not statistically different from the values detected at 2 mM in all the three timepoints. At the reference condition (2 mM), not statistically different *VviNRT3.1* transcript

abundances were detected among the three timepoints. The other combination of treatments and timepoints showed the lowest values. *VviGS* transcripts were abundant in leaves treated with 0 mM $Ca(NO_3)_2$ at T2, while the lowest values were detected in leaves treated with 5 mM $Ca(NO_3)_2$ (Figure 4.1.5B). The other combination of treatments and timepoints showed intermediate values. The abundance of *VviAS1* transcripts was not affected neither by treatment nor by time. No statistically significant differences were observed (Figure 4.1.5C).

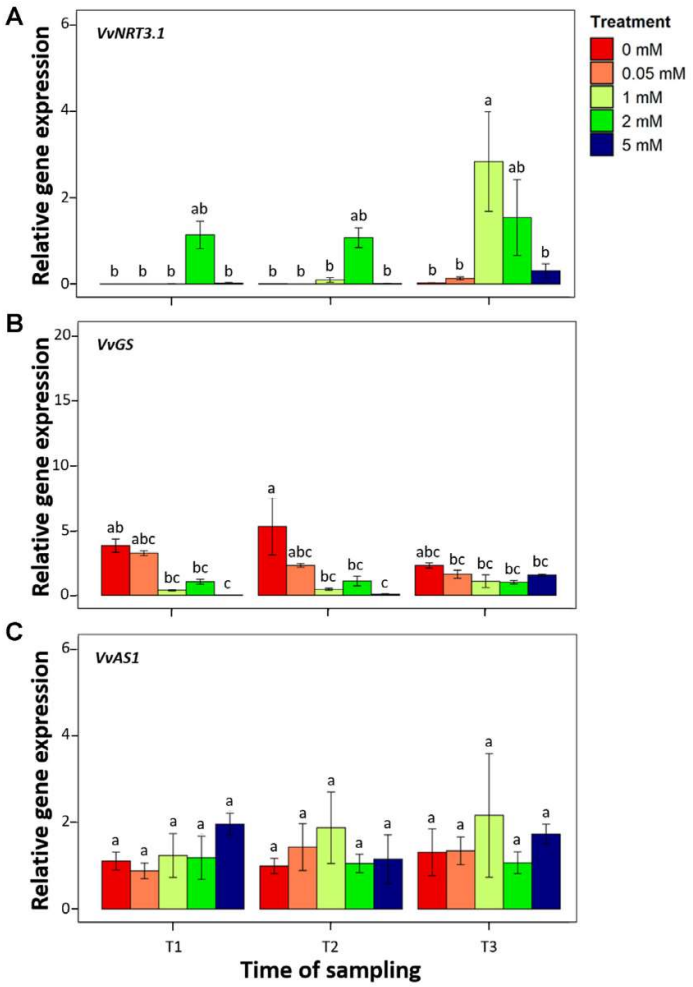

Figure 4.1.5 Relative expression level ($2^{-\Delta\Delta Ct}$ method) of genes involved in the N metabolism detected in leaves of Pinot noir plants grown under different N concentrations (0, 0.05, 1, 2 and 5 mM $Ca(NO_3)_2$) at different timepoints (T1, T2 and T3). (**A**) Nitrate transporter (*VviNRT3.1*). (**B**) Glutamine synthetase (*VviGS*). (**C**) Asparagine synthetase (*VviAS1*). Bars represent the standard deviation. Different letters indicate statistically significant differences.

4.1.4 Discussion

4.1.4.1 N Fertilization Influences Leaf N Content and the Photosynthesis

Nitrate (NO_3^-), the primary source of N for grapevine, is absorbed by roots and either stored in the vacuoles of the root cells or transported to the shoots through the xylem (Keller, 2005). Before flowering, leaves and stems are the major N sinks. They are supplied initially by stored N reserves and successively by soil N (Ferrara et al., 2018). The high nitrate concentration induced by fertilizer application can lead to N accumulation in the leaves (Keller, 2005), as observed in this study, where the treatment with 2 mM $Ca(NO_3)_2$ led to a significantly higher foliar N % than the absence or very limited (0.05 mM) fertilization.

As a macronutrient, N plays a key role in plant metabolism, entering in the composition of key metabolites such as proteins, DNA, RNA, and chlorophyll (Verdenal et al., 2021). N concentration in leaves is correlated with the chlorophyll index. Chlorophyll meter assays, such as chlorophyll fluorescence, reflect the intensity of leaf green color and are correlated with leaf chlorophyll and N concentrations (Verdenal et al., 2021). Thus, chlorophyll fluorescence can be used to diagnose plant N status (De Oliveira et al., 2021), as observed in our experimental conditions, where the treatment with optimal N fertilization (2 mM $Ca(NO_3)_2$) showed MQY values higher than the ones with non-optimal fertilization (0, 0.5 and 5 mM $Ca(NO_3)_2$).

4.1.4.2 Pathogen Development and Disease Severity Are Reduced in Absence of N Fertilization

Compared to the reference concentration (2 mM), the treatments with 1 and 5 mM $Ca(NO_3)_2$ induced statistically analogous SA at all timepoints, indicating that halving or increasing by 2.5 times the optimal N supply to the plant did not influence the ability of the pathogen to cause disease. Conversely, the plants that were subjected to no fertilization or to a 40 times reduction in the optimal N value registered the least disease severity values at T1 (for 0.05 mM concentration) and T3 (for no fertilization), indicating that only a substantial or

complete lack in N supply reduces the ability of *P. viticola* to cause disease. This result confirms that the greatest responses to N fertilization are generally observed between deficiency and physiological sufficiency (Huber and Thompson, 2007). The results achieved at T3 are the most indicative of plants response to the different N treatments: at this timepoint, we can observe the greatest variability in the plant response to the pathogen, with SA values that are significantly different and PSA distributions that show a progressive decrease at decreasing nitrate supply (from 2 to 0 mM). This could be linked to the contemporaneous reduction in leaf N content that was observed in the 0 mM samples starting from T2 but was particularly marked at T3. The positive linear correlation observed between the SA and N content of the samples suggests that the disease severity is increased by N fertilization. Leaf nitrogen content, indeed, was already reported as one of the most important parameters influencing the diseased leaf area in field studies (De Oliveira et al., 2021) and high N fertilization has been associated with increased susceptibility to *P. viticola* in a previous greenhouse experiment (Bavaresco and Eibach, 1987). An analogous situation was already observed for other biotrophs such as the rust agents *Puccinia striiformis* f.sp. *tritici* (the yellow rust of winter wheat) (Neumann et al., 2004), *Puccinia coronata* f. sp. *avenae* (the crown oat rust) (Dietz et al., 2019) and the wheat powdery mildew agent *Blumeria graminis* f. sp. *tritici* (Luo et al., 2021).

The reasons behind the reduced susceptibility of plant to *P. viticola* at the low N content might be explained by the biotrophic nature of *P. viticola*. Most oomycetes use the major nitrogen sources found in planta (amino acids, ammonium, and nitrate), but the biotrophs have a greater reliance on the host because of their reduced metabolic capabilities (Judelson and Ah-Fong, 2019). Recently, it has been demonstrated that, like other obligate biotrophs (Duplessis et al., 2011), *P. viticola* lost genes encoding nitrate and nitrite reductase enzymes, becoming totally dependent from its host for acquiring nitrogen in its reduced form (Brilli et al., 2018). In general, nitrogen-deficient plants are not able to provide the nutrients that are necessary for the obligate pathogens (Huber and Thompson, 2007). This is testified by the poor vegetative growth of *P. viticola*

observed at the microscope in leaf samples collected from 0 mM $Ca(NO_3)_2$ treated plants. Once penetrated through the stomata, the pathogen differentiated very short hyphae with few haustoria and sporadic sporangiophores; an indication that leaf tissue conditions were not favorable for its growth and asexual reproduction, as confirmed by the low sporangia production.

One of the interesting outcomes of the positive linear correlation obtained between the quantification of sporangia and sporulated area (SA) is that image analysis can be used for accurately estimating the sporangia production. This can help to reduce the amount of work needed for the phenotypic evaluation of the interaction between *P. viticola* and grapevine, which is time consuming and a limiting factor in the research of several features of downy mildew (Possamai and Wiedemann-Merdinoglu, 2022; Massi et al., 2022). Quantifying the sporangia produced by *P. viticola* is important for biological and epidemiological reasons, because it is a fitness component and it can be used to estimate the inoculum produced by the pathogen to infect new plants and tissues (Bove and Rossi, 2020; Delmotte et al., 2014; Toffolatti et al. 2012; Kennelly et al., 2007). This type of analysis is time consuming, since it must be performed at the microscope after detaching the sporangia from the leaves. Image analysis, on the contrary, is quite fast and simple because it is based on a picture of the sporulating leaf or leaf disc that is processed with a common image analysis software, it can be automated, and it provides more precise and reliable data than the traditional visual assessment methods (Hernández et al., 2022).

4.1.4.3 The Expression of the Candidate Susceptibility/Resistance Genes Is Not Influenced by N Fertilization

Nitrogen is an essential nutrient for plants (Tomasi et al., 2015) that can acquire both nitrate (NO_3^-) or ammonium (NH_4^+) mineral forms (The et al., 2021). Its uptake and allocation are mediated by carrier proteins showing different affinities (low- and high-affinity transporters, NRT) for N (NO_3^- and NH_4^+) forms (Lejay and Gojon, 2018). At nitrate concentrations above 1 mM, N acquisition is mainly operated by Low-Affinity Transport System (LATS), while when the nitrate

concentration is below 1 mM, N acquisition is mainly operated by High-Affinity Transport System (HATS) (Dechorgnat et al., 2011). *NRT3.1* is considered to be a high-affinity transporter proved to be responsive to nitrate induction in *Arabidopsis thaliana* (Okamoto et al., 2006). In this work, *VviNRT3.1* acted as a low-affinity transporter. It was expressed 27 days after treatment (T3) with 1 mM nitrate, suggesting its involvement in nitrate transport at low nitrate supply level (Fagard et al., 2014; Toffolatti et al., 2018). In higher plants, glutamine synthetase catalyzes the incorporation of ammonia into glutamate to generate glutamine, being a major enzyme responsible for the assimilation of ammonium absorbed from the growth medium or generated by NO_3^- reduction (Lea et al., 1990). GS activity seemed to not or only slightly be affected by N form (Woodall and Forde, 1996). In our experimental conditions, *VviGS* was slightly active at low nitrate concentration (0 and 0.05 mM), 7 and 17 days (T1 and T2) after the beginning of treatment, meaning that the plant is perceiving a non-optimal N condition (Fagard et al., 2014; Toffolatti et al., 2018; Asselberg et al., 2007; Liu et al., 2010). Asparagine synthetase catalyzes the synthesis of asparagine from aspartate, playing a role in both N assimilation and remobilization (Moison et al., 2018; Lee et al., 2020). The expression of gene encoding for this enzyme has been found to be affected by both form and content. In *A. thaliana*, the expression level of *AtAS2* gene is induced by NH_4^+, while *AS* genes are induced by NO_3^- in *Phaseolus vulgaris* and soybean (Wong et al., 2004; Osuna et al., 2001; Antunes et al., 2008), but the expression level of *VviAS1* in leaves of cv Pinot noir seems not to be affected by NO_3^- treatments (Toffolatti et al., 2018; Seifi et al., 2014; Hwang et al., 2011).

All of these genes are induced in response to pathogens. In *A. thaliana*, two *NRT* genes are involved in the response to *Pseudomonas syringae* and to *Erwinia amylovora* (Camañes et al., 2012). In grapevine, *VviNRT3.1* seems to be involved in the response to *P. viticola* infection. It was upregulated in infected leaves of cv Bianca, and was downregulated in infected leaves of cv Pinot noir (Toffolatti et al., 2018). *GS1* was upregulated in tomato cultivars resistant to *Botrytis cinerea* (Asselbergh et al., 2007) and the expression *GS1* has been shown to be induced in *A. thaliana* upon fungal infections (Liu et al., 2010). The

GS1 involvement in plant stress response has been observed also in grapevine. *VviGS1* was differentially expressed in resistant cultivars infected with *P. viticola* (Toffolatti et al., 2018). In non-optimal N conditions, it can be hypothesized that the activation of *VviNRT3.1* and *VviGS1* could lead the plant to show a less susceptible phenotype. *AS1* is required not only for plant nitrogen assimilation, but also for defense response to microbial pathogens (Seifi et al., 2014; Hwang et al., 2011). *VviAS1* has been identified to be involved in the response of grapevine to *P. viticola* infection. Its expression was down-regulated in cv Bianca and upregulated in cv Pinot noir infected leaves (Toffolatti et al., 2018). The activation of *VviAS1* in infected leaves of cv Pinot noir may play a role in promoting *P. viticola* pathogenesis by providing a rich source of N for the pathogen. The putative role in pathogenicity and its steady expression in optimal and non-optimal N conditions make *VviAS1* a good candidate susceptibility gene.

4.1.5 Conclusions

The results highlighted that only a very low level of nitrogen availability could reduce the downy mildew severity, while small increases or decreases of N supply compared to the standard reference $Ca(NO_3)_2$ concentration (2 mM) did not show any sensible effect on the management of the disease. *VviNRT3.1*, *VviGS* and *VviAS1* are good candidate resistance and susceptibility genes, because their expression was not influenced by nitrogen nutrition. Further analyses are needed to assess the effect of other nitrogen nutritional levels on the expression of these genes, and to evaluate the role of the proteins encoded by the candidate resistance/susceptibility genes in the plant-pathogen interaction. However, the present achievements strongly indicate that these genes can be exploited for the selection and development of disease management tools. In particular, susceptibility genes could be transiently knocked down by exploiting target specific dsRNA to inhibit the pathogen development, or stably knocked out by genome editing, while resistance genes could be exploited as markers of the plant response to the pathogen.

4.2 *VviAS1* as a candidate gene of susceptiblity to downy mildew: validation assay by transient RNAi interference

4.2.1 Introduction

RNA interference (RNAi) is a biological mechanism used by different organisms to regulate gene expression. It is based on transcriptional and post transcriptional gene silencing (PTGS) triggered by double stranded RNA (dsRNA) molecules, to prevent the aberrant or exogenous expression of specific genes (Bosher and Labouesse, 2000). RNAi silencing mechanism starts with enzyme Dicer, that is able to process and convert dsRNA silencing trigger to smaller molecules of 20-26 nucleotides, the small interfering RNAs (siRNAs). After that, the siRNA antisense strand become specific to an endonuclease-protein complex named RNA-induced silencing complex (RISC). The complex is able to target the homologous RNA and to degrade it at specific sites, resulting in the knock-down of the gene expression (Younis *et al.*, 2014). Due to its nature, RNAi mechanism can be employed as a gene regulatory approach in functional genomics studies. In this way, precise down-regulation of target genes of interest can be achivied, and their role can be efficiently explored (Dalakouras *et al.*, 2016).

In particular, this approach can be particularly useful to silence susceptibility genes, with the scope of achieving resistance to plant diseases. S-genes are genes that facilitate the compatibility between plant and pathogen, and are essential for their interaction, especially for biotrophic pathogens. As a consequence, loss-of-function mutation of S-genes can limit pathogens success in establishing the infection, resulting, indirectly, in plant resistance against the disease (Van Schie and Takken, 2014).

In the previous chapter (4.1), a new candidate gene of susceptibility to downy mildew, *Asparagine synthetase 1* (*VviAS1*), was indentified. The gene is involved in nitrogen metabolism, playing a role in both N assimilation and remobilization by catalyzing the synthesis of asparagine from aspartate (Moison *et al.*, 2018; Lee *et al.*, 2020). In previous studies, its expression during grapevine infection with *P. viticola* (causal agent of downy mildew) was found to be compatible with

S-genes patterns of expression. The gene was strongly up-regulated by susceptible variety Pinot noir, and down-regulated by resistant variety Bianca (Toffolatti *et al.*, 2018, 2020).

In this work, the role of *VviAS1* as candidate gene of susceptibility to downy mildew was evaluated trough a transient RNAi approach based on exogenous application of dsRNA. The assay was performed following guidelines reported in (Marcianò *et al.*, 2021)(Chapter 3). Furthermore, to gain new information about dsRNA dosage and plant age effect, information scarcely available in literature, the experiment was performed with some modifications. i) Grapevine plants more advanced in the vegetative growth stage were employed; ii) Compared to the previous experiment, an increased dsRNA quantity was used (200 ug per plant instead of 100 ug per plant); iii) To prove the target-dsRNA specificity of action, an internal control gene (*VviUFGT*) was included in the experiment.

4.2.2 Material and Methods

4.2.2.1 Plant material

Treatments with *VviAS1* and *VviUFGT* dsRNA were carried out on 6-year-old Pinot noir plants grafted onto SO4, maintained in a greenhouse in 5-L pots filled with sand-peat mixture (7:3 v/v), regularly watered via a drip system and fertilized twice a year with Osmocote Topdress fertilizer (ICL Specialty Fertilizers, Italy), as reported in Marcianò et al., (2021). The plants, grown in a greenhouse, never came in contact with *P. viticola* and were regularly inspected for disease symptoms.

4.2.2.2 *VviAS1* and *VviUFGT* dsRNA Design and Synthesis

In order to synthesize the dsRNA molecules, *VviAS1* (LOC100241610) candidate S – gene and *VviUFGT* (NM_001397857) control gene were partially amplified. *VviUFGT V. vinifera anthocyanidin 3-O-glucosyltransferase 2* was

used as an internal control for the experiment. The aim of its use was to demonstrate that it's not the application of whichever dsRNA to impact the expression of target genes, but the application of a specific dsRNA for a specific target.

To allow the synthesis of dsRNA template of proper dimension (400–500 bp) through PCR, primers for *VviAS1* (VviAS1_RNAi3_F and VviAS1_RNAi3_R; Table 4.2.1) and *VviUFGT* (VviUFGT_RNAi3_F and VviUFGT_RNAi3_R) were designed on the available sequence using the Primer3 Plus software and NCBI Primer-BLAST. NetPrimer was used to predict primers quality. In order to reduce the probability of off-target amplicons, the partial *VviAS1 and VviUFGT* sequence were amplified starting from cDNA samples obtained in the "4.1.2.5 Gene Expression Analysis subsection" of chapter 4.1. PCR reaction was carried out using the same protocol of chapter 3 "3.1.2.2 *VviLBDIf7* dsRNA Design and Synthesis" subsession. PCR fragments were visualized on 1.2 % agarose gel electrophoresis stained with Midori Green Advance (Nippon Genetics, Düren, Germany). Due to the presence of aspecific fragments, PCR target products were gel purified through Wizard SV Gel and PCR Clean-Up System (Promega, Fitchburg, WI) and the PCR fragments were cloned in the pJET1.2 plasmid using the CloneJET PCR cloning kit (Thermo Fisher Scientific, Whaltam, MA), following manufacturer intructions.

The cloning products were used as a template for another PCR following the previous protocol and, afterwards, PCR products were used as templete for another PCR reaction using RNAi primers 5′ attached with T7 RNA polymerase promoter sequences (VviAS1_T7_F and VviAS1_T7_R; VviUFGT_T7_F and VviUFGT_T7_R; Table 4.2.1), as requested by MEGAscript RNAi Kit protocol (Thermo Fisher Scientific). PCR reaction was carried out using 1 μl of amplification product, and following the protocol described in chapter 3 "3.1.2.2 *VviLBDIf7* dsRNA Design and Synthesis" subsession. PCR products were solved on 1.2 % agarose gel electrophoresis stained with Midori Green Advance (Nippon Genetics). Replicates of PCR product were pooled and quantified using Qubit™ 3.0 fluorometer (Thermo Fisher Scientific), using the Qubit™ dsDNA HS Assay Kit (Thermo Fisher Scientific). Template samples were Sanger sequenced

by Macrogen Europe B.V. in two replicates, using RNAiT7 primers. Sequences were aligned to reference sequence using ClustalW (Thompson et al., 1994). The obtained template was used in the dsRNA synthesis reaction using MEGAscript RNAi Kit (Thermo Fisher Scientific), according to the manufacturer's instructions. Synthetized dsRNA was solved on 1% agarose gel electrophoresis stained with Midori Green Advance (Nippon Genetics) and quantified by NanoDrop 1000 Spectrophotometer (Thermo Fisher Scientific).

Table 4.2.1 List of primers used in this work to synthetize the dsRNAs and to evaluete target genes expression. VviUFGT_RNAi3_F and VviUFGT_RNAi3_R, VviAS1_RNAi3_F and VviAS1_RNAi3_R primers were used to amplify the partial sequence of target genes to synthetize the dsRNAs. VviUFGT_T7_F and VviUFGT_T7_R, VviAS1_T7_F and VviAS1_T7_R primers were used to perform MEGAscript RNAi Kit protocol. VviUFGT_Rt_F and VviUFGT_Rt_R, VviAS1_Rt_F and VviAS1_Rt_R primers were used to evaluate the expression of *VviAS1* and *VviUFGT* genes on dsRNA- and water-treated leaves. VviUFGT_RNAi3_R and VviUFGT_Rt_R primers share the same sequence.

Primer ID	Gene	Sequence (5'-3')	Tm	GC%
VviUFGT_RNAi3_F	*VviUFGT*	AAGACCAGAGGGTACGGAAT	57.75	50.00
VviUFGT_RNAi3_R	*VviUFGT*	CAGGTGGTACAAGCAACAGT	58.03	50.00
VviAS1_RNAi3_F	*VviAS1*	CATGTCGCAAGATAAAGGCACTC	60.24	47.83
VviAS1_RNAi3_R	*VviAS1*	CGGAACAGTCAGCCTAGCTG	60.46	60.00
VviUFGT_ T7_F	*VviUFGT*	TAATACGACTCACTATAGGGAGA AAGACCAGAGGGTACGGAAT	77.57	44.19
VviUFGT_ T7_R	*VviUFGT*	TAATACGACTCACTATAGGGAGA CAGGTGGTACAAGCAACAGT	77.15	44.19
VviAS1_ T7_F	*VviAS1*	TAATACGACTCACTATAGGGAGA CATGTCGCAAGATAAAGGCACTC	79.77	43.48
VviAS1_ T7_R	*VviAS1*	TAATACGACTCACTATAGGGAGA CGGAACAGTCAGCCTAGCTG	79.23	48.84
VviUFGT_Rt_F	*VviUFGT*	CTGAGGGAAAATCTGGGAGC	57.95	55.00
VviUFGT_Rt_R	*VviUFGT*	CAGGTGGTACAAGCAACAGT	58.03	50.00
VviAS1_Rt_2_F	*VviAS1*	GCAATGGATATTGACCCTGAGTG	59,43	47,83
VviAS1_Rt_2_R	*VviAS1*	AAAAGCCCTCCTGAGAACCC	59,59	55.00

4.2.2.3 *VviAS1* and *VviUFGT* dsRNA Treatment

Three plants were treated with 200 μg per plant of *VviAS1* dsRNA dissolved in 6 ml of sterilized water, three plants were treated with 200 μg per plant of *VviUFGT* dsRNA dissolved in 6 ml of sterilized water and three were treated with only

sterilized water (6 ml per plant). Treatments were performed with an airbrush on both sides of leaves of a single vine shoot (vines had 10 leaves each) per plant. One sprayed leaf per plant was randomly collected at 3, 5, 7 and 10 days after treatment (dat) (Figure 4.2.1). From each leaf (biological replication), nine 1.5-cm-diameter disks (technical replication) were excised and inoculated with the pathogen. The remaining leaf tissue was frozen in liquid nitrogen and stored at −80°C until gene expression analysis.

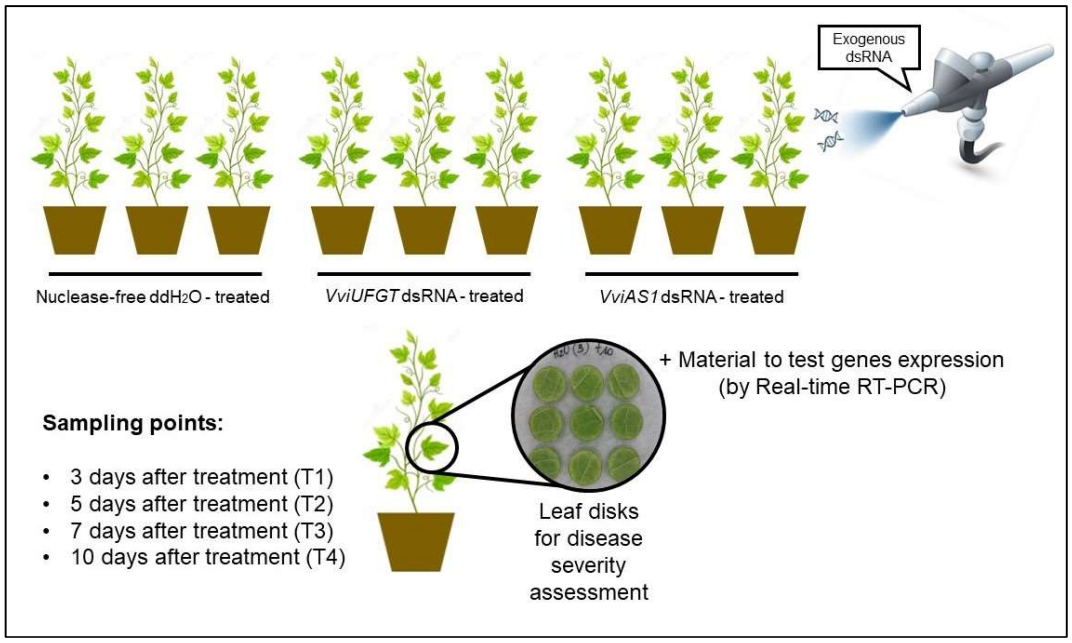

Figure 4.2.1 Scheme of the treatment and sampling carried out in the dsRNA assay experiment.

4.2.2.4 *VviAS1* and *VviUFGT* Gene Expression Analysis on dsRNA- and Water-Treated Leaves

Expression of the candidate S-gene and the control-gene on dsRNA- and water-treated samples was evaluated through RT-qPCR. RNA extraction, RT-qPCR, and comparison of Ct values were carried out following the procedures described in the "Basal expression of *VviLBDIf7* subsection" of chapter 3, with some modifications: (i) to ensure the specific retrotranscription of only functional mRNAs, only oligo(dT) primers were used in RT-PCR; (ii) to avoid the amplification of undesidered cDNA sequences of similar members from the same

gene families of target genes, qPCR primers (VviAS1_Rt_F and VviAS1_Rt_R; VviUFGT_Rt_F and VviUFGT_Rt_R, Table 4.2.1) were specifically designed, using Primer3 Plus software and NCBI Primer-BLAST.

The target genes expression at all the time points was calculated by comparing $2^{-\Delta\Delta Ct}$ (Ct = cycle threshold) values (Livak and Schmittgen, 2001).

4.2.2.5 Inoculation of *P. viticola* on Treated Leaves and Phenotypic Characterization of the Plant–Pathogen Interaction

Experimental inoculation of the leaf discs with the pathogen were carried out by mixing *P. viticola* sporangia coming from Western and Eastern Italian field populations (Maddalena *et al.*, 2020). Nine leaf discs (1.5 cm diameter), sampled at each time point, were placed, lower surface upward, in a Petri dish (9 cm diameter) containing moistened filter paper. Three plates per treatment were prepared. The leaf discs were sprayed a sporangia suspension (5×10^4 sporangia ml^{-1}) obtained by collecting sporangia in sterile distilled water, and incubated in a growth chamber at 22°C with a 16:8 h photoperiod.

Disease incidence was evaluated as Infection Frequency Rate (IFR), the proportion of the inoculated discs exhibiting sporulation over the total inoculated discs (where 0 = disc not sporulated; 1 = disc sporulated) (Bove *et al.*, 2019). Disease severity was evaluated as the percentage of leaf disk area covered by sporulation (PSA) (Toffolatti *et al.*, 2012).

4.2.2.6 Statistical Analysis

All the statistical analyses were performed using R (R core team, 2019) in R studio 9.1 (R team, 2020).

For gene expression, the $2^{-\Delta\Delta Ct}$ values were subjected to Levene's test to assess homogeneity of variance in R software. LSD (least significant difference) test was performed in R to evaluate differences among dsRNA- and water-treated leaves in *VviAS1* and *VviUFGT* gene expression values.

For *P. viticola* infection data, the binary outcome provided by disease incidence was investigated by fitting a binary logistic regression via glm() function in R .

$$g(y)=\beta 0 + \beta iXi$$

with β = intercept, β0 = the model's intercept; i = (ith treatment; H_2O; *VviUFGT* dsRNA; *VviAS1* dsRNA); g(•) = logit as the link function. To assess the difference in probabilities at the response level (IFR) EMMs were employed. Pairwise comparisons among EMMs were calculated through the pairs() function in the emmeans package (Lenth et al., 2020).

PSA values were assumed to be a sample from beta distribution; PSA values were expressed as proportions (x) and transformed to include extreme values (0 and 1) as y = (x * (n − 1) + 0.5)/n, with n = sample size (Smithson and Verkuilen, 2006). Then, a multiple beta-regression model (BRM) was fitted on proportion responses using betareg() (Cribari-Neto et al., 2010):

$$g(y)=\beta 0 + \beta iXi$$

with β = intercept, β0 = the model's intercept; i = (ith treatment; ith treatment; H_2O; *VviUFGT* dsRNA; *VviAS1* dsRNA); g(•) = logit as the link function; and a constant ϕ (precision parameter). The Xi parameter is represented by a categorical factor; for this reason, to compare among different estimated marginal means (EMMs) were retrieved from the fitted model over the Xi variable via emmeans(). The overall effect of independent variables was tested by the ANOVA-like type III test performed through a joint_test(). In addition, pairwise comparisons among estimated EMMs were calculated through the pairs() function in the emmeans package (Lenth et al., 2020).

4.2.3 Results

4.2.3.1 dsRNA Treatment Increases *VvAS1* and *VvUFGT* Gene Expression

A dsRNA 443-bp was synthetized on the *VviAS1* candidate S-gene sequence, and a 429-bp long dsRNA was synthetized on the *VviUFGT* control gene sequence. The synthetized dsRNAs were applied in the transient RNAi experiment (Figure 4.2.1).

Pinot noir plants grafted onto SO4 were treated with the dsRNAs and the knock-down of the target genes was assessed at 3, 5, 7, and 10 after dsRNA treatment (dat). A statistically significant increase in the expression of both *VviAS1* and *VviUFGT* expression was observed between dsRNA- and water-treated leaves at all timepoints (Figure 4.2.2A, B). *VviAS1* expression highest increase was observed at 5 dat, with the gene showing a statistically significant over-expression in dsRNA-treated samples equal to 30 thousand times the value of the control conditions (Figure 4.2.2A). The over-expression of the gene decreased gradually in the following timepoints (Figure 4.2.2A).

VviUFGT highest expression value was observed at 3 dat, in dsRNA-treated samples, showing an 800-fold change increase in the gene expression compared to control conditions. As for the case of *VviAS1*, the over-expression of the gene decreased over time (Figure 4.2.2B).

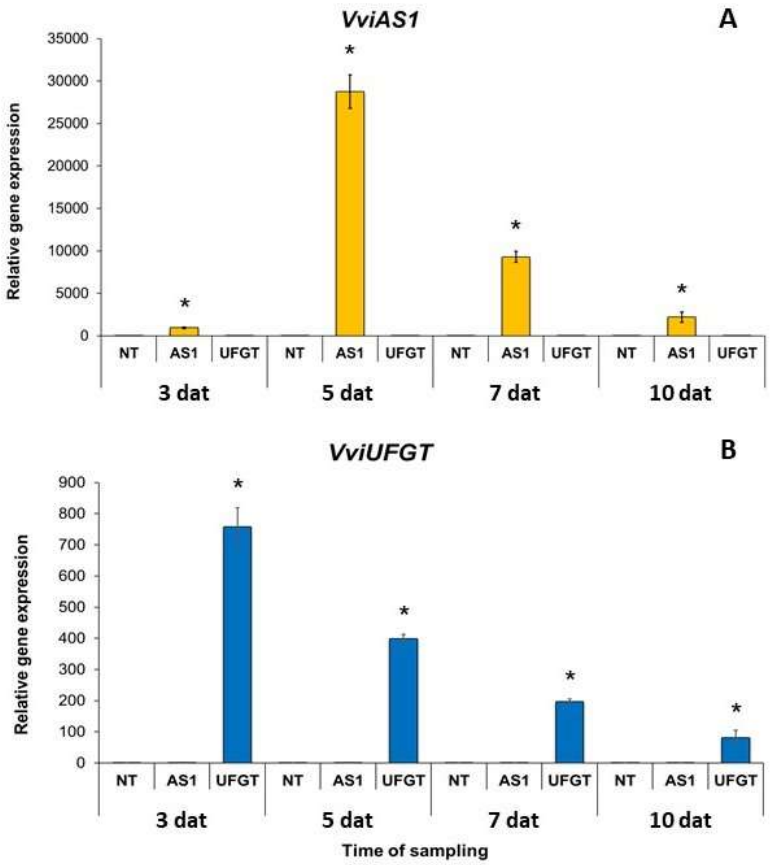

Figure 4.2.2 Effect of dsRNA treatment on *VviAS1* (**A**) and *VviUFGT* (**B**) gene expression. The genes expression analysis was determined based on the $2^{-\Delta\Delta Ct}$ method at 3, 5, 7, and 10 days after treatment (dat) on Pinot noir plants leaves. Bars represent standard errors. Asterisks indicate statistically significant differences among the dsRNA- and water-treated conditions at each time point (*p-value = 0.05).

4.2.3.2 dsRNA Treatment at 3 Days After Treatment Reduces Pathogen Infection and Sporulation

DsRNA- and water-treated leaf tissues were experimentally inoculated with *P. viticola* to investigate whether the dsRNA treatment induced changes in the downy mildew disease extent. Inoculated leaf tissues were used to evaluate phenotypic traits such as disease severity, estimated through PSA and sporangia production. Phenotyping was carried out at 3 dat, because inoculation was unsuccessful in the other timepoints (Figure 4.2.4).

PSA values of water-treated samples ranged from accounted to 2.70 ± 1.74% (Figure 4.2.3A, Table 4.2.2). A significant difference was found among PSA values of dsRNA- and water-treated samples inoculated at 3 dat, where *VviAS1* dsRNA treated samples showed a decreased value equal to 0.37 ± 0.59 %, and *VviUFGT* dsRNA-treated samples 1.16 ± 1.36 (Table 4.2.2). Although some differences were observed between PSA values of *VviAS1* and *VviUFGT* dsRNA-treated samples, they were found to be not statistically significant (Table 4.2.2, Figure 4.2.4).

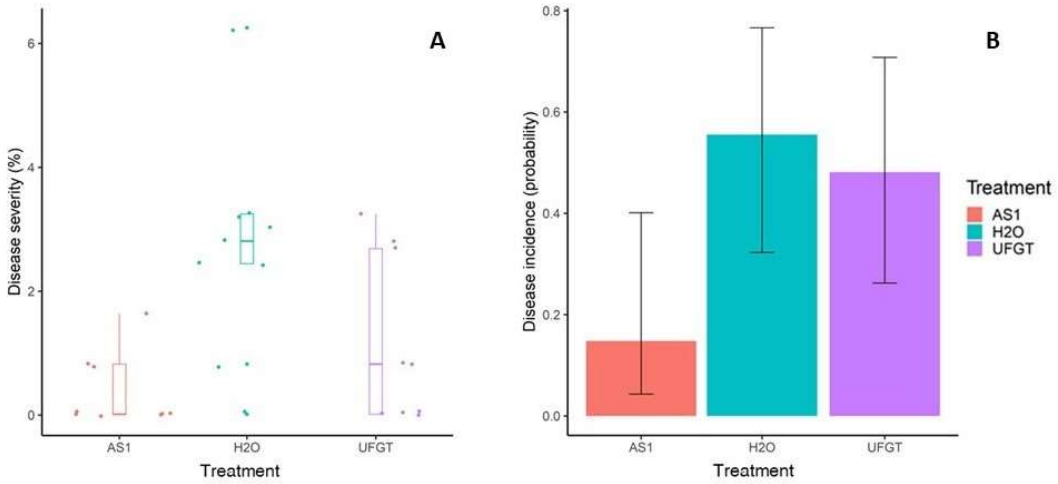

Figura 4.2.3 Effect of dsRNA treatment on percentage of sporulating area (PSA) and infection frequency rate (IFR) of leaf disks replicates evaluated 7 days after *P. viticola* inoculation. PSA evaluated on Pinot noir plants grafted onto SO4 at 3 days after treatment (dat) (**A**), and disease incidence evaluated on Pinot noir plants grafted onto SO4 at 3 days after treatment (dat) (**B**). Bars represent standard deviation.

Table 4.2.2 Disease severity assessment of leaf disks as percentage of sporulating area (PSA) in samples treated with dsRNA *vs* control treatment (H_2O). Disks were evaluated on samples collected at 3 days after treatment, 7 days after *P. viticola* inoculation. Letters indicate ANOVA like test (F = 3.85; df = 3; *p*-value = 0.0091) results.

Treatment	Severity (%) ± SD	EMM (95%) CI
H2O	2.70 ± 1.74	2.41 (0.82-4) a
VviUFGT dsRNA	1.16 ± 1.36	0.9 (0.10-1.69) bc
VviAS1 dsRNA	0.37 ± 0.59	0.61 (0.03-1.18) c

As expected, disease incidence followed the same trend of PSA analysis results (Figure 4.2.3B, Figure 4.2.4), with water-treated samples showing 55.56% of IFR, against a significantly lower value 14.8 % in *VviAS1* dsRNA-treated samples and 48.1 of *VviUFGT* dsRNA-treated samples (Table 4.2.3). In this case, only the IFR values differences between water-treated and *VviAS1* dsRNA-treated samples were found to be statistically significant (Table 4.2.3, Figure 4.2.4).

Table 4.2.3 Disease incidence evaluated as Infection Frequency Rate (IFR) of leaf disks treated with dsRNA *vs* control treatment (H_2O). IFR rapresents the proportion of the inoculated discs exhibiting sporulation over the total of discs replicates inoculated with *P. viticola*. Disks were evaluated on samples collected at 3 days after treatment, 7 days after *P. viticola* inoculation. Letters indicate ANOVA like test (F = 3.85; df = 3; *p*-value = 0.0091) results.

Treatment	N of infected disks/total (27)	IFR (%)	EMM (95% CI)
H_2O	15	55.56	55.6 (32.27-76.60) b
VviUFGT dsRNA	13	48.15	48.1 (26.24-70.80) ab
VviAS1 dsRNA	4	14.81	14.8 (4.32-40.1) a

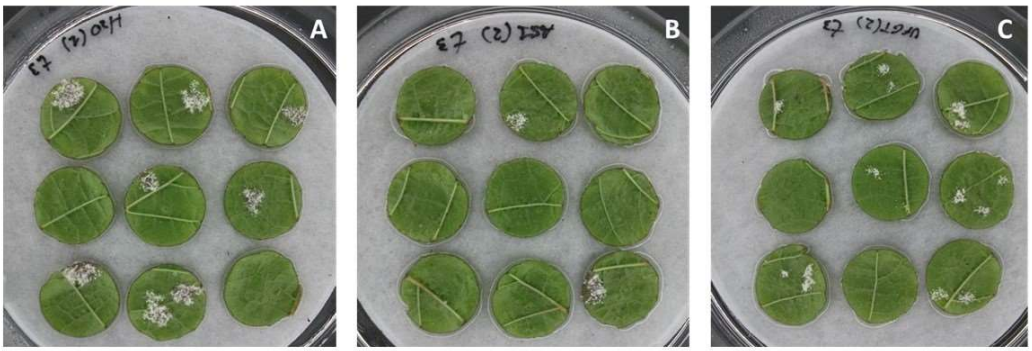

Figura 4.2.4 Pinot noir leaves disks sampled at 3 days after treatment, 7 days after inoculation with *P. viticola*. Disks of leaves treated with water (**A**), candidate gene of susceptibility to *P. viticola VviAS1* dsRNA (**B**) and internal control gene *VviUFGT* dsRNA (**C**).

4.2.4 Discussion

4.2.4.1 Exogenous dsRNA strongly increased expression *VviAS1 and VviUFGT* genes

Susceptibility genes (S-genes), are plant genes exploited by pathogens to support a compatible plant-pathogen interaction and succeed with the infection (Van Schie and Takken, 2014). Therefore, the silencing of S-genes disrupts the advantage the pathogen has in the establishment of the infection, potentially causing pathogen-specific resistance (Pavan *et al.*, 2010; Thatcher *et al.*, 2012). In this work, dsRNA exogenous application by high-pressure spraying has been used to silence *VviAS1,* the candidate gene of susceptibility to downy mildew, and the internal control gene *VviUFGT*. This approach has already been successfully applied to target essential interaction genes in plants (S-genes) or to control plant pathogens and pests by gene silencing induction (Zaidi, Mukhtar and Mansoor, 2018; Dubrovina and Kiselev, 2019; Dalakouras *et al.*, 2020). In the chapter 3 of this thesis, this approach was used to perform the knock-down of *VviLBDIF7*, another candidate gene of susceptibility to downy mildew (Marcianò *et al.*, 2021). Nevertheless, contrary to the previous work, this experiment exhibited some issues.

In this work, the foliar application of *VviAS1* and *VviUFGT* dsRNAs led to a strong over-expression of the target genes. This result could be a consequence of different hypothesis or a combination of them. Assuming that the genes expressions were truthfully assessed, one possible explanation is based mainly on the experimental design. In the experiment, for the leaves sampling after the treatment, the timing of the previous experiment on *VviLBDIf7* (Chapter 3) was followed, however, in this experiment twice the concentration of dsRNA was used to treat the plants (200 ug/plant instead of 100 ug/plant in the former). This could have led to a faster down-regulation of the genes expression that we were not able to capture, due to the samplings starting only 3 days after treatment. All the main studies reported in literature are based on the same quantity of dsRNA application, and not many information regarding change in dsRNA dosage in relation to the speed of the RNAi machinery activation are available (Dubrovina

and Kiselev, 2019; Nerva *et al.*, 2020). To cover this possible occurrence, in future experiments featuring this dsRNA concentration (200 ug/plant), a timepoint at 1 day after treatment need to be added.

The second possible explanation is related to the first and could rely on role of these genes in the plant metabolism. *VviAS1* and *VviUFGT* are both genes part of the core metabolism of plants (Offen *et al.*, 2006; Gaufichon *et al.*, 2010). Assuming that the first hypothesis is true, what is observed could be the over-expression of these genes by the plant as an attempt to recover from their abrupt silencing, because of to their fundamental role in metabolism. Similarly, considering the first hypothesis false, a failed silencing could have occurred, due to some sort of fight response by the plant, perceiving the dsRNA application as a threat against the fundamental genes that were instead over-expressed as a preventive measure. Another possibility related to the second hypothesis, could be in the quantity of dsRNA itself. It could be possible that high quantity of dsRNA could be perceived by the plant as some sort of attack and thus some preventive measures are activated to avoid the exploitation of the RNA interference machinery.

Finally, related to the third explanation, the last possible one could be the more extreme one. Considering the phenotypic data in which we observed significant changes among *VviAS1* dsRNA-treated and water-treated samples, it could be possible that no down-regulation of the target genes occurred (Ebbesen *et al.*, 2008; Ambesajir *et al.*, 2012). Instead, the over-expression of the target genes was the result of the treatment. As a consequence, the cause of the decreased infection rate in dsRNA-treated samples is *VviAS1* over-expression. No certain information is available in literature, where cases of over-expression of certain *AS* genes causing a decrease of viral and microbial pathogens infections are reported (Hwang, An and Hwang, 2011; Liu *et al.*, 2022), together with experiments showing other *AS* genes down-regulation leading to the same results in fungal diseases (Seifi *et al.*, 2014).

On top of the previous hypothesis, it is necessary to consider the scenario in which, because of technical reasons, genes expression might have been not correctly assessed. In this work, gene expression was evaluated by real-time

RT-PCR, where primers specific for target genes were employed (Table 4.2.1). However, there is the possibility that due to limitation of this technique, it wasn't possible to assess the real expression of the genes. It could be possible that among the cDNA captured by the primers, there were some fragments synthtized from RNAi-processed target genes. These fragments could have been picked up by the primers, even if they represented only partial (and thus non-functional) mRNAs sequences. Moreover, the primer design was really complicated due to the presence of strong similarities in the sequences of the target genes with other members of gene families. As a consequence, it could be possible that it was measured the expression of more members of the same gene family. To exclude this possibility, another approach of gene expression evaluation will be applied for the future replicate of this experiment. As an alternative, different methods of primers design (Sharbati-Tehrani *et al.*, 2008; Wan, Lim and Too, 2010; Czimmerer *et al.*, 2013) and RNA-sequencing of the degradome can be employed to correctly assess target genes expression (Ma *et al.*, 2020).

4.2.4.2 *VviAS1* dsRNA treated samples show a reduced susceptibility to *P. viticola*

The phenotype assessment of this work was carried out only at 3 dat. This was because of the unsuccessful inoculation at the other timepoints. Some possible causes of the failure could lay in laboratory equipment issues that negatively impacted the inoculum growth.

Independently from inoculum quality, at 3 dat a significant reduction of both PSA and IFR were shown between the samples treated with *VviAS1* dsRNA and water. As discussed in the previous section, it will be interesting to understand what is the cause of these differences, whether it will be because of overexpression or down-regulation of the gene. This could reveal if an effective candidate gene of susceptibility to downy mildew is being discussed or, unexpectedly, a resistance one. However, at the moment, due to the unreliability of gene expression data, no conclusion on the origin of these differences can be drawn.

Interesting, although some differences were observed between *VviAS1* and *VviUFGT* dsRNA treated samples, no statistically significant ones were found. However, this could be due to the quality of the inoculum itself, that could have caused some issues in the reliable assessment of the existing differences.

4.2.5 Conclusions

Gene silencing via dsRNA is a molecular mechanism used to regulate gene expression by suppressing the activity of specific genes, with applications ranging from functional genomics to plant defence. In this work, due to different technical issues occurred during this work, no definitive conclusion could be drawn on the function of candidate gene of suscpetibility to *P. viticola VviAS1*. We were able to successfully prove the specificity of dsRNA treatment using the control gene *VviUFGT*, however we weren't able to determine the effective down-regulation of the target genes. Moreover, the inoculation failure did not allow us to perform an effective and reliable evaluation of the downy mildew infection. In the near future, the experiment will be repeated according to the adjustments that this work allowed us to discover. Their discovery was fundamental for the set-up of a comprehensive and efficient dsRNA assay, to validate new candidate genes of susceptibility to downy mildew.

Chapter 5: Identification of powdery mildew and downy mildew resistance loci in Caucasian germplasm

5.1 Introduction

Vitis vinifera L., the European grapevine, is a widely cultivated species native to the Eurasian region (Olmo et al., 1995). As of 2020, it was estimated that approximately 7.3 million hectares of arable land around the World were dedicated to grapevine cultivation, yielding a production of around 77.8 million tons of grapes. Only in Europe, the hectares are more than 3 million, with a production of around 27 million tons. Its production is mainly used for winemaking purposes (more than 50%), while less then 40% is reserved for consumption as table grapes, and less than 10% is used in producing raisins (https://www.oiv.int/public/medias/7909/oiv-state-of-the-world-vitivinicultural-sector-in-2020.pdf; https://www.fao.org/faostat/en/#data).

Grapevine is susceptible to many diseases, including downy mildew (DM), powdery mildew (PM) and grapevine trunk diseases, which can cause significant economic losses in grapevine cultivation (Rienth *et al.*, 2021). The most devastating ones are DM and PM, caused by *Plasmopara viticola* (Berk. e Curt.) Berl. e De Toni and *Erysiphe necator Schw.*, respectively (Armijo *et al.*, 2016). *P. viticola* causes significant damage to grapevines by infecting leaves, shoots, and green berries. Symptom disease are yellow spots on the leaves and stunted growth, causing reduced fruit quality and yield (Gessler, Pertot and Perazzolli, 2011). *E. necator* infects leaves, stems, flowers and berries of the grapevine, leading to a white powdery growth on the surface of the infected organs. The disease can affect grapevine growth and development, reducing yields and quality of grapes (Gadoury *et al.*, 2012). Management of DM and PM relies on the use of fungicides, due to the ineffectiveness of agronomical practices, although the use of resistance genotypes is a more sustainable approach (Merdinoglu *et al.*, 2018). Indeed, the European Union (EU) has issued several directives aimed at reducing the use of agrochemicals in agricultural practices, including the Directive 2009/128/EC on the Sustainable Use of Pesticides. The

directive sets out principles for the sustainable use of pesticides, such as the reduction of risks and impacts on human health and the environment, the promotion of integrated pest management practices, and the encouragement of the use of alternative approaches to pesticides.

Breeding of grapevine varieties with genetic resistance to diseases is a sustainable approach to reduce the use of agrochemicals. The identification of genetic loci associated with disease resistance, such as those associated with DM and PM resistance, has facilitated the development of new grapevine varieties with improved disease resistance, such as the PIWI varieties bred by some institutions in European Countries, such as Germany, France, Austria and Italy (https://www.internationalwinechallenge. com/Canopy-Articles/piwis-the-most-promising-varieties.html). The loci associated with the DM resistance (*Rpv*) are 35 (Merdinoglu et al., 2003; Fischer et al., 2004; Wiedemann-Merdinoglu et al., 2006; Welter et al., 2007; Bellin et al., 2009; Marguerit et al., 2009; Blasi et al., 2011; Moreira et al., 2011; Schwander et al., 2012; Venuti et al., 2013; Ochssner et al., 2016; Divilov et al., 2018; Sapkota et al., 2019; Lin et al., 2019; Sargolzaei et al., 2020; Fu et al., 2020; Bhattarai et al., 2021; Pap et al., in preparation; Malagol et al., in preparation; Zou et al., 2023). Most of them originate from North American and Asian wild Vitis species, only three (*Rpv29-31*) originate from *vinifera* germplasm, coming from Caucasus (Sargolzaei et al., 2020). While, the loci associated with the PM resistance (*Ren* and *Run*) are 15 (Dalbó et al., 2001; Adam-Blondon et al., 2004; Barker et al., 2005; Welter et al., 2007; Hoffmann et al., 2008; Riaz et al., 2011; Blanc et al., 2012; Feechan et al., 2013; Zyprian et al., 2016; Pap et al., 2016; Teh et al., 2017; Zendler et al., 2017; Karn et al., 2021; Possamai et al., 2021; Cadle-Davidson et al., in preparation), originate from North American and Asian wild *Vitis* species. All those loci have been identified via QTL (Quantitative Trait Loci) analysis, a powerful method used in genetics to identify regions of the genome that are associated with variation in quantitative traits (Kearsey and Farquhar, 1998). The loci lie in regions where there are genes encoding putative nucleotide-binding leucine-rich repeat (NBS-LRR) proteins, such as *Rpv1*, *Rpv3* and *Run1* (Merdinoglu et al., 2003; Bellin et al., 2009; Feechan et al., 2013).

GWAS (Genome-Wide Association Studies) is a powerful method used to identify genetic variations that contribute to complex traits or diseases in various organisms. This method involves analyzing large numbers of genetic variants (usually Single Nucleotide Polymorphism, SNP) across the genome of individuals with and without the target trait. The method is able to identify genetic variants that are more common in individuals holding the target trait (Korte and Farlow, 2013). GWAS has been successfully used to identify genetic variants associated with many plant complex traits, such as yield, abiotic stress tolerance and disease resistance (Sakiroglu and Brummer, 2017; Kim and Reinke, 2019; Abdelraheem et al., 2021). GWAS turned out to be a valuable tool for understanding the genetic basis of complex traits and diseases and for developing strategies to improve crop breeding. It has been successfully used in grapevine research to identify genetic markers associated with important traits, such as fruit quality (Laucou et al., 2018; Guo et al., 2019; Flutre et al., 2022), disease resistance (Zhang et al., 2017; Sargolzaei et al., 2020) and abiotic stress tolerance (Trenti et al., 2021).

Although European grapevine germplasm has been considered susceptible to DM and PM, some researches have disproved the fact. Indeed, DM resistance genotypes have been identified in the germplasm of Caucasus, one of the two grapevine domestication centers (Dong et al., 2023), such as Mgaloblishvili and other genotypes (Bitsadze et al., 2015; Toffolatti et al., 2016, 2018). Likewise, Caucasian germplasm can boast genotypes resistant to PM, such as Kishmish vatkana, Shavtsitska and Tskhvedianis tetra (Hoffmann et al., 2008; Possamai et al., 2021). These data make this germplasm a valuable genetic resource to breed disease-resistant grapevine varieties.

The aim of this work was to identify new loci associated with the resistance to *P. viticola* and *E. necator* in *V. vinifera* germplasm, through a GWA approach. The genotypes (88), coming from wild and cultivated compartments of Caucasus, Iran and Uzbekistan, were: i) genotyped with 13 SSR (Simple Sequence Repeat) loci for cultivar identification; ii) genotyped with six SSR loci associated with the resistance to DM and PM; iii) genotyped with the *Vitis*18kSNP genotyping chip array and phenotyped for the resistance to DM and PM to perform GWAS.

5.2 Material and methods

5.2.1 Plant material and DNA extraction

The grapevine accessions analyzed in this study accounted for 88 genotypes, wild (*V. vinifera* subsp. *sylvestris*) and cultivated (*V. vinifera* subsp. *sativa*), coming from Armenia, Azerbaijan, Georgia, Iran and Uzbekistan (Table S5.1), grown in pot (20 cm diamiter) at the University of Milan screenhouse, located in Tavazzano con Villavesco (Lodi, Italy).

Young leaves were collected from each accession, sampled into 2 ml tubes and lyophilized. DNA was purified using DNeasy Plant Mini Kit (Qiagen, Hilden, Germany), following manufacturer's instructions. DNA was quantified and quality checked with the NanoDrop™ One/One spectrofotomer (ThermoFisher Scientific, Waltham, Massachusetts, USA).

5.2.2 SSR genotyping

Genotyping of all accessions was performed with 13 SSR markers, encompassing the nine internationally adopted (VVS2, VVMD5, VVMD7, VVMD25, VVMD27, VVMD28, VVDM32, VrZAG62, VrZAG79; Maul et al., 2012), plus additional four (ISV2, ISV3, ISV4 and VMCNG4b9; Crespan, 2003; Welter et al., 2007). Two multiplex PCRs combining 7 and 4 SSR loci (VVS2, VVMD7, VVMD28, VrZAG79, ISV2, ISV4 and VMC4B9; VVMD25, VVMD27, VVMD32 and VrZAG62) and one single PCR (for VVMD5 locus) were performed, in 10 µL final volume, as follow: MyTaq (Bioline Reagents LTD, London, United Kingdom), primers (from 14 to 50 nM, depending by the primer), DNA (10 ng). Amplification conditions were: denaturation at 95° C for 3 min; followed by 35 cycles of 95° C for 30 sec, 57° C for 30 sec, 72° C for 30 sec; final elongation step 10° C ∞. 0.5 µL of PCR products were mixed with Genescan-500(LIZ) (Life Technologies, Foster City, CA, USA) as internal size standard and HI-DI formamide (Life Technologies), denatured and separated by capillary electrophoresis using an ABI 3130xl genetic analyzer (Life Technologies). Allele

calling was performed with GeneMapper 4 (Life Technologies) software and a home-made bin-set built with reference varieties.

5.2.3 Genotyping for loci associated with resistance to downy and powdery mildew

All accessions were genotyped using SSR markers associated with known *Ren1*, *Rpv1-Run1* and *Ren3-Ren9* resistance loci to DM and PM (Possamai et al., 2021). Three multiplex PCR combining pairs of SSRs linked to resistance loci were performed. PCR mix and amplification conditions were as for sample identification. Primer quantity varied from 7 to 14 nM (depending by the primer). Capillary electrophoresis has been performed as reported above. Allele calling was performed after building a bin-set with the reference varieties Artaban, Floreal, Vidoc, Voltis and Kishmish vatkana grown at VCR repository (Rauscedo, Pordenone, Italy), and Regent from CREA-VE collection in Susegana (Treviso, Italy).

5.2.4 Disease resistance evaluation

5.2.4.1 Downy mildew

Resistance to *P. viticola* has been investigated following the protocol reported in Sargolazaei et al., 2020. Briefly, naturally infected grapevine leaves of plants were collected from vineyard plots not treated with fungicides acting against the downy mildew agent located in Santa Maria della Versa (Pavia, Italy; North-Eastern Italian *P. viticola* population) and Casarsa della Delizia (Pordenone, Italy; North-Western Italian *P. viticola* population) (Maddalena et al., 2020). Sporangia were collected from the infected leaves and resuspended in distilled, sterile water to reach a $5x10^4$ sporangia/mL concentration. Three technical replicates constituted by leaf discs (1.5 cm in diameter), cut from three different leaves (biological replicates) collected from the 3rd–5th leaf starting from the shoot apex of the plants, were sprayed with 1 mL of sporangia suspension by using an airbrush. The leaf discs, placed in Petri dishes (9 cm diameter) containing

moistened filter paper and incubated at 22 °C for 10 days, were then scored for the area covered by sporulation by using the OIV 452 resistance scoring method (OIV, 2009). Each leaf disc was attribute with the following classes: 1, when all leaf disc surface was covered by sporulation; 3, when most leaf disc surface was covered by sporulation; 5, when sporulation was limited to less than a half of the leaf disc surface; 7, when very few sporulating spots were visible; 9, when no sporulation was visible (Bove et al., 2019).

5.2.4.2 Powdery mildew

Resistance to the powdery mildew agent, *E. necator*, was evaluated by experimentally inoculating leaves on potted plants. Three leaves, starting from the third fully expanded leaf, from three replicate shoots per genotype were inoculated with *E. necator* conidia by gently touching an infected leaf onto the target leaf (Fung et al., 2008). Infected leaves were collected from naturally infected plants grown in the same location, outside from the screenhouse. The inoculum used represents a mixed strain population of *E. necator* (Welter et al., 2017). The leaves were scored for resistance by using the OIV 455 scoring method (OIV, 2009), by attributing the following classes: 1 where leaves and other tissue types were covered with unlimited patches of powdery mildew infection; 3 to vast numbers of powdery mildew infection spots and abundant mycelium growth; ; 5 patches of infection that were bigger than 5 cm in diameter; 7 when limited patches of powdery mildew infection (< 2 cm) were visible; 9 when no disease symptoms or a tiny spot was visible (Riaz et al., 2011). An average OIV score was calculated for each accession.

5.2.4.3 Phenotype classification

Phenotyping was carried out for three years and only accessions with at least two years of data were considered for genotyping. The score “0” was attributed to susceptible accessions (OIV<7) and “1” to resistant accessions (OIV≥7).

5.2.5 SNP genotyping

The 88 samples were genotyped using the Vitis18kSNP genotyping array (Illumina Inc., San Diego, CA, United States), holding 18,071 SNPs. Hybridization was carried out on 200 ng of genomic DNA at the laboratory of Fondazione Edmund Much (San Michele all'Adige, Trento, Italy). SNP data were filtered following these parameters, as reported in De Lorenzis (2015): i) samples showing a call quality value (p50GC) lower than 0.54 to be removed; ii) loci with a GenTrain (GT) score value lower than 0.6 to be removed; iii) samples with a marker missing rate > 20% to be removed; iv) loci with a minor allele frequency (MAF) < 5% to be removed.

5.2.6 GWA analysis

poppr package (Kamvar et al., 2014) for R software (R Core Team, 2021) was used to build a circular UPGMA (Unweighted Pair Group Method with Arithmetic Mean) phylogenetic tree, based on the Nei's coefficient distance matrix. Principal Component Analysis (PCA) was performed in R using adegenet package (Jombart, 2008). The values of first two components were plotted on a 2-D scatterplot. LEA package (Frichot and François, 2015) was used to perform structure analysis, varying the number of ancestral genetic groups (K) from 1 to 10. For each K value, ten repetition runs were performed. LEA cross-validation method was used to determine the most likely K value. The LD (linkage disequilibrium) estimation was evaluated by PLINK software (Purcell et al., 2007) using the following setting: --ld-window-r2 0, --ld-window 99999, --ld-window-kb 10000. The distances between loci were categorized into intervals of a fixed length (100 kb) and, for each interval, average r^2 (Pearson's squared correlation coefficient) was calculated. R was used to plot the average r^2 values. LD decay was defined identifying the distance at which half of the maximum LD ($LD_{½,90}$) has decayed (Vos et al., 2017).

GAPIT package (Wang and Zhang, 2021) for R was used to perform GWAS. The following algorithms were run: i) BLINK (Bayesian-information and Linkage-

disequilibrium Iteratively Nested Keyway); ii) FarmCPU (Fixed and random model Circulating Probability Unification); iii) GLM (General Linear Model); iv) MLM (Mixed Linear Model). The first two PCs were estimated by GAPIT to assess the population structure and control the false marker-trait association. The *p*-value of each SNP was calculated, and only SNPs showing $-\log_{10}(p)$ values higher than Bonferroni's threshold were considered significantly associated with the resistance. The GWA algorithm performances were evaluated through quantile-quantile (QQ) plots.

Significant SNP loci were identified on both grapevine PN40024 v4 reference genome (Velt *et al.*, 2023) and Mgaloblishvili genome (Chapter 2; Toffolatti et al., 2018). To do that, the SNP probes identifying the signals were mapped against both genomes using BLASTn-short (Altschul *et al.*, 1990). The annotated genes, in linkage regions with the SNP probe location, were identified as the putative candidate genes likely involved in disease resistance. To avoid possible annotations mistakes, the genes of each locus in the reference genome were mapped against Mgaloblishvili genome haplotypes and *viceversa* using GMAP (Wu et al., 2005).

5.3 Results

5.3.1 Varietal identification and screening for resistance loci

DNA analysis with the set of 13 SSR markers revealed 88 unique molecular profiles (Table S5.1). After comparing these profiles with the ones reported in the *Vitis* International Variety Catalogue molecular database, 54 profiles were identified as new. Some accessions showed to be triallelic, like Absheron Gelinbarmaghy B. (G4) at VVMD5 locus. Some genotypes showed a peculiarity at the VVMD28 locus: the combination of the allele pair 236 and 238 with a third allele profiles (Table S5.1).

Regarding the presence of already known sources of resistance to DM and PM, no positive results were obtained for *Rpv1-Run1* and *Ren3-Ren9* loci. For *Ren1* locus, the allelic combination associated with the resistance identified in

Kishmish vatkana was found in two genotypes, Tchumuta and Nakhiduri 04, while the one identified in Shavtsitska and in Tskhvedianis tetra was detected in 14 genotypes (Aladasturi, Alexandrouli, Atcharuli tetri, Barisakho turning 01, Chachkhriala – 01, Chkhaveri, Dzvelshavi, Kakhet, Khupishij, Kvelouri, Samebis seri 02, Seura, Skra 01, Tushis tbebi 02, six of them are wild genotypes). Interestingly, in the Georgian *sylvestris* Barisakho turning 01, the resistance could be in a homozygous state, unless for the presence of null allele profile (Table S5.1).

5.3.2 SNP genetic diversity

SNP profiles obtained by the hybridization of DNA with the Vitis18kSNP genotyping array after filtering accounted for 13,213 loci (Table S5.2). The filtered profiles were used to assess the genetic diversity of plant material, performing clustering analysis, PCA and structure analysis. Cluster analysis clearly discriminated between wild and cultivated samples (Figure 5.1A). Only four genotypes labelled as wild samples were clustered together with cultivated ones. Similarly, PCA discriminated between wild and cultivated samples, with some wild genotypes grouped together with cultivated ones (Figure 5.1B). The two compartments were mainly discriminated along the first principal component (PC1), accounting for 8% of genetic variability. While, the PC2, accounting for the 6% of genetic variability, discriminated among the cultivated genotypes. According to the cross-validation plot, structure analysis identified K = 3, as the most likely number of ancestral populations, two for cultivated individuals (groups 1 and 2) and one for wild ones (Figure 5.1C). The percentage of admixed genotypes (with a membership probability < 80%) was 50% (Table S5.4). The 51% of cultivated genotypes were admixed, while the wild admixed accessions accounted for around 53%. As expected, LD decreased with the increase in physical distance between marker loci (Figure 5.1D). $LD_{½,90}$ ($r^2 = 0.05$) value was observed at around 0.9 Mb.

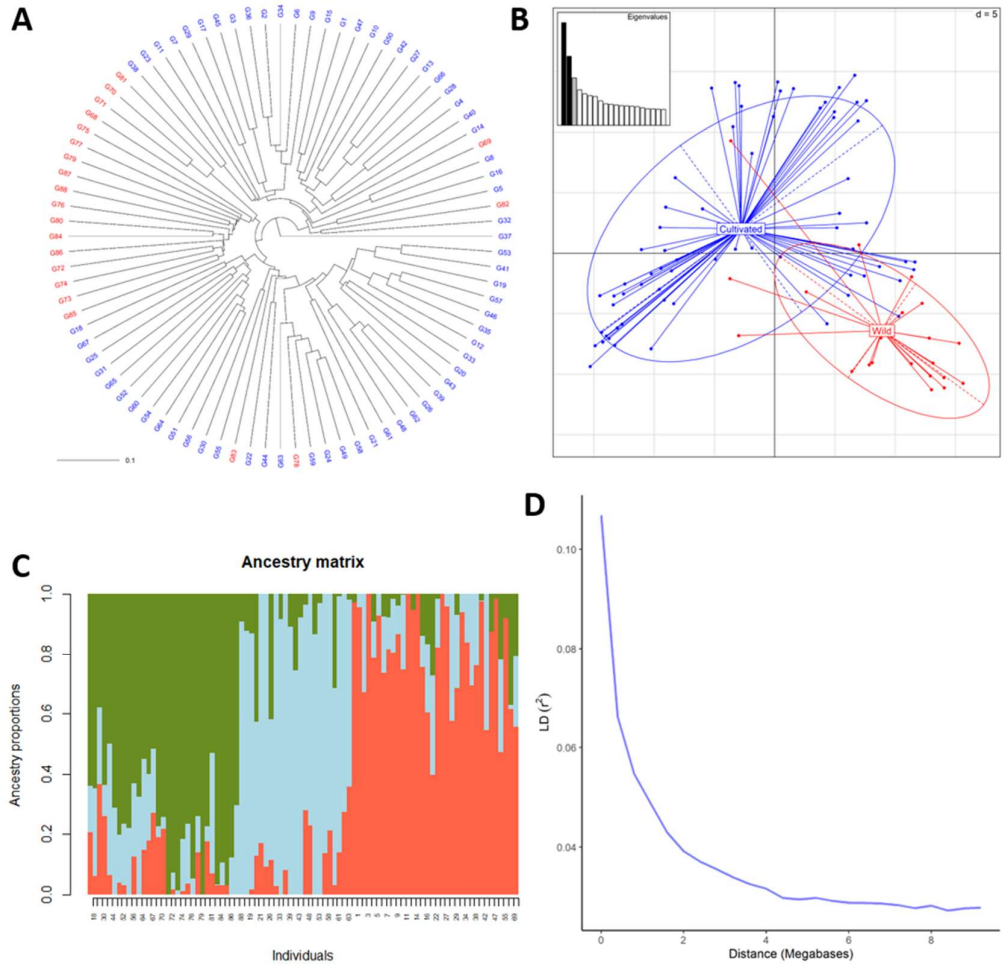

Figure 5.1 Genetic diversity of 88 cultivated and wild grapevine accessions, coming from Caucasus, Iran and Uzbekistan, genotyped using the *Vitis*18kSNP array. (**A**) UPGMA dendrogram showing relationships among cultivated (blue) and wild (red) individuals. (**B**) Scatterplot relationships among cultivated (blue) and wild (red) individuals, as represented by the first two principal components (PC1 along the horizontal axis, PC2 along the vertical axis) of PCA. (**C**) Admixture proportions as estimated by LEA package at K = 3, displayed in a barplot. Each sample is represented as a vertical bar, reflecting assignment probabilities to each of the three groups. (**D**) Decay of average linkage disequilibrium (LD r^2) over distance (Mb).

5.3.3 Phenotypic diversity

Phenotypic data allowed us to identify DM and PM resistant varieties among the analysed population. In the end, seven DM (OIV score ≥ 7) and twenty-five PM resistant varieties (OIV score ≥ 7) were identified (Table S5.4).

5.3.4 Loci associated with DM and PM resistance

Four different statistical models (BLINK, FarmCPU, MLM and GLM) were tested to detect the loci associated with DM e PM resistance. Because PCA was able to capture the differences among the genotypes better than structure analysis, the values of the first two PCs have been used as covariate in the GWA analysis. All the four GWAS models allowed to identify at least one significant SNP locus associated with DM resistance, showing $-\log_{10}(p)$ values higher than Bonferroni's threshold. All the significant SNP loci were at least detected by two models. BLINK and FarmCPU identified one locus each, while GLM and MLM models identified two loci each. These loci are: i) mu_s_G_A_chr15_11771804 SNP located in the chromosome 15 at position 11,771,804, identified by BLINK, GLM and MLM models; ii) chr16_8343864_A_G SNP located in the chromosome 16 at position 8,343,864, identified by FarmCPU, GLM and MLM models (Figure 5.2). *p*-values ranged from 1.84^{e-8}, for mu_s_G_A_chr15_11771804 locus identified under the BLINK model to 4.19^{e-6}, for chr16_8343864_A_G locus identified under the MLM model (Table 5.1).

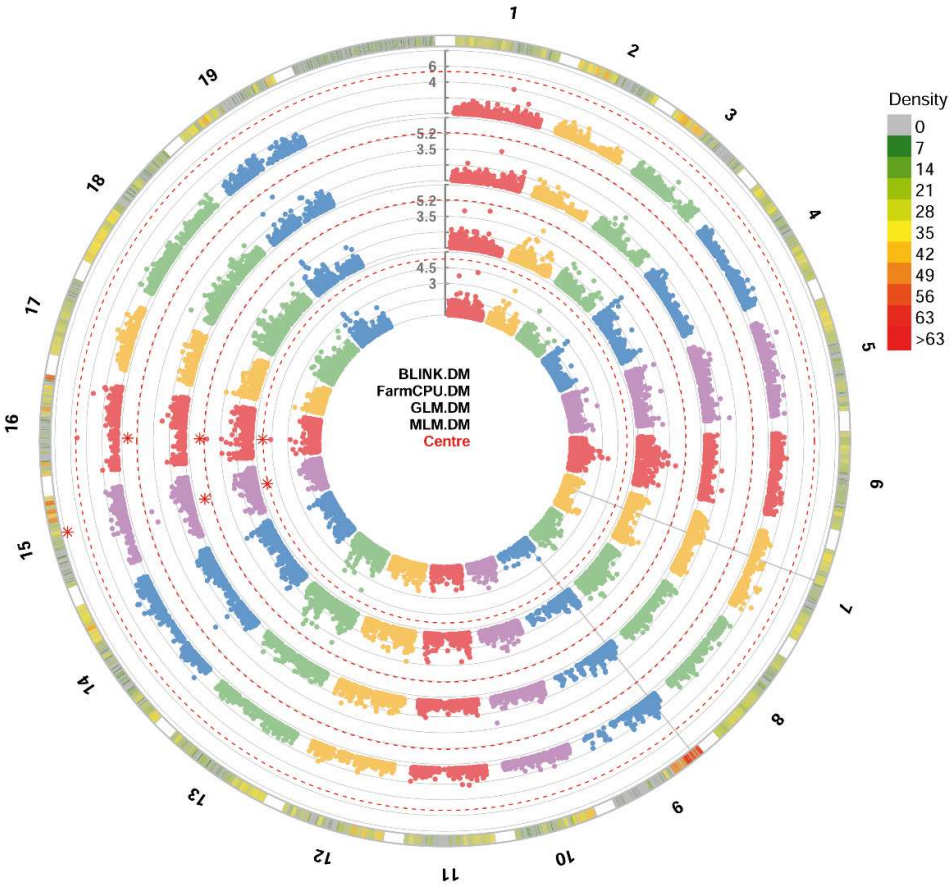

Figure 5.2 Circular Manhattan plot of -$\log_{10}$ *p*-values estimated for binary (resistant *vs.* susceptible) coded phenotypic response to downy mildew (DM) in a panel of 88 cultivated and wild grapevine accessions genotyped by 18 k SNPs and subjected to GWAS. Significant SNPs are starts above the Bonferroni-adjusted threshold (red dotted line). Association analysis results of BLINK, FarmCPU, MLM and GLM (from the outer to the inner circle) models.

QQ-plot showed that all the four models used in GWAS were able to account for population structure (Figure S5.1). The phenotypic variance explained by the two detected SNP loci ranged from 18%, for chr16_8343864_A_G locus identified under the GLM and MLM models, to 81%, for mu_s_G_A_chr15_11771804 locus identified under the BLINK model (Table 5.1).

Table 5.1 List of significant SNP loci associated with downy and powdery mildew resistance. Per each SNP, chromosome, position (PN40024 v4 genome), *p*-value, phenotype variance explained and GWAS models are reported.

SNP ID	Chr	Position PN40024 v2 (bp)	Position PN40024 v4 (bp)	*p*-value	Phenotype variance explained (%)	GWAS model
Downy mildew						
mu_s_G_A_chr15_11771804	15	11,771,804	13,090,527	1.84E-08	80.6	BLINK
				9.92E-07	43.5	GLM
				3.78E-06	43.5	MLM
chr16_8343864_A_G	16	8,343,864	7,156,839	4.56E-07	65.6	FarmCPU
				1.59E-06	18.5	GLM
				4.19E-06	18.5	MLM
Powdery mildew						
chr6_18189932_G_T	6	18,189,932	18,138,148	6.73E-08	11.4	BLINK
				3.94E-07	7.75	GLM
				2.00E-06	11.4	MLM
be_C_T_chr17_16451257	17	16,451,257	18,308,269	1.63E-07	14	BLINK
				2.02E-07	7.72	GLM
				4.88E-07	14.1	MLM

For PM resistance, all the four GWAS models allowed to identify significant SNP loci associated with the resistance, showing $-\log_{10}(p)$ values higher than Bonferroni's threshold. Since some of these loci were identified by only a model, only loci identified by at least two models were taken into account. These loci identified with BLINK, GLM and MLM models are: i) chr6_18189932_G_T SNP located in the chromosome 6 at position 18,189,932; ii) be_C_T_chr17_16451257 SNP located in the chromosome 17 at position 16,451,257 (Figure 5.3). *p*-values ranged from 6.73^{e-8}, for chr6_18189932_G_T SNP locus identified under the BLINK model, to 2.00^{e-6}, for chr6_18189932_G_T SNP locus identified under the MLM model (Table 5.1). QQ-plot showed that all the models used in GWAS were able to account for population structure, except for GLM model (Figure S5.2). The phenotypic variance explained by the two detected SNP loci ranged from 7.7%, for be_C_T_chr17_16451257 locus identified under the GLM model, to 14%, for be_C_T_chr17_16451257 locus identified under the BLINK model (Table 5.1).

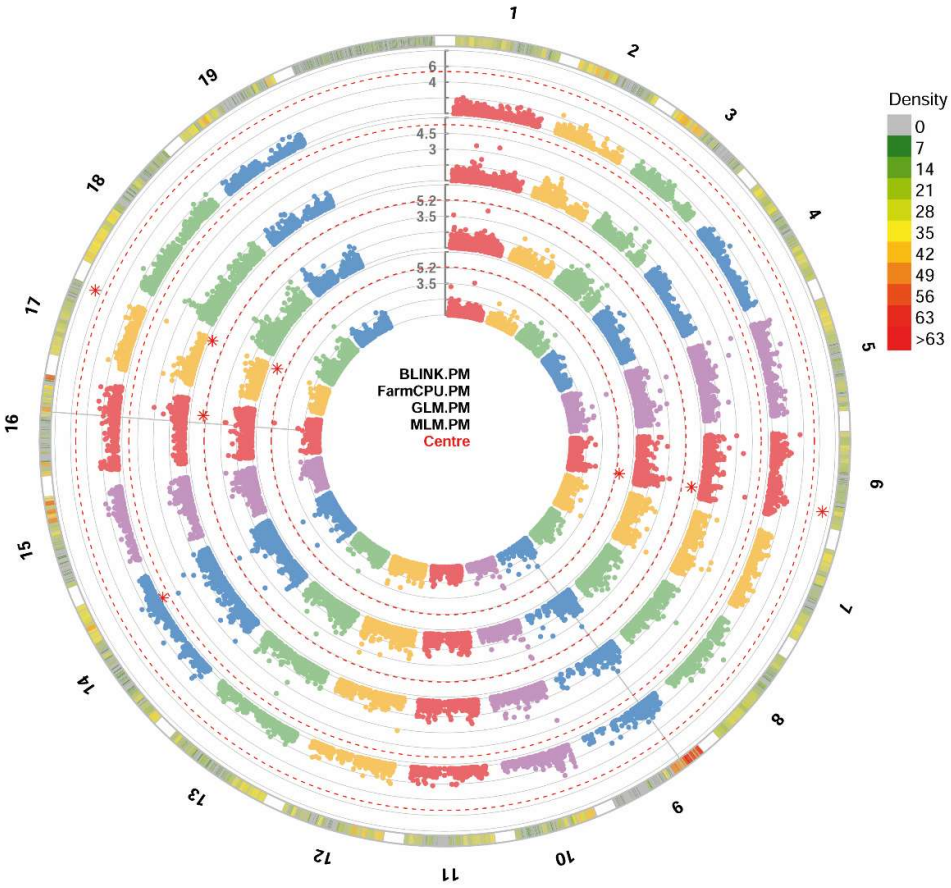

Figure 5.3 Circular Manhattan plot of -$\log_{10}$ *p*-values estimated for binary (resistant vs. susceptible) coded phenotypic response to powdery mildew (PM) in a panel of 88 cultivated and wild grapevine accessions genotyped by 18 k SNPs and subjected to GWAS. Significant SNPs are starts above the Bonferroni-adjusted threshold (red dotted line). Association analysis results of BLINK, FarmCPU, MLM and GLM (from the outer to the inner circle) models.

5.3.5 Candidate gene prediction

The four SNP loci associated with DM and PM resistance were mapped to *V. vinifera* reference genome (PN40024v4) and to the genome of DM resistant variety Mgaloblishvili to identify putative genes related to DM and PM resistance trait. To search for candidate genes, due to $LD_{½,90}$ (r^2 = 0.05) value, a window of

0.5 Mb upstream and downstream the four SNPs associated with DM and PM resistance has been used.

In PN40024, 43 genes were found in the surrounding regions of the mu_s_G_A_chr15_11771804 SNP (chromosome 15), while in Mgaloblishvili genome, 41 genes were identified in haplotype 1 and forty-four in haplotype 2 (Table S5.5). The region seemed to be relatively conserved between PN40024 and Mgaloblishvili. Among the conserved genes between the two genomes, there were ankyrin repeat family proteins (1 gene in PN40024, 3 genes in both Mgaloblishvili haplotypes), a WRKY transcriptional factor (12), some phospholipases A DAD1 genes (3 genes in PN40024 and Mgaloblishvili haplotype 2, and 2 genes in Mgaloblishvili haplotype 1), a serine/threonine-protein kinase D6PK-like and different ethylene-responsive transcription factors 1A – like (four genes in PN40024 and Mgaloblishvili haplotypes) (Table S5.5). A cytochrome P450 78A5 – like gene and a VASCULAR ASSOCIATED DEATH 1 protein were present only in the Mgaloblishvili haplotypes (Table S5.5).

The surrounding regions of the chr16_8343864_A_G SNP (chromosome 16) were more diverse in the two genomes. The gene content varied a lot even between the Mgaloblishvili haplotypes (Table S5.5). In PN40024, 44 genes were identified, while 32 genes were found in Mgaloblishvili haplotype 1 and 45 genes in haplotype 2. Some conserved genes were receptors-like proteins, a rust resistance kinase Lr10-like, a ceramide kinase and a derlin-2 protein gene (Table S5.5). Nevertheless, the gene content between the two genomes was very different for the major part, with Mgaloblishvili possessing more genes related to biotic stress responses compared to PN40024. Examples of these genes are an F-box/kelch-repeat plant protein, two WD-repeat-containing proteins, an armadillo/beta-catenin repeat family protein gene, a subtilase-like protease gene, ubiquinol-cytochrome-c reductase complex assembly factor 1 and a ubiquinol-cytochrome-c reductase complex assembly factor 1. Interestingly, Mgaloblishvili haplotype 2 carried also a MLO family protein gene and a Cf-4/9 disease resistance-like family protein gene, together with a higher number of MYB transcriptional factors (Table S5.5).

The surrounding regions of the chr6_18189932_G_T SNP (chromosome 6) were denser in gene content compared to the other loci. PN40024 holds 105 genes, Mgaloblishvili haplotype-1 85 and haplotype-2 91 genes (Table S5.5). The gene content varied greatly in terms of performed function, nevertheless most genes were found to be directly or indirectly involved in biotic stress responses, such as some serine kinases, genes related to the production of secondary metabolites (i.e. (+)-neomenthol dehydrogenase-like genes and 4-coumarate--CoA ligase-like 7 genes), some proteases genes, genes involved in auxins signaling pathway and some transporters (Table S5.5).

Fifty-one genes were found in the surrounding regions of the be_C_T_chr17_16451257 SNP (chromosome 17) for PN40024, and 42 and 41 for Mgaloblishvili haplotype 1 and 2, respectively (Table S5.5). In this case, the genes and their functions were more conserved between the two genomes. The majority of genes, functions appeared to be related to receptors and signaling pathways, plant core metabolism and, interestingly, to abiotic stress responses (Table S.5.5). Some of those genes where a proteasome subunit alpha type-1-A-like, a putative LRR receptor-like serine/threonine-protein kinase gene, a COP9 signalosome complex subunit 2 gene and Ubiquitin-like-specific protease ESD4 gene, all present in both PN40024 and Mgaloblishvili.

5.4 Discussion

Identifying loci of resistance to DM and PM in grapevines is of critical significance for advancing the sustainable management of viticulture. By pinpointing the specific genetic regions in grapevines associated with resistance to these pathogens, researchers and viticulturists can develop targeted breeding programs to cultivate grape varieties with built-in resistance. The identification of resistant cultivars with a *vinifera* background could be a promising solution to simplify breeding programs of resistant varieties. In this work, two new loci associated with DM resistance and two new loci associated with PM were identified adopting an association mapping approach.

5.4.1 New SNP loci associated with DM and PM resistance

To date, 34 QTLs conferring resistance to DM and 15 QTLs conferring resistance to PM have been identified within *Vitis* spp. and *V. vinifera.* In spite of the high number of loci, very few of them are characterized to gene level, *Rpv1* (Feechan *et al.*, 2013), *Rpv3* (Foria *et al.*, 2018), *Rpv33* (Zou *et al.*, 2023); and *Ren2*, *Ren3*, *Ren4*, *Ren6*, *Ren11*, *Ren12* and *Run1* (Massonnet *et al.*, 2022; Sapkota *et al.*, 2023). The scarce availability of grapevine complete genomes in the past years, and the complications related to mapping population development due to grapevine peculiarities (high heterozygosity and perennial life cycle), are probably responsible for this lack (Shi *et al.*, 2023). To avoid incurring in part of those issues, in this work the SNP probe location data (based on PN40024 12X v2) were used to obtain information about their location in the newest version of PN40024 genome (v4). In PN40024 v4, the probes revealed to be shifted in their location, in some cases (be_C_T_chr17_16451257 SNP, chromosome 17) even with a shift of ~4 Mb. This information was used to correctly retrieve information about the gene content of the regions associated with GWAS signal. However, to compare the position of GWAS signals with the ones of previously reported loci, we used also PN40024 12X v2 information. In this way, comparability of data could be maintained.

All the four signals identified in this work did not co-localize with previously known loci. Nonetheless, it was interesting to notice the proximity of the signal mu_s_G_A_chr15_11771804 SNP (chromosome 15, 11.7 Mb in PN40024 12x v2, 13.1 Mb in PN40024 v4), associated with *P. viticola* resistance, with *Ren3* (associated to *E. necator* resistance) location in the old version of PN40024 genome (12x v2) (Zendler *et al.*, 2017). It could suggest an evolutionary specialization of that chromosome region. For DM resistance, the signal related to chr16_8343864_A_G SNP is located on chromosome 16 (8.3 Mb in PN40024 12x v2 and 7.2 Mb in PN40024 v4). According to literature, *Rpv31* (Sargolzaei et al., 2020; Chapter 2) is also located on chromosome 16, but its position was identified to encompass the region between 22.09 and 22.28 Mb (Chapter 2). Altogether, because the SNPs identified in this work do not physically co-locate

with the QTL already identified, it is possible to conclude that the four loci are novel associations.

5.4.2 The gene content of the identified regions varies between PN40024 and Mgaloblishvili genome

To assure the most accurate content prediction for the genomic regions identified in this work, the SNP probes on both PN40024 versions (v2 and v4). Moreover, the probes were mapped on Mgaloblishvili genome, the first identified *V. vinifera* DM resistant variety ((Toffolatti *et al.*, 2018); Chapter 2). In this way, a comparison with a resistant variety with a nearer genetic background to PN40024 became available for this study. Nonetheless, it must be specified that no such similar comparison can be done in the case of PM resistance, given the susceptibility of Mgaloblishvili to the disease.

In the studied genomes, the gene content was conserved with varying degrees between the two varieties. The most conserved locus was the one identified by mu_s_G_A_chr15_11771804 SNP (chromosome 15) for the resistance to DM, while the most different was the one identified by chr6_18189932_G_T SNP (chromosome 6) for the resistance to PM. Frequently, one of the two haplotypes of Mgaloblishvili showed a more similar content to PN40024 genome, suggesting a greater genetic proximity to the reference, compared to the other haplotype that instead varied a lot (Magris *et al.*, 2021). Based on chapter 2 results, this difference could be based on structural variation of the locus between the compared genomes. If that will be revealed to be true, the difference could be interpreted as a bigger genetic distance between PN40024 and the higly different Mgaloblishvili haplotypes. Furthermore, it could suggest a high degree of differenciation of the region in *V. vinifera* varities, that could contribute to explain the existing variability among the distribution of PM resistance phenotypes in *V. vinifera* populations.

5.4.3 Regions associated with DM and PM resistance are related to biotic stress response

Plants have evolved various mechanisms to defend themselves against biotic stress, which includes threats from pathogens and herbivores. Some of the key defense mechanisms include: hormonal signaling, physical barriers, chemical defense. These mechanisms are part of a complex and dynamic interplay between plants and their biotic environment, allowing them to adapt and defend themselves against a wide range of stressors (Iqbal *et al.*, 2021). In this work, both genomes revealed that the regions contained at least a core of genes related to biotic stress responses, with interesting overlaps with abiotic stress responses. Usually, a higher content of genes specifically involved in plant defense against biotic stress was found in Mgaloblishvili, compared to PN40024. Nevertheless, also PN40024 showed at least a core of genes involved in the same functions. Regarding regions associated with DM, the mu_s_G_A_chr15_11771804 SNP (chromosome 15) identified a region that was very conserved between PN40024 and Mgaloblishvili genomes. Among the conserved genes between the two genomes, the majority appeared to be involved in response to pathogens, and within them some were present in cluster. The first interesting candidates were ankyrin repeat family proteins genes. In Mgaloblishvili, these genes were present in more copies (3) compared to PN40024 (1). According to literature, they act as receptors-like proteins and regulate plant immunity (Yang *et al.*, 2012). Other present receptors were the serine/threonine-protein kinase genes, that nowadays are considered well-established players in the defense response against many different pathogens, from fungi (such as thus causing PM) to viruses (Cao *et al.*, 2011). In this case, however, the genes were present with in the same number of copies (2) in PN40024 Mgaloblishvili haplotypes. Strictly related to these genes is the function of another cluster of genes found in this region and conserved between the two genomes, the phospholipase A DAD1 genes, involved in lipid metabolism and activated in response to pathogens infection, they are essential players in the mechanisms related to plant immunity (Lee and Park, 2019). These genes had the same number of copies in PN40024 and Mgaloblishvili haplotype 2 (3), while

they differend in Mgaloblishvili haplotype 1 (2 copies). Interestingly, in this chr 15 region there are also numerous transcription factors, such as WRKY transcription factor 12, whose over-expression results in the reduction of soft rot symptoms in *Arabidopsis thaliana* and Chinese cabbage (Kim *et al.*, 2014), and a cluster of ethylene-responsive transcription factors 2, notoriously involved in the regulation of defense responses in many plant species (Pré *et al.*, 2008; Licausi, Ohme-Takagi and Perata, 2013). Differently from the previous gene, those genes were present in the same number of copies in both the analysed genomes. Nevertheless, in general, in Mgaloblishvili, the gene content seemed to be even more specialized toward defense response against pathogen, with the presence of genes like a cytochrome P450 78A5 – like gene, involved in secondary metabolites production as a response to stresses (Chakraborty *et al.*, 2023) and the VASCULAR ASSOCIATED DEATH 1 protein gene. This gene is a regulator of cell death and is involved in defense responses in vascular tissues against pathogens like *Pseudomonas syringae* (Lorrain *et al.*, 2004).

The region identified by chr16_8343864_A_G SNP (chromosome 16) exhibited significant variation among the two genomes, compared to the first one. Even in this region, many genes were receptors-like proteins, such as a kinase Lr10-like, from literature involved in resistant to rust disease (Feuillet *et al.*, 2003). In a previous work studying the transcriptome of Mgaloblishvili during infection with *P. viticola,* several kinases Lr10-like genes were up-reguted by the variety after inoculation with the pathogen (Toffolatti *et al.*, 2018). In general, the majority of genes related to pathogens defense was found in Mgaloblishvili. Among the most interesting genes, it has been found a F-box/kelch-repeat plant protein gene and subtilase-like protease gene. Surprisingly, the first gene is involved in tolerance against PM in grapevine. It is a component of the E3 ubiquitin ligase complex (whose components were found in the regions identified in this work), and its over-expression leads to enhanced tolerance against the pathogen through the proteasome system pathway (Wang *et al.*, 2017). The second gene, subtilase-like protease, is known to be involved in the response against both *P. viticola* and *E. necator*, by contributing to the successful establishment of resistance response (Figueiredo, Sousa Silva and Figueiredo, 2018). The genes were

present also in Rpv31 locus of Mgaloblishvili genome (Chapter 2), once again confirming their important role in the defense against these pathogens. Within this region, the two Mgaloblishvili haplotypes exhibited substantial dissimilarity, with notable significance in haplotype 2 due to the presence of an MLO family protein gene and a Cf-4/9 disease resistance-like family protein gene. MLO protein gene is a well-known susceptibility gene to PM (Pessina *et al.*, 2016), while Cf-4/9 disease resistance-like family protein gene is known to confer resistant to *Cladosporium fulvum* in tomato. The resistance gene recognizes the Avirulence factor 9 (Avr9) produced by the pathogen and activates the pathway that leads to hypersensitive response (HR) (Kruijt, Brandwagt and De Wit, 2004). The regions associated to PM resistance were the less conserved between PN40024 and Mgaloblishvili. The first signal, chr6_18189932_G_T SNP (chromosome 6), pinpointed a region characterized by significantly higher gene density compared to the others (105 genes in PN40024, 85 in Mgaloblishvili haplotype 1 and 91 genes in haplotype 2). Despite the great variability in the performed functions, most genes were found to be involved in biotic stress responses. Among those genes, we discovered some serine kinases (previously described in chr15 and chr 16 identified regions) and some genes involved in the production of secondary metabolites for defense purposes, such as (+)-neomenthol dehydrogenase-like genes and 4-coumarate--CoA ligase gene. (+)-neomenthol dehydrogenase is a defense antimicrobial protein that is involved in the neomenthol biosynthesis induced in response to pathogen attack (Munhoz *et al.*, 2015). These findings reinforce what was discovered in previous studies about the defense mechanism of Mgaloblishvili. It was demonstrated that the variety porduces secondary metabolites compouds (such as volatile organic compounds – VOCs) in response to *P. viticola* infection, indicating a pivotal role of this mechanism in the cultivar defense strategy (Toffolatti *et al.*, 2018; Ricciardi *et al.*, 2021). The second gene synthetizes 4-coumarate--CoA ligase, this enzyme is known to be involved in the cotton plants resistance to *Verticillium dahlia*, by promoting vascular lignification and metabolic flux through jasmonic acid signaling pathway (Alariqi *et al.*, 2023). OtheR-genes in this region were discovered to be involved in auxin signaling pathway, notoriously known to have

a role in biotic stress responses (Kazan and Manners, 2009; Kunkel and Harper, 2018), and transport of nutrients and compounds.

As in the case of the other analyzed regions, the be_C_T_chr17_16451257 SNP (chromosome 17) identified a region with many genes related to pathogens responses, such as different receptors, like LRR receptor-like serine/threonine-protein kinase (Gururani *et al.*, 2012), genes involved in production and transformation of secondary metabolites (Erb and Kliebenstein, 2020), such as some amine- and polyamine- oxidases (Cona *et al.*, 2006), and components of the ubiquitination and proteasome complexes (Dielen *et al.*, 2010).

5.4.4 The gene content of the identified regions could be involved in both biotic and abiotic stress responses

Starting with the chr15 region analyzed, it was interesting to notice that some of the genes identified in this work were linked to both biotic and abiotic stress responses. An example is the case of the transporter genes and the COP9 signalosome complex subunit-like protein genes. In particular, these genes were present both in the region related to DM resistance in chromosome 15 and in the region related to PM resistance in chromosome 17, and conserved between PN40024 and Mgaloblishvili genomes. COP9 signalosome complex subunit-like protein genes are involved in the regulation of development and hormones, and in response against pathogens, like Tobacco mosaic virus and *Botrytis cinerea* and abiotic stresses, such as oxidative stress and salt stress (Hind et al., 2011; Stratmann and Gusmaroli, 2012; Tan et al., 2016; Wei et al., 2018).

For be_C_T_chr17_16451257 (chromosome 17) SNP identified region, the involvement of genes in abiotic stress response was true also for other candidates in the region, such as NAC domain-containing protein 86-like, present in both genomes, and scarecrow-like protein 23 in Mgaloblishvili haplotype 1. NAC domain-containing protein genes are known to be involved in the response to different pathogens, like *Pseudomonas syringae*, *B. cinerea*, *Alternaria brassicola* and *Puccinia striiformis*, and to different abiotic stresses such as drought and salt stress (Xia *et al.*, 2010; Tariq *et al.*, 2022). Scarecrow-

like protein genes are involved mainly in abiotic stress responses, through auxins and gibberellins signaling pathways (Wang *et al*., 2020).

5.5 Conclusions

In this work, GWAS was used to identify loci associated with the resistance to grapevine DM and PM. The analysis allowed the discovery of two new loci associated with *P. viticola* resistance and two loci associated with *E. necator* resistance, in a population of *V. vinifera* varieties coming from one of grapevine domestication centers. The four loci were found to be located in chromosomal regions enriched with genes involved in defense against biotic stresses, suggesting promising bases for their future exploitation in breeding programs of resistant varieties. To use them with the most efficient gain, further functional characterization studies could be performed, employing approaches such as CRISPR (Clustered Regularly Interspaced Short Palindromic Repeats) based systems or RNA interference technologies.

Employing resistance sources from *V. vinifera* germplasm could confer a great advantage to breeding programs, compared to using non-*vinifera* species. This is because they make possible to obtain crosses with cultivated varieties in a faster way, while maintaining a good resistance level against specific pathogens. Moreover, they can provide a product free from the unpleasant characteristics typical of wild species crosses. The development of resistant grapevine varieties with high enological potential not only leads to a reduced dependence on chemical interventions but also promote a transition towards environmentally friendly vineyard practices, resulting in decreased production costs and ultimately fostering greater sustainability within the wine industry.

Chapter 6: General conclusions and future perspectives

Every year, downy mildew and powdery mildew cause huge grape losses worldwide. The massive use of fungicides to treat these diseases is considered no more sustainable for the viticulture sector. To achieve viticulture eco-friendly disease management, part of the solution could be the development of resistant varieties breeding programs. In this scenario, the aim of this PhD project was to contribute to breeding programs with the identification and characterization of resistance and susceptibility genes.

Different results were achieved. First, the genome of the first identified *V. vinifera* DM resistant variety, Mgaloblishvili, was assembled and studied. The three R loci of the variety, *Rpv29*, *Rpv30* and *Rpv31*, were identified and analyzed for their gene content and expression during the infection with *P. viticola*. After that, using a transient RNAi approach based on the exogenous application of dsRNA, the candidate gene of susceptibility to downy mildew *VviLBDIf7* was successfully proven to reduce downy mildew infections. On the following work, other two candidate gene of susceptibility to downy mildew, involved in nitrogen metabolism, were identified. One of them, *VviAS1*, was the subject of another validation assay through transient RNAi, although the assay needs to be repeated. Finally, a GWA study on *V. vinifera* varieties from the Caucasus and neighboring regions allowed the discovery of two new DM and two new PM resistance loci. For each locus, some interesting candidate genes were hypothesized using the grapevine reference genome PN40024 and the newly assembled Mgaloblishvili genome, the first reference genome for DM resistant *V. vinifera* varieties.

Functions and roles of the candidate R and S genes will be explored in the future using New Breeding Techniques, such as RNAi and genome editing based on CRISPR-Cas9 system, and by employing last generation genomics and transcriptomics approaches. Once validated, all these genetic resources will contribute to the knowlenge about downy mildew- and powdery mildew-grapevine pathosystem. Moreover, they will be available for breeding programs aiming to develop grapevine resistant varieties. The introgression of resistance

sources based on different mechanisms (R-genes and S-genes) could substantially improve the durability of the traits, avoiding the eventual onset of resistance breakthrough by the pathogens. In this way, hopefully, the current drawbacks of resistant varieties breeding programs will be significantly reduced.

Supplementary materials

Supplementary materials can be found in the following onedrive folder:

https://unimi2013-my.sharepoint.com/:f:/g/personal/valentina_ricciardi_unimi_it/EoyELbnknqdJqANrA5oEuOoB0GFmoULNYNsEDqJld0H89g?e=cmAr0l

Chapter 2

Figure S2.1A Identification of recombination events on chromosome 14 (*Rpv29* location) of accession 97 (DM resistant). The accession is part of Mgalobllishvili self-cross progeny. DNA-seq reads alignments against chromosome 14 of Mgaloblishvili genome haplotypes (parental haplotypes) are shown. Blue line represents the average distribution value of reads in homozygous allelic state for a determined parental haplotype. Red line represents the average distribution value of reads in heterozygous allelic state for the parental haplotypes. Green vertical line indicates putative recombination event. Red arrow indicates *Rpv* locus of interest.

Figure S2.1B Identification of recombination events on chromosome 03 (*Rpv30* location) of accession 97 (DM resistant). The accession is part of Mgalobllishvili self-cross progeny. DNA-seq reads alignments against chromosome 03 of Mgaloblishvili genome haplotypes (parental haplotypes) are shown. Blue line represents the average distribution value of reads in homozygous allelic state for a determined parental haplotype. Red line represents the average distribution value of reads in heterozygous allelic state for the parental haplotypes. Green vertical line indicates putative recombination event. Red arrow indicates *Rpv* locus of interest.

Figure S2.1C Identification of recombination events on chromosome 16 (*Rpv31* location) of accession 97 (DM resistant). The accession is part of Mgalobllishvili self-cross progeny. DNA-seq reads alignments against chromosome 16 of Mgaloblishvili genome haplotypes (parental haplotypes) are shown. Blue line represents the average distribution value of reads in homozygous allelic state for a determined parental haplotype. Red line represents the average distribution value of reads in heterozygous allelic state for the parental haplotypes. Green vertical line indicates putative recombination event. Red arrow indicates *Rpv* locus of interest.

Figure S2.1D Identification of recombination events on chromosome 14 (*Rpv29* location) of accession 124 (DM resistant). The accession is part of Mgalobllishvili self-cross progeny. DNA-seq reads alignments against chromosome 14 of Mgaloblishvili genome haplotypes (parental haplotypes) are shown. Blue line represents the average distribution value of reads in homozygous allelic state for a determined parental haplotype. Red line represents the average distribution value of reads in heterozygous allelic state for the parental haplotypes. Green vertical line indicates putative recombination event. Red arrow indicates *Rpv* locus of interest.

Figure S2.1E Identification of recombination events on chromosome 03 (*Rpv30* location) of accession 124 (DM resistant). The accession is part of Mgalobllishvili self-cross progeny. DNA-seq reads alignments against chromosome 03 of Mgaloblishvili genome haplotypes (parental haplotypes) are shown. Blue line represents the average distribution value of reads in homozygous allelic state for a determined parental haplotype. Red line represents the average distribution value of reads in heterozygous allelic state for the parental haplotypes. Green vertical line indicates putative recombination event. Red arrow indicates *Rpv* locus of interest.

Figure S2.1F Identification of recombination events on chromosome 16 (*Rpv31* location) of accession 124 (DM resistant). The accession is part of Mgalobllishvili self-cross progeny. DNA-

seq reads alignments against chromosome 16 of Mgaloblishvili genome haplotypes (parental haplotypes) are shown. Blue line represents the average distribution value of reads in homozygous allelic state for a determined parental haplotype. Red line represents the average distribution value of reads in heterozygous allelic state for the parental haplotypes. Green vertical line indicates putative recombination event. Red arrow indicates *Rpv* locus of interest.

Figure S2.2A Analysis of *Rpv29 (chr14)*, *Rpv30 (chr03)* and *Rpv31(chr16)* allelic state in accession 97 (DM resistant). The accession is part of Mgalobllishvili self-cross progeny and was analysed to determine the resistance haplotype of the target loci. DNA-seq reads alignments against the three loci regions in Mgaloblishvili genome haplotypes (parental haplotypes) are shown. Blue line represents the average distribution value of reads in homozygous allelic state for a determined parental haplotype. Red line represents the average distribution value of reads in heterozygous allelic state for the parental haplotypes.

Figure S2.2B Analysis of *Rpv29 (chr14)*, *Rpv30 (chr03)* and *Rpv31(chr16)* allelic state in accession 124 (DM resistant). The accession is part of Mgalobllishvili self-cross progeny and was analysed to determine the resistance haplotype of the target loci. DNA-seq reads alignments against the three loci regions in Mgaloblishvili genome haplotypes (parental haplotypes) are shown. Blue line represents the average distribution value of reads in homozygous allelic state for a determined parental haplotype. Red line represents the average distribution value of reads in heterozygous allelic state for the parental haplotypes.

Figure S2.2C Analysis of *Rpv29 (chr14)*, *Rpv30 (chr03)* and *Rpv31(chr16)* allelic state in accession 145LIB (DM susceptible). The accession is part of Mgalobllishvili self-cross progeny and was analysed to determine the resistance haplotype of the target loci. DNA-seq reads alignments against the three loci regions in Mgaloblishvili genome haplotypes (parental haplotypes) are shown. Blue line represents the average distribution value of reads in homozygous allelic state for a determined parental haplotype. Red line represents the average distribution value of reads in heterozygous allelic state for the parental haplotypes.

Figure S2.2D Analysis of *Rpv29 (chr14)*, *Rpv30 (chr03)* and *Rpv31(chr16)* allelic state in accession 157M (DM susceptible). The accession is part of Mgalobllishvili self-cross progeny and was analysed to determine the resistance haplotype of the target loci. DNA-seq reads alignments against the three loci regions in Mgaloblishvili genome haplotypes (parental haplotypes) are shown. Blue line represents the average distribution value of reads in homozygous allelic state for a determined parental haplotype. Red line represents the average distribution value of reads in heterozygous allelic state for the parental haplotypes.

Figure S2.3 Barplots showing structural variants (SVs) identified between PN40024 v4 genome and Mgaloblishvili haplotypes, represented as their length sums in base pairs (bp). SVs length sums of *Rpv29* (**A**) and *Rpv31* (**B**) are shown. Each SV is represented by a different color.

Table S2.1 Results of *Rpv29-*, *Rpv30-*, and *Rpv31-indentifying* SNP probes mapping against PN40024 v2 genome, PN40024 v4 genome and Mgaloblishvili haplotypes. BLASTn-short was used to perform the alignment. The probes sequences were retrived from the Vitis18k genotyping array (Laucou et al., 2018).

Table S2.2 *Rpv29*, *Rpv30* and *Rpv31* loci reconstruction using NUCmer tool suite output. The reconstruction was performed using alignements of the loci between PN40024 v4 and both Mgaloblishvili haplotypes. Tables summarizing loci coordites are also reported.

Table S2.3 Whole genome, Rpv29 and Rpv31 descriptive statistics (length sums, mean length, count) of detected structural variants (SVs). SVs are reported divided by type: CID = complex insertion-deletion, DEL = deletion, DUP = duplication, INV = inversion, TRA = translocation, INS = insertion.

Table S2.4 Summary of structural varints (SVs) and single nucleotide polymorphism (SNPs) impacting *Rpv29* and *Rpv31* genes, in both Mgaloblishvili haplotypes. Per each gene, position, length and type of variant are reported, as well as the comparison from which they were indentified (PN40024 v4 *vs* Mgaloblishvili haplotype 1 or Mgaloblishvili haplotype 2). SVs are reported divided by type: CID = complex insertion-deletion, DEL = deletion, DUP = duplication, INV = inversion, TRA = translocation, INS = insertion.

Table S2.5 Expression of *Rpv29*, *Rpv30* and *Rpv31* genes in leaves of Mgaloblishvili, during infection with *P. vicola*. The analysis was performed on both haplotypes of Mgaloblishvili loci. Results are shown for the four analyzed timepoints: T0 (leaves not-inoculated with *P. viticola*), T1 (24 days after incolutaion with *P. viticola*), T2 (48 days after incolutaion with *P. viticola*), and T3. Gene expression is indicated as transcript per millions (TPM) values. Per each gene ID, gene position, expression values at the different timepoints, ad functions are shown. A table summuryzing the total number of differentially expressed genes (DEGS) identified by DEseq2 (R) analysis is also reported.

Table S2.6 Summary of genome assembly qualitative parameters. Mgaloblishvili genome assembly statistics, chromosomes lengths for PN40024 v2, PN40024 v4 and Mgaloblishvili genomes are reported. BUSCO parameters of Mgaloblishvili genome assembly are also shown.

Chapter 3

File S3.1 dsRNA sequence, 412 bp long, targeting *VviLBDIf7* S-gene.

Figure S3.1 Scheme of the leaf choice and treatment. **A**) Leaves chosen for the water/dsRNA treatment (2nd to the 6th fully developed leaf from the apex of the shoot). **B**) Spraying of the water/dsRNA treatment on the upper side of the leaf. **C**) Spraying of the water/dsRNA treatment on the underside of the leaf. For each treatment, a single leaf per plant was randomly sampled at different time points (3, 5, 7 and 15 dat in the first experiment; 5 and 7 dat in the second experiment) for the experimental inoculation with *P. viticola*.

Figure S3.2 Picture of the agarose gel showing the absence of amplification in some of the leaf samples used for the experimental inoculation of *P. viticola* and in negative controls (*Botrytis cinerea* DNA and water) and the presence of the band corresponding to *P. viticola* samples (sporangia and infected leaf). Ladder 50 bp biotechrabbit GmbH, Henningsdorf DE.

Chapter 5

Figure S5.1. Quantile-quantile (QQ) plot of expected *vs*. observed -$\log_{10}$ *p*-values estimated for binary (resistant *vs*. susceptible) coded phenotypic response to downy mildew (DM) in a panel of 88 cultivated and wild grapevine accessions genotyped by 18 k SNPs. Results of BLINK, FarmCPU, MLM and GLM association models.

Figure S5.2. Quantile-quantile (QQ) plot of expected *vs*. observed -$\log_{10}$ *p*-values estimated for binary (resistant *vs*. susceptible) coded phenotypic response to powdery mildew (PM) in a panel of 88 cultivated and wild grapevine accessions genotyped by 18 k SNPs. Results of BLINK, FarmCPU, MLM and GLM association models.

Table S5.1. List of 88 grapevine genotypes, cultivated and wild, coming from Caucasus, Iran and Uzbekistan and SSR profiles. VVS2, VVMD5, VVMD7, VVMD25, VVMD27, VVMD28, VVDM32, VrZAG62, VrZAG79, ISV2, ISV3, ISV4 and VMCNG4b9 loci were used for varietal identification. *Ren1*, *Rpv1-Run1* and *Ren3-Ren9* loci were amplified for identification of alleles associated with resistance to downy and powdery mildew.

Table S5.2. SNP profiles of 88 grapevine genotypes, cultivated and wild, coming from Caucasus, Iran and Uzbekistan, genotyped at 18 k loci.

Table S5.3. List of grapevine accessions, cultivated and wild, coming from Caucasus, Iran and Uzbekistan, analyzed in this study. Information about subspecies, origin and resistance/susceptibility to *P. viticola* and *E. necator* are reported. 1: resistant; 0: susceptible.

Table S5.4. Ancestry values at K = 3 detected for SNP profiles of 88 grapevine accessions (wild and cultivated from Caucasus, Iran and Uzbekistan), genotyped at 18 k loci.

Table S5.5. List of candidate genes in a window of 0.5 Mb upstream and downstream the four SNPs associated to *P. viticola* and *E. necator* resistance trait.

References

Abashidze, E. et al. (2015) Evaluation of eno-carpological traits in Georgian grapevine varieties from Skra germplasm repository.

Abdelraheem, A., Thyssen, G. N., Fang, D. D., Jenkins, J. N., McCarty, J. C., Wedegaertner, T., et al. (2021). GWAS reveals consistent QTL for drought and salt tolerance in a MAGIC population of 550 lines derived from intermating of 11 Upland cotton (Gossypium hirsutum) parents. Mol. Genet. Genomics 296, 119–129. doi:10.1007/s00438-020-01733-2.

Acevedo-Garcia, J., Kusch, S. and Panstruga, R. (2014). Magical mystery tour: MLO proteins in plant immunity and beyond. Journal of Physiology. Blackwell Publishing Ltd, pp. 273–281. doi: https://doi.org/10.1111/nph.12889.

Adam-Blondon, a-F., Roux, C., Claux, D., Butterlin, G., Merdinoglu, D., and This, P. (2004). Mapping 245 SSR markers on the Vitis vinifera genome: a tool for grape genetics. Theor. Appl. Genet. 109, 1017–27. doi:10.1007/s00122-004-1704-y.

Agudelo-Romero, P., Erban, A., Rego, C., Carbonell-Bejerano, P., Nascimento, T., Sousa, L., et al. (2015). Transcriptome and metabolome reprogramming in Vitis vinifera cv. Trincadeira berries upon infection with Botrytis cinerea. J. Exp. Bot. 66, 1769–1785. doi: 10.1093/jxb/eru517

Alariqi, M. et al. (2023) 'Cotton 4-coumarate-CoA ligase 3 enhanced plant resistance to Verticillium dahliae by promoting jasmonic acid signaling-mediated vascular lignification and metabolic flux', Plant Journal, 115(1), pp. 190–204. Doi: https://doi.org/10.1111/tpj.16223.

Albertazzi, G., Milc, J., Caffagni, A., Francia, E., Roncaglia, E., Ferrari, F., et al. (2009). Gene expression in grapevine cultivars in response to bois noir phytoplasma infection. Plant Sci. 176, 792–804. doi: 10.1021/jf104297n

Alexander, D. L., Mellor, E. A., and Langdale, J. A. (2005). CORKSCREW1 defines a novel mechanism of domain specification in the maize shoot. Plant Physiol. 138, 1396–1408. doi: 10.1104/pp.105.063909

Altschul, S.F. et al. (1990). Basic Local Alignment Search Tool. Journal of Molecular Biology.

Ambesajir, A. et al. (2012). RNA interference: A futuristic tool and its therapeutic applications. Saudi Journal of Biological Sciences, pp. 395–403. doi: https://doi.org/10.1016/j.sjbs.2012.08.001.

Antunes, F.; Aguilar, M.; Pineda, M.; Sodek, L. (2008). Nitrogen stress and the expression of asparagine synthetase in roots and nodules of soybean (Glycine max). Physiol. Plant, 133, 736–743.

Armijo, G. et al. (2016). Grapevine pathogenic microorganisms: Understanding infection strategies and host response scenarios. Frontiers in Plant Science. doi: https://doi.org/10.3389/fpls.2016.00382.

Asselbergh, B.; Curvers, K.; Franca, S.C.; Audenaert, K.; Vuylsteke, M.; Van Breusegem, F.; Höfte, M. (2007) Resistance to Botrytis cinerea in sitiens, an Abscisic Acid-Deficient Tomato Mutant, Involves Timely Production of Hydrogen Peroxide and Cell Wall Modifications in the Epidermis. Plant Physiol. 144, 1863–1877.

Bachewich, C., and Heath, I. B. (1999). Cytoplasmic migrations and vacuolation are associated with growth recovery in hyphae of Saprolegnia, and are dependent on the cytoskeleton. Mycol. Res. 103, 849–858.

Barker, C. L., Donald, T., Pauquet, J., Ratnaparkhe, M. B., Bouquet, A., Adam-Blondon, A.-F., et al. (2005). Genetic and physical mapping of the grapevine powdery mildew resistance gene, Run1, using a bacterial artificial chromosome library. Theor. Appl. Genet. 111, 370–377. doi:10.1007/s00122-005-2030-8.

Bavaresco, L.; Eibach, R. Investigations on the influence of N fertilizer on resistance to powdery mildew (Oidium tuckeri), downy mildew (Plasmopara viticola) and on phytoalexin synthesis in different grapevine varieties. Vitis 1987, 26, 192–200.

Bellin, D., Peressotti, E., Merdinoglu, D., Wiedemann-Merdinoglu, S., Adam-Blondon, A. F., Cipriani, G., et al. (2009). Resistance to Plasmopara viticola in grapevine 'Bianca' is controlled by a major dominant gene causing localised necrosis at the infection site. Theor. Appl. Genet. 120, 163–176. doi:10.1007/s00122-009-1167-2.

Bhattarai, G., Fennell, A., Londo, J. P., Coleman, C., and Kovacs, L. G. (2021). A Novel Grape Downy Mildew Resistance Locus from Vitis rupestris. Am. J. Enol. Vitic. 72, 12–20.

Bianchi, D., Brancadoro, L. and De Lorenzis, G. (2020). Genetic diversity and population structure in a Vitis spp. core collection investigated by SNP markers. Diversity, 12(3). doi: https://doi.org/10.3390/d12030103.

Bianchi, D.; Brancadoro, L. (2021). Water use efficiency and nutritional status of a new grapevine rootstock selection. Horticulturae, 7, 503.

Biedenkopf, D., Will, T., Knauer, T., Jelonek, L., Furch, A. C. U., Busche, T., et al. (2020). Systemic spreading of exogenous applied RNA biopesticides in the crop plant Hordeum vulgare. ExRNA 2:12.

Bitsadze, N., Aznarashvili, M., Vercesi, A., Chipashvili, R., Failla, O., and Maghradze, D. (2015). Screening of Georgian grapevine germplasm for susceptibility to downy mildew (Plasmopara viticola). Vitis - J. Grapevine Res. 54, 193–196. doi:10.17660/ActaHortic.2014.1032.25.

Blanc, S., Wiedemann-Merdinoglu, S., Dumas, V., Mestre, P., and Merdinoglu, D. (2012). A reference genetic map of Muscadinia rotundifolia and identification of Ren5, a new major locus for resistance to grapevine powdery mildew. Theor. Appl. Genet. 125, 1663–1675. doi:10.1007/s00122-012-1942-3.

Blasi, P., Blanc, S., Prado, E., Rühl, E. H., Mestre, P., and Merdinoglu, D. (2011). Construction of a reference linkage map of Vitis amurensis and genetic mapping of Rpv8, a locus conferring resistance to grapevine downy mildew. Theor. Appl. Genet. 123, 43–53. doi:10.1007/s00122-011-1565-0.

Bock, C.H.; Barbedo, J.G.A.; Del Ponte, E.M.; Bohnenkamp, D.; Mahlein, A.-K. (2020). From visual estimates to fully automated sensor-based measurements of plant disease severity: Status and challenges for improving accuracy. Phytopathol. Res. 2, 9.

Bosher, J.M. and Labouesse, M. (2000) RNA interference: genetic wand and genetic watchdog, NATURE CELL BIOLOGY.

Bourguet, D. et al. (2016). Combining selective pressures to enhance the durability of disease resistance genes. Frontiers in Plant Science. doi: https://doi.org/10.3389/fpls.2016.01916.

Bove, F. et al. (2019) 'Assessment of Resistance Components for Improved Phenotyping of Grapevine Varieties Resistant to Downy Mildew', Frontiers in Plant Science, 10. doi: https://doi.org/10.3389/fpls.2019.01559.

Bove, F.; Rossi, V. (2020). Components of partial resistance to Plasmopara viticola enable complete phenotypic characterization of grapevine varieties. Sci. Rep.10, 585.

Bozkurt, T.O. et al. (2012). Oomycetes, effectors, and all that jazz. Current Opinion in Plant Biology, pp. 483–492. Doi: https://doi.org/10.1016/j.pbi.2012.03.008.

Brancadoro, L.; Rabotti, G.; Scienza, A.; Zocchi, G. (1995). Mechanisms of Fe-efficiency in roots of Vitis spp. in response to iron deficiency stress. Plant Soil, 171, 229–234.

Brilli, M.; Asquini, E.; Moser, M.; Bianchedi, P.L.; Perazzolli, M.; Si-Ammour, A. (2018). A multi-omics study of the grapevine-downy mildew (Plasmopara viticola) pathosystem unveils a complex protein coding-A nd noncoding-based arms race during infection. Sci. Rep. 8, 757.

Buonassisi, D., Colombo, M., Migliaro, D., Dolzani, C., Peressotti, E., Mizzotti, C., et al. (2017). Breeding for grapevine downy mildew resistance: a review of “omics” approaches. Euphytica 213, 1–21. doi: 10.1007/s10681-017-1882-8

Cadle-Davidson, L., Chicoine, D.R. and Consolie, N.H. (2011). Variation within and among Vitis spp. for foliar resistance to the powdery mildew pathogen Erysiphe necator. Plant Disease, 95(2), pp. 202–211. doi: https://doi.org/10.1094/PDIS-02-10-0092.

Cagliari, D., Avila dos Santos, E., Dias, N., Smagghe, G., and Zotti, M. (2019). Nontransformative strategies for RNAi in crop protection in Modulating Gene Expression - Abridging the RNAi and CRISPR-Cas9 Technologies, eds A. Singh and M. W. Khan (IntechOpen).

Camañes, G.; Pastor, V.; Cerezo, M.; García-Andrade, J.; Vicedo, B.; García-Agustín, P.; Flors, V. (2012). A deletion in NRT2.1 attenuates Pseudomonas syringae-induced hormonal perturbation, resulting in primed plant defenses. Plant Physiol. 158, 1054–1066.

Campbell, M.A. et al. (2006). Comprehensive analysis of alternative splicing in rice and comparative analyses with Arabidopsis. BMC. Genomics., 7, p. 327. doi: https://doi.org/10.1186/1471-2164-7-327.

Canaguier, A., Grimplet, J., Di Gaspero, G., Scalabrin, S., Duchêne, E., Choisne, N., et al. (2017). A new version of the grapevine reference genome assembly (12X.v2) and of its annotation (VCost.v3). Genomics Data 14, 56–62. doi: 10.1016/j.gdata.2017.09.002

Cao, A. et al. (2011). Serine/threonine kinase gene Stpk-V, a key member of powdery mildew resistance gene Pm21, confers powdery mildew resistance in wheat. Proceedings of the National Academy of Sciences of the United States of America, 108(19), pp. 7727–7732. Doi: https://doi.org/10.1073/pnas.1016981108.

Capriotti, L., Baraldi, E., Mezzetti, B., Limera, C., and Sabbadini, S. (2020). Biotechnological approaches: gene overexpression, gene silencing, and genome editing to control fungal and oomycete diseases in grapevine. Int. J. Mol. Sci. 21:5701. doi: 10.3390/ijms21165701

Chakraborty, P. et al. (2023). Cytochrome P450 Gene Families: Role in Plant Secondary Metabolites Production and Plant Defense. Journal of Xenobiotics, 13(3), pp. 402–423. doi: https://doi.org/10.3390/jox13030026.

Chen, J., Moreau, C., Liu, Y., Kawaguchi, M., Hofer, J., Ellis, N., et al. (2012). Conserved genetic determinant of motor organ identity in medicago truncatula and related legumes. Proc. Natl. Acad. Sci.U.S.A. 109, 11723–11728. doi: 10.1073/pnas.1204566109

Chen, W., Zhang, X., Fan, Y., Li, B., Ryabov, E., Shi, N., et al. (2018). A genetic network for systemic RNA silencing in plants. Plant Physiol. 176, 2700–2719.

Cheng, H. et al. (2021). Haplotype-resolved de novo assembly using phased assembly graphs with hifiasm. Nature Methods, 18(2), pp. 170–175. doi: https://doi.org/10.1038/s41592-020-01056-5.

Chin, C.S. et al. (2016). Phased diploid genome assembly with single-molecule real-time sequencing. Nature Methods, 13(12), pp. 1050–1054. Doi: https://doi.org/10.1038/nmeth.4035.

Chong, J. et al. (2014). The SWEET family of sugar transporters in grapevine: VvSWEET4 is involved in the interaction with Botrytis cinerea. Journal of Experimental Botany, 65(22), pp. 6589–6601. doi: https://doi.org/10.1093/jxb/eru375.

Cochetel, N. et al. (2021). Diploid chromosome-scale assembly of the Muscadinia rotundifolia genome supports chromosome fusion and disease resistance gene expansion during Vitis and Muscadinia divergence. G3: Genes, Genomes, Genetics, 11(4). doi: https://doi.org/10.1093/g3journal/jkab033.

Colombo, M.; Masiero, S.; Rosa, S.; Caporali, E.; Toffolatti, S.L.; Mizzotti, C.; Tadini, L.; Rossi, F.; Pellegrino, S.; Musetti, R.; et al. (2020). NoPv1: A synthetic antimicrobial peptide aptamer targeting the causal agents of grapevine downy mildew and potato late blight. Sci. Rep. 10, 17574.

Cona, A. et al. (2006). Functions of amine oxidases in plant development and defence. Trends in Plant Science, pp. 80–88. doi: https://doi.org/10.1016/j.tplants.2005.12.009.

Conklin, A.; Stilwell, T. World Food; John Wiley & Sons: Hoboken, NJ, USA, 2007; ISBN 9780470043820.

Conrath, U. (2006). Systemic acquired resistance. Plant Signaling and Behavior, pp. 179–184. doi: https://doi.org/10.4161/psb.1.4.3221.

Consonni, C. et al. (2006). Conserved requirement for a plant host cell protein in powdery mildew pathogenesis. Nature Genetics, 38(6), pp. 716–720. doi: https://doi.org/10.1038/ng1806.

Crespan, M. (2003). The parentage of Muscat of Hamburg. Vitis - J. Grapevine Res. 42, 193–197. doi:10.5073/vitis.2003.42.193-197.

Cribari-Neto, F.; Zeileis, A. Beta. (2010). Regression in R. J. Stat. Softw. 34, 1–24.

Czimmerer, Z. et al. (2013). A Versatile Method to Design Stem-Loop Primer-Based Quantitative PCR Assays for Detecting Small Regulatory RNA Molecules', PLoS ONE, 8(1). doi: https://doi.org/10.1371/journal.pone.0055168.

D'Onofrio, C. et al. (2021). Parentage Atlas of Italian Grapevine Varieties as Inferred From SNP Genotyping. Frontiers in Plant Science, 11. doi: https://doi.org/10.3389/fpls.2020.605934.

Da Silva, C. et al. (2013). The high polyphenol content of grapevine cultivar tannat berries is conferred primarily by genes that are not shared with the reference genome. Plant Cell, 25(12), pp. 4777–4788. doi: https://doi.org/10.1105/tpc.113.118810.

Dalakouras, A., Wassenegger, M., Dadami, E., Ganopoulos, I., Pappas, M. L., and Papadopoulou, K. (2020). Genetically modified organism-free RNA interference: exogenous application of RNA molecules in plants. Plant Physiol. 182, 38–50. doi: 10.1104/pp.19.00570

Dalakouras, A., Wassenegger, M., McMillan, J. N., Cardoza, V., Maegele, I., Dadami, E., et al. (2016). Induction of silencing in plants by high-pressure spraying of in vitro-synthesized small RNAs. Front. Plant Sci. 7:1327. doi: 10.3389/fpls.2016.01327

Dalbó, M. A., Ye, G. N., Weeden, N. F., Wilcox, W. F., and Reisch, B. I. (2001). Marker-assisted Selection for Powdery Mildew Resistance in Grapes. J. Am. Soc. Hortic. Sci. 126, 83–89. doi:10.21273/JASHS.126.1.83.

Danecek, P. et al. (2021) 'Twelve years of SAMtools and BCFtools', GigaScience, 10(2). doi: https://doi.org/10.1093/gigascience/giab008.

Dangl, J. and Jones, J. (2001). Plant pathogens and integrated defence responses to infection. Nature.

Das, P. R., and Sherif, S. M. (2020). Application of exogenous dsRNAs-induced RNAi in agriculture: challenges and triumphs. Front. Plant Sci. 11:946. doi: 10.3389/fpls.2020.00946

De Lorenzis, G., Chipashvili, R., Failla, O., and Maghradze, D. (2015). Study of genetic variability in Vitis vinifera L. germplasm by high-throughput Vitis18kSNP array: The case of Georgian genetic resources. BMC Plant Biol., 15, 154. doi:10.1186/s12870-015-0510-9.

De Mendiburu, F.; Simon, R. (2015). Agricolae-Ten years of an open source statistical tool for experiments in breeding, agriculture and biology. PeerJ PrePrints, 3, e1404v1.

De Oliveira, A.F.; Serra, S.; Ligios, V.; Satta, D.; Nieddu, G. (2021). Assessing the effects of vineyard soil management on downy and powdery mildew development. Horticulturae, 7, 209.

Dechorgnat, J.; Nguyen, C.T.; Armengaud, P.; Jossier, M.; Diatloff, E.; Filleur, S.; Daniel-Vedele, F. (2011). From the soil to the seeds: The long journey of nitrate in plants. J. Exp. Bot., 62, 1349–1359.

Delmotte, F.; Mestre, P.; Schneider, C.; Kassemeyer, H.H.; Kozma, P.; Richart-Cervera, S.; Rouxel, M.; Delière, L. (2014). Rapid and multiregional adaptation to host partial resistance in a plant pathogenic oomycete: Evidence from European populations of Plasmopara viticola, the causal agent of grapevine downy mildew. Infect. Genet. Evol., 27, 500–508.

Delventhal, R. et al. (2017). A comparative analysis of nonhost resistance across the two Triticeae crop species wheat and barley. BMC Plant Biology, 17(1). doi: https://doi.org/10.1186/s12870-017-1178-0.

Dielen, A.S. et al. (2010) 'The ubiquitin/26S proteasome system in plant-pathogen interactions: A never-ending hide-and-seek game', Molecular Plant Pathology, pp. 293–308. doi: https://doi.org/10.1111/j.1364-3703.2009.00596.x.

Dietz, J.I.; Schierenbeck, M.; Simón, M.R. (2019). Impact of foliar diseases and its interaction with nitrogen fertilization and fungicides mixtures on green leaf area dynamics and yield in oat genotypes with different resistance. Crop Prot., 121, 80–88.

Díez-Navajas, A. M., Greif, C., Poutaraud, A., and Merdinoglu, D. (2007). Two simplified fluorescent staining techniques to observe infection structures of the oomycete Plasmopara viticola in grapevine leaf tissues. Micron 38, 680–683. doi: 10.1016/j.micron.2006.09.009

Divilov, K., Barba, P., Cadle, L., and Bruce, D. (2018). Single and multiple phenotype QTL analyses of downy mildew resistance in interspecific grapevines. Theor. Appl. Genet., 131, 1133–1143.

Dong, Y., Duan, S., Xia, Q., Liang, Z., Dong, X., Margaryan, K., et al. (2023). Dual domestications and origin of traits in grapevine evolution. Science (80). 379, 892–901. doi:10.1126/science.add8655.

Dubrovina, A. S., Aleynova, O. A., Kalachev, A. V., Suprun, A. R., Ogneva, Z. V., and Kiselev, K. V. (2019). Induction of transgene suppression in plants via external application of synthetic dsRNA. Int. J. Mol. Sci., 20:1585. doi: 10.3390/ijms20071585

Dubrovina, A.S. and Kiselev, K. V. (2019). Exogenous RNAs for gene regulation and plant resistance. International Journal of Molecular Sciences, 20(9). doi: https://doi.org/10.3390/ijms20092282.

Duplessis, S.; Cuomo, C.A.; Lin, Y.C.; Aerts, A.; Tisserant, E.; Veneault-Fourrey, C.; Joly, D.L.; Hacquard, S.; Amselem, J.; Cantarel, B.L.; et al. (2011). Obligate biotrophy features unraveled by the genomic analysis of rust fungi. Proc. Natl. Acad. Sci. USA, 108, 9166–9171.

Ebbesen, M. et al. (2008). Ethical Perspectives on RNA Interference Therapeutics, International Journal of Medical Sciences.

Eichmann, R., Schultheiss, H., Kogel, K.-H., and Hückelhoven, R. (2004). The barley apoptosis suppressor homologue bax inhibitor-1 compromises nonhost penetration resistance of barley to the inappropriate pathogen blumeria graminis f. sp. tritici. Mol. Plant-Microbe Interact. 17, 484–490. doi: 10.1094/MPMI.2004.17.5.484

Ellis, J., Dodds, P. and Pryor, T. (2000). Structure, function and evolution of plant disease resistance genes. Current Opinion in Plant Biology.

Erb, M. and Kliebenstein, D.J. (2020). Plant Secondary Metabolites as Defenses, Regulators, and Primary Metabolites: The Blurred Functional Trichotomy. Plant Physiology, pp. 39–52. doi: https://doi.org/10.1104/PP.20.00433.

Fagard, M.; Launay, A.; Clement, G.; Courtial, J.; Dellagi, A.; Farjad, M.; Krapp, A.; Soulie, M.-C.; Masclaux-Daubresse, C. (2014). Nitrogen metabolism meets phytopathology. J. Exp. Bot., 65, 5643–5656.

Fasoli, M., Dal Santo, S., Zenoni, S., Tornielli, G. B., Farina, L., Zamboni, A., et al. (2012). The grapevine expression atlas reveals a deep transcriptome shift driving the entire plant into a maturation program. Plant Cell, 24, 3489–3505. doi: 10.1105/tpc.112.100230

Feechan, A., Anderson, C., Torregrosa, L., Jermakow, A., Mestre, P., Wiedemann-Merdinoglu, S., et al. (2013). Genetic dissection of a TIR-NB-LRR locus from the wild North American grapevine species Muscadinia rotundifolia identifies paralogous genes conferring resistance to major fungal and oomycete pathogens in cultivated grapevine. Plant J., 76, 661–674. doi:10.1111/tpj.12327.

Ferrara, G.; Malerba, A.D.; Matarrese, A.M.S.; Mondelli, D.; Mazzeo, A. (2018). Nitrogen Distribution in Annual Growth of 'Italia' Table Grape Vines. Front. Plant Sci., 9, 1374.

Feuillet, C. et al. (2003) Map-based isolation of the leaf rust disease resistance gene Lr10 from the hexaploid wheat (Triticum aestivum L.) genome. doi: www.pnas.orgcgidoi10.1073pnas.2435133100.

Figueiredo, A., Monteiro, F. and Sebastiana, M. (2014). Subtilisin-like proteases in plant–pathogen recognition and immune priming: A perspective. Frontiers in Plant Science, 5(DEC). doi: https://doi.org/10.3389/fpls.2014.00739.

Figueiredo, A.; Monteiro, F.; Sebastiana, M. (2015). First clues on a jasmonic acid role in grapevine resistance against the biotrophic fungus Plasmopara viticola. Eur. J. Plant Pathol., 142, 645–652. doi: https://doi.org/10.1111/mpp.12567.

Fischer, B., Salakhutdinov, I., Akkurt, M., Eibach, R., Edwards, K., Toepfer, R., et al. (2004). Quantitative trait locus analysis of fungal disease resistance factors on a molecular map of grapevine. Theor. Appl. Genet., 108, 501–515. doi: 10.1007/s00122-003-1445-3.

Flutre, T., Le Cunff, L., Fodor, A., Launay, A., Romieu, C., Berger, G., et al. (2022). A genome-wide association and prediction study in grapevine deciphers the genetic architecture of multiple traits and identifies genes under many new QTLs. G3 Genes|Genomes|Genetics, 12. doi: 10.1093/g3journal/jkac103.

Foria, S. et al. (2018). The genetic background modulates the intensity of Rpv3-dependent downy mildew resistance in grapevine. Plant Breeding, 137(2), pp. 220–228. doi: https://doi.org/10.1111/pbr.12564.

Frichot, E., and François, O. (2015). LEA: An R package for landscape and ecological association studies. Methods Ecol. Evol., 6, 925–929. doi: 10.1111/2041-210X.12382.

Fröbel, S.; Zyprian, E. (2019). Colonization of Different Grapevine Tissues by Plasmopara viticola—A Histological Study. Front. Plant Sci., 10, 951. doi: https://doi.org/10.3389/fpls.2019.00951.

Fu, P., Wu, W., Lai, G., Li, R., Peng, Y., Yang, B., et al. (2020). Identifying Plasmopara viticola resistance Loci in grapevine (Vitis amurensis) via genotyping-by-sequencing-based QTL mapping. Plant Physiol. Biochem., 154, 75–84.

Fujita, A., Soma, N., Goto-yamamoto, N., Mizuno, A., Kiso, K., and Hashizume, K. (2007). Effect of shading on proanthocyanidin biosynthesis in the grape berry. J. Japanese Soc. Hortic. Sci., 76, 112–119.

Gadoury, D.M. et al. (2007). Effects of diffuse colonization of grape berries by Uncinula necator on bunch rots, berry microflora, and juice and wine quality. Phytopathology, 97(10), pp. 1356–1365. doi: https://doi.org/10.1094/PHYTO-97-10-1356.

Gadoury, D.M. et al. (2012). Grapevine powdery mildew (Erysiphe necator): A fascinating system for the study of the biology, ecology and epidemiology of an obligate biotroph. Molecular Plant Pathology, 13(1), pp. 1–16. doi: https://doi.org/10.1111/j.1364-3703.2011.00728.x.

Gaufichon, L. et al. (2010). Biological functions of asparagine synthetase in plants. Plant Science, pp. 141–153. doi: https://doi.org/10.1016/j.plantsci.2010.04.010.

Gessler, C., Pertot, I., and Perazzolli, M. (2011). Plasmopara viticola: a review of knowledge on downy mildew of grapevine and effective disease management. Phytopathol. Mediterr., 50, 3–44. doi: 10.14601/Phytopathol_Mediterr-9360

Ghosh, S. K. B., Hunter, W. B., Park, A. L., and Gundersen-Rindal, D. E. (2018). Double-stranded RNA oral delivery methods to induce RNA interference in phloem and plant-sap-feeding hemipteran insects. J. Vis. Exp. 135:57390. doi: 10.3791/57390

Giacomelli, L. et al. (2023). Simultaneous editing of two DMR6 genes in grapevine results in reduced susceptibility to downy mildew', Frontiers in Plant Science, 14. doi: https://doi.org/10.3389/fpls.2023.1242240.

Gorshkov, V. and Tsers, I. (2022). Plant susceptible responses: the underestimated side of plant–pathogen interactions. Biological Reviews, 97(1), pp. 45–66. doi: https://doi.org/10.1111/brv.12789.

Grimplet, J., Pimentel, D., Agudelo-Romero, P., Martinez-Zapater, J. M., and Fortes, A. M. (2017). The lateral organ boundaries domain gene family in grapevine: genome-wide

characterization and expression analyses during developmental processes and stress responses. Sci. Rep., 7: 15968. doi: 10.1038/s41598-017-16240-5

Gu, K.-X., Song, X.-S., Xiao, X.-M., Duan, X.-X., Wang, J.-X., Duan, Y.-B., et al. (2019). A β-tubulin dsRNA derived from Fusarium asiaticum confers plant resistance to multiple phytopathogens and reduces fungicide resistance. Pestic. Biochem. Physiol., 153, 36–46. doi: 10.1016/j.pestbp.2018.10.005

Guo, D.-L., Zhao, H.-L., Li, Q., Zhang, G.-H., Jiang, J.-F., Liu, C.-H., et al. (2019). Genome-wide association study of berry-related traits in grape [Vitis vinifera L.] based on genotyping-by-sequencing markers. Hortic. Res., 6, 11. doi: 10.1038/s41438-018-0089-z.

Gururani, M.A. et al. (2012). Plant disease resistance genes: Current status and future directions. Physiological and Molecular Plant Pathology, pp. 51–65. doi: https://doi.org/10.1016/j.pmpp.2012.01.002.

Haas, B.J. et al. (2003). Improving the Arabidopsis genome annotation using maximal transcript alignment assemblies. Nucleic acids research, 31(19), pp. 5654–66. doi: https://doi.org/10.1093/nar/gkg770.

Haas, B.J. et al. (2008). Automated eukaryotic gene structure annotation using EVidenceModeler and the Program to Assemble Spliced Alignments. Genome biology, 9(1), p. R7. doi: https://doi.org/10.1186/gb-2008-9-1-r7.

Hernández, I.; Gutiérrez, S.; Ceballos, S.; Palacios, F.; Toffolatti, S.L.; Maddalena, G.; Diago, M.P.; Tardaguila, J. (2022). Assessment of downy mildew in grapevine using computer vision and fuzzy logic. Development and validation of a new method. OENO One, 56, 41–53.

Hervé, M. (2020). Package 'RVAideMemoire'. See https://CRAN. R-project. org/package= RVAideMemoire, 0-9.

Hill, M.S., Vande Zande, P. and Wittkopp, P.J. (2021). Molecular and evolutionary processes generating variation in gene expression. Nature Reviews Genetics., pp. 203–215. doi: https://doi.org/10.1038/s41576-020-00304-w.

Hind, S.R. et al. (2011). The COP9 signalosome controls jasmonic acid synthesis and plant responses to herbivory and pathogens. Plant Journal, 65(3), pp. 480–491. doi: https://doi.org/10.1111/j.1365-313X.2010.04437.x.

Hintze, J.L.; Nelson, R.D. (1998). Violin plots: A box plot-density trace synergism. Am. Stat., 52, 181–184.

Hoffmann, S., Di Gaspero, G., Kovács, L., Howard, S., Kiss, E., Galbács, Z., et al. (2008). Resistance to Erysiphe necator in the grapevine 'Kishmish vatkana' is controlled by a single locus through restriction of hyphal growth. Theor. Appl. Genet., 116, 427–438. doi: 10.1007/s00122-007-0680-4.

Hood, M., and Shew, H. (1996). Applications of KOH-aniline blue fluorescence in the study of plant-fungal interactions. Phytopathology, 86:704.

Huang, X., Liu, G., and Zhang, W. (2018). Genome-wide analysis of LBD (lateral organ boundaries domain) gene family in brassica rapa. Brazilian Arch. Biol. Technol., 61:e18180049.

Huber, D.; Thompson, I. (2007). Nitrogen and plant disease. In Mineral Nutrition and Plant Disease; Datnoff, L., Elmer, W., Huber, D., Eds.; APS Press: St. Paul, MN, USA, pp. 31–44.

Hwang, I.S., An, S.H. and Hwang, B.K. (2011). Pepper asparagine synthetase 1 (CaAS1) is required for plant nitrogen assimilation and defense responses to microbial pathogens. Plant Journal, 67(5), pp. 749–762. doi: https://doi.org/10.1111/j.1365-313X.2011.04622.x.

Iqbal, Z. et al. (2021). Plant Defense Responses to Biotic Stress and Its Interplay With Fluctuating Dark/Light Conditions. Frontiers in Plant Science. doi: https://doi.org/10.3389/fpls.2021.631810.

Jaillon, O. et al. (2007). The grapevine genome sequence suggests ancestral hexaploidization in major angiosperm phyla. Nature, 449(7161), pp. 463–467. doi: https://doi.org/10.1038/nature06148.

Jia, H. et al. (2017). Genome editing of the disease susceptibility gene CsLOB1 in citrus confers resistance to citrus canker. Plant Biotechnology Journal, 15(7), pp. 817–823. doi: https://doi.org/10.1111/pbi.12677.

Jombart, T. (2008). ADEGENET: A R package for the multivariate analysis of genetic markers. Bioinformatics 24, 1403–1405. doi: 10.1093/bioinformatics/btn129.

Jones, J. D. G., and Dangl, J. L. (2006). The plant immune system. Nature 444, 323–329. doi: 10.1038/nature05286

Jones, P. et al. (2014). InterProScan 5: genome-scale protein function classification. Bioinformatics (Oxford, England), 30(9), pp. 1236–40.

Judelson, H. S., and Ah-Fong, A. M. V. (2019). Exchanges at the plant-oomycete interface that influence disease. Plant Physiol. 179, 1198–1211. doi: 10.1104/pp.18.00979

Kamvar, Z. N., Tabima, J. F., and Grünwald, N. J. (2014). Poppr: an R package for genetic analysis of populations with clonal, partially clonal, and/or sexual reproduction. PeerJ 2, e281. doi: 10.7717/peerj.281.

Karn, A., Zou, C., Brooks, S., Fresnedo-Ramírez, J., Gabler, F., Sun, Q., et al. (2021). Discovery of the REN11 Locus From Vitis aestivalis for Stable Resistance to Grapevine Powdery Mildew in a Family Segregating for Several Unstable and Tissue-Specific Quantitative Resistance Loci. Front. Plant Sci., 12. doi: 10.3389/fpls.2021.733899.

Kazan, K. and Manners, J.M. (2009). Linking development to defense: auxin in plant-pathogen interactions. Trends in Plant Science, pp. 373–382. doi: https://doi.org/10.1016/j.tplants.2009.04.005.

Kearsey, M. J., and Farquhar, A. G. L. (1998). QTL analysis in plants; where are we now? Heredity (Edinb). 80, 137–142. doi: 10.1046/j.1365-2540.1998.00500.x.

Keller, M. (2015). The Science of Grapevines: Anatomy and Physiology.

Keller, M. (2005). Deficit Irrigation and Vine Mineral Nutrition. Am. J. Enol. Vitic., 56, 267–283.

Kennelly, M.M.; Gadoury, D.M.; Wilcox, W.F.; Magarey, P.A.; Seem, R.C. (2007). Primary infection, lesion productivity, and survival of sporangia in the grapevine downy mildew pathogen Plasmopara viticola. Phytopathology, 97, 512–522.

Kerschen, A., Napoli, C. A., Jorgensen, R. A., and Müller, A. E. (2004). Effectiveness of RNA interference in transgenic plants. FEBS Lett. 566, 223–228.

Kim, D. et al. (2019). Graph-based genome alignment and genotyping with HISAT2 and HISAT-genotype. Nature Biotechnology, 37(8), pp. 907–915. doi: https://doi.org/10.1038/s41587-019-0201-4.

Kim, D. H., and Rossi, J. J. (2007). Strategies for silencing human disease using RNA interference. Nat. Rev. Genet. 8, 173–184.

Kim, H.S. et al. (2014). Overexpression of the Brassica rapa transcription factor WRKY12 results in reduced soft rot symptoms caused by Pectobacterium carotovorum in Arabidopsis and Chinese cabbage. Plant Biology, 16(5), pp. 973–981. doi: https://doi.org/10.1111/plb.12149.

Kim, M.-J., Kim, M., Lee, M. R., Park, S. K., and Kim, J. (2015). Lateral organ boundaries domain (LBD)10 interacts with SIDECAR POLLEN / LBD27 to control pollen development in Arabidopsis. Plant J. 81, 794–809. doi: 10.1111/tpj.12767

Kim, S.-M., and Reinke, R. F. (2019). A novel resistance gene for bacterial blight in rice, Xa43(t) identified by GWAS, confirmed by QTL mapping using a bi-parental population. PLoS One 14, e0211775. doi: 10.1371/journal.pone.0211775.

Konakalla, N. C., Kaldis, A., Berbati, M., Masarapu, H., and Voloudakis, A. E. (2016). Exogenous application of double-stranded RNA molecules from TMV p126 and CP genes confers resistance against TMV in tobacco. Planta 244, 961–969. doi: 10.1007/s00425-016-2567-6

Korf, I. (2004). Gene finding in novel genomes. BMC bioinformatics, 5, p. 59. doi: https://doi.org/10.1186/1471-2105-5-59.

Korte, A., and Farlow, A. (2013). The advantages and limitations of trait analysis with GWAS: a review. Plant Methods 9, 1–9.

Kruijt, M., Brandwagt, B.F. and De Wit, P.J.G.M. (2004). Rearrangements in the Cf-9 disease resistance gene cluster of wild tomato have resulted in three genes that mediate Avr9 responsiveness. Genetics, 168(3), pp. 1655–1663. doi: https://doi.org/10.1534/genetics.104.028985.

Kunkel, B.N. and Harper, C.P. (2018). The roles of auxin during interactions between bacterial plant pathogens and their hosts. Journal of Experimental Botany. Oxford University Press, pp. 245–254. doi: https://doi.org/10.1093/jxb/erx447.

Kusch, S., and Panstruga, R. (2017). Mlo -based resistance: an apparently universal “weapon” to defeat powdery mildew disease. Mol. Plant-Microbe Interact. 30, 179–189. doi: 10.1094/MPMI-12-16-0255-CR

Lai, S.H. and Chye, M.L. (2021). Plant acyl-CoA-binding proteins—their lipid and protein interactors in abiotic and biotic stresses. Cells. MDPI. doi: https://doi.org/10.3390/cells10051064.

Laucou, V., Launay, A., Bacilieri, R., Lacombe, T., Adam-Blondon, A.-F., Bérard, A., et al. (2018). Extended diversity analysis of cultivated grapevine Vitis vinifera with 10K genome-wide SNPs. PLoS One, 13, 1–27. doi: https://doi.org/10.1371/journal.pone.0192540

Lea, P.J.; Blackwell, R.D.; Chen, F.-L.; Hecht, U. (1990). Enzymes of Ammonia Assimilation. In Enzymes of Primary Metabolism; Elsevier: Amsterdam, The Netherlands, pp. 257–276.

Lee, H.J. and Park, O.K. (2019). Lipases associated with plant defense against pathogens. Plant Science. Elsevier Ireland Ltd, pp. 51–58. doi: https://doi.org/10.1016/j.plantsci.2018.07.003.

Lee, S.; Park, J.; Lee, J.; Shin, D.; Marmagne, A.; Lim, P.O.; Masclaux-Daubresse, C.; An, G.; Nam, H.G. (2020). OsASN1 Overexpression in Rice Increases Grain Protein Content and Yield under Nitrogen-Limiting Conditions. Plant Cell Physiol., 61, 1309–1320. doi: https://doi.org/10.1093/PCP/PCAA060.

Lejay, L.; Gojon, A. (2018). Root Nitrate Uptake. In Membrane Transport in Plants; Elsevier: Amsterdam, The Netherlands, pp. 139–169.

Lenth, R. (2021). Emmeans: Estimated Marginal Means, Aka Least-Squares Means. R Package Version 1.5.3. doi: https://CRAN.R-project.org/package=emmeans

Li, X., Wu, J., Yin, L., Zhang, Y., Qu, J., and Lu, J. (2015). Comparative transcriptome analysis reveals defense-related genes and pathways against downy mildew in Vitis amurensis grapevine. Plant Physiol. Biochem. 95, 1–14. doi: 10.1016/j.plaphy.2015.06.016

Licausi, F., Ohme-Takagi, M. and Perata, P. (2013). APETALA2/Ethylene Responsive Factor (AP2/ERF) transcription factors: mediators of stress responses and developmental programs. The New phytologist, pp. 639–649. doi: https://doi.org/10.1111/nph.12291.

Lin, H., Leng, H., Guo, Y., Kondo, S., Zhao, Y., Shi, G., et al. (2019). QTLs and candidate genes for downy mildew resistance conferred by interspecific grape (V. vinifera L. × V. amurensis Rupr.) crossing. Sci. Hortic. (Amsterdam). 244, 200–207.

Liu, C. et al. (2022). Nicotiana benthamiana asparagine synthetase associates with IP-L and confers resistance against tobacco mosaic virus via the asparagine-induced salicylic acid signalling pathway. Molecular Plant Pathology, 23(1), pp. 60–77. doi: https://doi.org/10.1111/mpp.13143.

Liu, G.; Ji, Y.; Bhuiyan, N.H.; Pilot, G.; Selvaraj, G.; Zou, J.; Wei, Y. (2010). Amino Acid Homeostasis Modulates Salicylic Acid–Associated Redox Status and Defense Responses in Arabidopsis. Plant Cell, 22, 3845–3863.

Liu, H., Wang, S., Yu, X., Yu, J., He, X., Zhang, S., et al. (2005). ARL1, a LOB-domain protein required for adventitious root formation in rice. Plant J. 43, 47–56. doi: 10.1111/j.1365-313X.2005.02434.x

Livak, K.J. and Schmittgen, T.D. (2001). Analysis of relative gene expression data using real-time quantitative PCR and the 2-ΔΔCT method. Methods, 25(4), pp. 402–408. doi: https://doi.org/10.1006/meth.2001.1262.

Lomsadze, A. et al. (2005). Gene identification in novel eukaryotic genomes by self-training algorithm. Nucleic Acids Research, 33(20), pp. 6494–6506. doi: https://doi.org/10.1093/nar/gki937.

Lorrain, S. et al. (2004). Vascular Associated Death1, a novel GRAM domain-containing protein, is a regulator of cell death and defence responses in vascular tissues. Plant Cell, 16(8), pp. 2217–2232. doi: https://doi.org/10.1105/tpc.104.022038.

Love, M.I., Huber, W. and Anders, S. (2014). Moderated estimation of fold change and dispersion for RNA-seq data with DESeq2. Genome Biology, 15(12). doi: https://doi.org/10.1186/s13059-014-0550-8.

Lu, Q., Shao, F., Macmillan, C., Wilson, I. W., van der Merwe, K., Hussey, S. G., et al. (2018). Genomewide analysis of the lateral organ boundaries domain gene family in Eucalyptus grandis reveals members that differentially impact secondary growth. Plant Biotechnol. J. 16, 124–136. doi: 10.1111/pbi.12754

Luo, C.; Ma, L.; Zhu, J.; Guo, Z.; Dong, K.; Dong, Y. (2021). Effects of Nitrogen and Intercropping on the Occurrence of Wheat Powdery Mildew and Stripe Rust and the Relationship With Crop Yield. Front. Plant Sci., 12, 637393.

Luo, Y., Chen, Q., Luan, J., Chung, S. H., Van Eck, J., Turgeon, R., et al. (2017). Towards an understanding of the molecular basis of effective RNAi against a global insect pest, the whitefly Bemisia tabaci. Insect Biochem. Mol. Biol. 88, 21–29. doi: 10.1016/j.ibmb.2017.07.005

Ma, X. et al. (2020). The RNA degradome: a precious resource for deciphering RNA processing and regulation codes in plants. RNA Biology, 17(9), pp. 1223–1227. doi: https://doi.org/10.1080/15476286.2020.1757898.

Maddalena, G., Delmotte, F., Bianco, P. A., De Lorenzis, G., and Toffolatti, S. L. (2020). Genetic structure of Italian population of the grapevine downy mildew agent, plasmopara viticola. Ann. Appl. Biol. 176, 257–267. doi: 10.1111/aab.12567

Magris, G. et al. (2021). The genomes of 204 Vitis vinifera accessions reveal the origin of European wine grapes. Nature Communications, 12(1). doi: https://doi.org/10.1038/s41467-021-27487-y.

Mangeon, A., Bell, E. M., Lin, W., Jablonska, B., and Springer, P. S. (2011). Misregulation of the LOB domain gene DDA1 suggests possible functions in auxin signalling and photomorphogenesis. J. Exp. Bot. 62, 221–233. doi: 10.1093/jxb/erq259

Marçais, G. et al. (2018). MUMmer4: A fast and versatile genome alignment system. PLoS Computational Biology, 14(1). doi: https://doi.org/10.1371/journal.pcbi.1005944.

Marcianò, D.; Ricciardi, V.; Marone Fassolo, E.; Passera, A.; Bianco, P.; Failla, O.; Casati, P.; Maddalena, G.; De Lorenzis, G.; Toffolatti, S. (2021). RNAi of a putative grapevine susceptibility gene as a possible downy mildew control strategy. Front. Plant Sci., 12, 667319. https://doi.org/10.3389/fpls.2021.667319.

Marguerit, E., Boury, C., Manicki, A., Donnart, M., Butterlin, G., Némorin, A., et al. (2009). Genetic dissection of sex determinism, inflorescence morphology and downy mildew resistance in grapevine. Theor. Appl. Genet. 118, 1261–1278. doi: 10.1007/s00122-009-0979-4.

Massi, F.; Marcianò, D.; Russo, G.; Stuknyté, M.; Arioli, S.; Mora, D.; Toffolatti, S.L. (2022). Evaluation of the characteristics and infectivity of the secondary inoculum produced by Plasmopara viticola on grapevine leaves by means of flow cytometry and cell sorting. Appl. Environ. Microbiol., 88, e01010-22.

Massonnet, M. et al. (2020). The genetic basis of sex determination in grapes. Nature Communications, 11(1). doi: https://doi.org/10.1038/s41467-020-16700-z.

Massonnet, M. et al. (2022). The grape powdery mildew resistance loci Ren2, Ren3, Ren4D, Ren4U, Run1, Run1.2b, Run2.1, and Run2.2 activate different transcriptional responses to Erysiphe necator. Frontiers in Plant Science, 13. doi: https://doi.org/10.3389/fpls.2022.1096862.

Mattos, A.P.; Tolentino Júnior, J.B.; Itako, A.T. (2020). Determination of the severity of Septoria leaf spot in tomato by using digital images. Australas. Plant Pathol., 49, 329–356.

Maul, E., Sudharma, K., Kecke, S., Marx, G., Müller, C., Audeguin, L., et al. (2012). The European Vitis Database (www.eu-vitis.de): A technical innovation through an online uploading and interactive modification system. Vitis - J. Grapevine Res. 51, 79–85.

Meister, G., Landthaler, M., Dorsett, Y., and Tuschl, T. (2004). Sequence-specific inhibition of microRNA- and siRNA-induced RNA silencing. RNA 10, 544–550. doi: 10.1261/rna.5235104

Melnyk, C. W., Molnar, A., and Baulcombe, D. C. (2011). Intercellular and systemic movement of RNA silencing signals. EMBO J. 30, 3553–3563.

Merdinoglu, D. et al. (2018). Breeding for durable resistance to downy and powdery mildew in grapevine. Oeno One, 52(3), pp. 189–195. doi: https://doi.org/10.20870/oeno-one.2018.52.3.2116.

Merdinoglu, D., Wiedeman-Merdinoglu, S., Coste, P., Dumas, V., Haetty, S., Butterlin, G., et al. (2003). Genetic analysis of downy mildew resistance derived from Muscadinia rotundifolia. Proceedings of the Eighth International Conference on Grape Genetics and Breeding. Acta Hortic. 603, 451–456.

Mezzetti, B., Smagghe, G., Arpaia, S., Christiaens, O., Dietz-Pfeilstetter, A., Jones, H., et al. (2020). RNAi: What is its position in agriculture? J. Pest Sci., 93, 1125–1130.

Minio, A. et al. (2018). Isoform-scale annotation and expression profiling of the Cabernet Sauvignon transcriptome using single-molecule sequencing of full-length cDNA. G3: Genes, Genomes, Genetics. doi: https://doi.org/10.1101/269530.

Minio, A. et al. (2022). Assembly of complete diploid-phased chromosomes from draft genome sequences. G3: Genes, Genomes, Genetics, 12(8). doi: https://doi.org/10.1093/g3journal/jkac143.

Minio, A., Massonnet, M., Figueroa-Balderas, R., Castro, A., et al. (2019). Diploid genome assembly of the wine grape carménère. G3: Genes, Genomes, Genetics, 9(5), pp. 1331–1337. doi: https://doi.org/10.1534/g3.119.400030.

Minio, A., Massonnet, M., Figueroa-Balderas, R., Vondras, A.M., et al. (2019). Iso-Seq allows genome-independent transcriptome profiling of grape berry development. G3: Genes, Genomes, Genetics, 9(3), pp. 755–767. doi: https://doi.org/10.1534/g3.118.201008.

Mitter, N., Worrall, E. A., Robinson, K. E., Li, P., Jain, R. G., Taochy, C., et al. (2017). Clay nanosheets for topical delivery of RNAi for sustained protection against plant viruses. Nat. Plants 3:16207. doi: 10.1038/nplants.2016.207

Moison, M.; Marmagne, A.; Dinant, S.; Soulay, F.; Azzopardi, M.; Lothier, J.; Citerne, S.; Morin, H.; Legay, N.; Chardon, F.; et al. (2018). Three cytosolic glutamine synthetase isoforms localized in different-order veins act together for N remobilization and seed filling in Arabidopsis. J. Exp. Bot., 69, 4379–4393. doi: https://doi.org/10.1093/jxb/ery217.

Monaghan, J. and Li, X. (2010). The HEAT repeat protein ILITYHIA is Required for plant immunity. Plant and Cell Physiology, 51(5), pp. 742–753. doi: https://doi.org/10.1093/pcp/pcq038.

Moreira, F. M., Madini, A., Marino, R., Zulini, L., Stefanini, M., Velasco, R., et al. (2011). Genetic linkage maps of two interspecific grape crosses (Vitis spp.) used to localize quantitative trait loci for downy mildew resistance. Tree Genet. Genomes 7, 153–167. doi:10.1007/s11295-010-0322-x.

Morozov, S. Y., Solovyev, A. G., Kalinina, N. O., and Taliansky, M. E. (2019). Double-stranded RNAs in plant protection against pathogenic organisms and viruses in agriculture. Acta Naturae 11, 13–21.

Munhoz, C.F. et al. (2015). Analysis of plant gene expression during passion fruit- Xanthomonas axonopodis interaction implicates lipoxygenase 2 in host defence. Annals of Applied Biology, 167(1), pp. 135–155. doi: https://doi.org/10.1111/aab.12215.

Myles, S. et al. (2011) 'Genetic structure and domestication history of the grape', Proceedings of the National Academy of Sciences of the United States of America, 108(9), pp. 3530–3535. Doi: https://doi.org/10.1073/pnas.1009363108.

Nerva, L., Sandrini, M., Gambino, G., and Chitarra, W. (2020). Double-stranded rnas (Dsrnas) as a sustainable tool against gray mold (botrytis cinerea) in grapevine: Effectiveness of different application methods in an open-air environment. Biomolecules 10:200. doi: 10.3390/biom10020200.

Neumann, S.; Paveley, N.D.; Beed, F.D.; Sylvester-Bradley, R. (2004). Nitrogen per unit leaf area affects the upper asymptote of Puccinia striiformis f.sp. tritici epidemics in winter wheat. Plant Pathol., 53, 725–732.

Newman, M. A., Sundelin, T., Nielsen, J. T., and Erbs, G. (2013). MAMP (microbe-associated molecular pattern) triggered immunity in plants. Front. Plant Sci., 4:139. doi: 10.3389/fpls.2013.00139

Niehl, A., Soininen, M., Poranen, M. M., and Heinlein, M. (2018). Synthetic biology approach for plant protection using dsRNA. Plant Biotechnol. J. 16, 1679–1687. doi: 10.1111/pbi.12904

Niks, R.E. and Marcel, T.C. (2009). Nonhost and basal resistance: How to explain specificity? New Phytologist, pp. 817–828. doi: https://doi.org/10.1111/j.1469-8137.2009.02849.x.

Ochssner, I., Hausmann, L., and Töpfer, R. (2016). Rpv14, a new genetic source for Plasmopara viticola resistance conferred by Vitis cinerea. Vitis 55, 79–81. doi:10.5073/vitis.2016.55.79-81.

Offen, W. et al. (2006). Structure of a flavonoid glucosyltransferase reveals the basis for plant natural product modification. EMBO Journal, 25(6), pp. 1396–1405. doi: https://doi.org/10.1038/sj.emboj.7600970.

Okamoto, M.; Kumar, A.; Li, W.; Wang, Y.; Siddiqi, M.Y.; Crawford, N.M.; Glass, A.D.M. (2006). High-Affinity Nitrate Transport in Roots of Arabidopsis Depends on Expression of the NAR2-Like Gene AtNRT3.1. Plant Physiol., 140, 1036–1046.

Okushima, Y., Fukaki, H., Onoda, M., Theologis, A., and Tasaka, M. (2007). ARF7 and ARF19 regulate lateral root formation via direct activation of LBD/ASL genes in arabidopsis. Plant Cell 19, 118–130. doi: 10.1105/tpc.106.047761

Ollat, N., Peccoux, A., Papura, D., Esmenjaud, D., Marguerit, E., Tandonnet, J. P., et al. (2015). “Rootstocks as a component of adaptation to environment,” in Grapevine in a Changing Environment: A Molecular and Ecophysiological Perspective, eds H. V. Gerós, M. M. Chaves, H. M. Gil, and S. Delrot (Chichester, UK), 68–94. doi: 10.1002/9781118735985.ch4

Olmo, H. P., McGovern, P. E., Fleming, S. J., and Katz, S. H. (1995). The Origins and Ancient History of Wine. McGovern P, éd. Orig. Anc. Hist. Wine. Amsterdam Gordon Breach 31, 43.

Osuna, D.; Gálvez-Valdivieso, G.; Piedras, P.; Pineda, M.; Aguilar, M. (2001). Cloning, characterization and mRNA expression analysis of PVAS1, a type I asparagine synthetase gene from Phaseolus vulgaris. Planta, 213, 402–410.

Panstruga, R. and Moscou, M.J. (2020). What is the molecular basis of nonhost resistance? Molecular Plant-Microbe Interactions. American Phytopathological Society, pp. 1253–1264. doi: https://doi.org/10.1094/MPMI-06-20-0161-CR.

Panthapulakkal Narayanan, S. et al. (2020). The overexpression of OsACBP5 protects transgenic rice against necrotrophic, hemibiotrophic and biotrophic pathogens. Scientific Reports, 10(1). doi: https://doi.org/10.1038/s41598-020-71851-9.

Pap, D., Riaz, S., Dry, I. B., Jermakow, A., Tenscher, A. C., Cantu, D., et al. (2016). Identification of two novel powdery mildew resistance loci, Ren6 and Ren7, from the wild Chinese grape species Vitis piasezkii. BMC Plant Biol. 16, 170. doi:10.1186/s12870-016-0855-8.

Patro, R. et al. (2017). Salmon provides fast and bias-aware quantification of transcript expression. Nature Methods, 14(4), pp. 417–419. doi: https://doi.org/10.1038/nmeth.4197.

Pavan, S., Jacobsen, E., Visser, R. G. F., and Bai, Y. (2010). Loss of susceptibility as a novel breeding strategy for durable and broad-spectrum resistance. Mol. Breed. 25, 1–12. doi: 10.1007/s11032-009-9323-6

Perreault, F.; Oukarroum, A.; Pirastru, L.; Sirois, L.; Gerson Matias, W.; Popovic, R. (2010). Evaluation of Copper Oxide Nanoparticles Toxicity Using Chlorophyll a Fluorescence Imaging in Lemna gibba. J. Bot., 2010, 763142.

Pessina, S., Lenzi, L., Perazzolli, M., Campa, M., Dalla Costa, L., Urso, S., et al. (2016). Knockdown of MLO genes reduces susceptibility to powdery mildew in grapevine. Hortic. Res. 3:16016. doi: 10.1038/hortres.2016.16

Pirrello, C. et al. (2019). Emergent Ascomycetes in Viticulture: An Interdisciplinary Overview. Frontiers in Plant Science. doi: https://doi.org/10.3389/fpls.2019.01394.

Pirrello, C. et al. (2022). Grapevine DMR6-1 Is a Candidate Gene for Susceptibility to Downy mildew. Biomolecules, 12(2). doi: https://doi.org/10.3390/biom12020182.

Pirrello, C., Zeilmaker, T., Bianco, L., Giacomelli, L., Moser, C., and Vezzulli, S. (2021). Mining grapevine downy mildew susceptibility genes: a resource for genomics-based breeding and tailored gene editing. Biomolecules 11, 1–23. doi: 10.3390/biom11020181

Possamai, T., Wiedemann-Merdinoglu, S., Merdinoglu, D., Migliaro, D., De Mori, G., Cipriani, G., et al. (2021). Construction of a high-density genetic map and detection of a major QTL of resistance to powdery mildew (Erysiphe necator Sch.) in Caucasian grapes (Vitis vinifera L.). BMC Plant Biol. 21, 528. doi:10.1186/s12870-021-03174-4.

Possamai, T.; Wiedemann-Merdinoglu, S. (2022). Phenotyping for QTL identification: A case study of resistance to Plasmopara viticola and Erysiphe necator in grapevine. Front. Plant Sci., 13, 930954.

Pré, M. et al. (2008). The AP2/ERF domain transcription factor ORA59 integrates jasmonic acid and ethylene signals in plant defense. Plant Physiology, 147(3), pp. 1347–1357. doi: https://doi.org/10.1104/pp.108.117523.

Pugliese, M., Gullino, M.L. and Garibaldi, A. (2011). Effect Of Climate Change On Infection Of Grapevine By Down And Powdery Mildew Under Controlled Environment. doi: https://www.researchgate.net/publication/227160227.

Purcell, S., Neale, B., Todd-Brown, K., Thomas, L., Ferreira, M. A. R., Bender, D., et al. (2007). PLINK: a tool set for whole-genome association and population-based linkage analyses. Am. J. Hum. Genet. 81, 559–575.

Quinlan, A.R. and Hall, I.M. (2010). BEDTools: A flexible suite of utilities for comparing genomic features. Bioinformatics, 26(6), pp. 841–842. doi: https://doi.org/10.1093/bioinformatics/btq033.

R Core Team (2021). R: A language and environment for statistical computing. R Found. Stat. Comput. Vienna, Austria.

R Core Team. (2019). R: A Language and Environment for Statistical Computing; R Foundation for Statistical Computing: Vienna, Austria; Available at: https://www.R-project.org/.

Rast, M. I., and Simon, R. (2012). Arabidopsis jagged lateral organs acts with asymmetric leaves2 to coordinate knox and pin expression in shoot and root meristems. Plant Cell 24, 2917–2933. doi: 10.1105/tpc.112.099978

Reid, K. E., Olsson, N., Schlosser, J., Peng, F., and Lund, S. T. (2006). An optimized grapevine RNA isolation procedure and statistical determination of reference genes for real-time RT-PCR during berry development. BMC Plant Biol. 6:27. doi: 10.1186/1471-2229-6-27

Riaz, S. et al. (2018). Genetic diversity analysis of cultivated and wild grapevine (Vitis vinifera L.) accessions around the Mediterranean basin and Central Asia. BMC Plant Biology, 18(1). doi: https://doi.org/10.1186/s12870-018-1351-0.

Riaz, S., Tenscher, A. C., Ramming, D. W., and Walker, M. A. (2011). Using a limited mapping strategy to identify major QTLs for resistance to grapevine powdery mildew (Erysiphe necator) and their use in marker-assisted breeding. Theor. Appl. Genet. 122, 1059–1073. doi: 10.1007/s00122-010-1511-6.

Ricciardi, V.; Marcianò, D.; Sargolzaei, M.; Maddalena, G.; Maghradze, D.; Tirelli, A.; Casati, P.; Bianco, P.A.; Failla, O.; Fracassetti, D.; et al. (2021). From plant resistance response to the discovery of antimicrobial compounds: The role of volatile organic compounds (VOCs) in grapevine downy mildew infection. Plant Physiol. Biochem., 160, 294–305. doi: 10.1016/j.plaphy.2021.01.035

Rienth, M. et al. (2021). Modifications of Grapevine Berry Composition Induced by Main Viral and Fungal Pathogens in a Climate Change Scenario. Frontiers in Plant Science. doi: https://doi.org/10.3389/fpls.2021.717223.

Robinson, J.T. et al. (2011). Integrative genomics viewer. Nature Biotechnology, pp. 24–26. doi: https://doi.org/10.1038/nbt.1754.

Rosa, C., Kuo, Y.-W., Wuriyanghan, H., and Falk, B. W. (2018). RNA interference mechanisms and applications in plant pathology. Annu. Rev. Phytopathol. 56, 581–610. doi: 10.1146/annurev-phyto-080417-050044

Rubin, G., Tohge, T., Matsuda, F., Saito, K., and Scheible, W.-R. (2009). Members of the LBD family of transcription factors repress anthocyanin synthesis and affect additional nitrogen responses in arabidopsis. Plant Cell 21, 3567–3584. doi: 10.1105/tpc.109.067041

Rumbolz, J., Wirtz, S., Kassemeyer, H.-H., Guggenheim, R., Schäfer, E., and Büche, C. (2002). Sporulation of plasmopara viticola: differentiation and light regulation. Plant Biol. 4, 413–422. doi: 10.1093/jxb/erv137

Rustioni, L. et al. (2019). Description of the vitis vinifera L. Phenotypic variability in eno-carpological traits by a Euro-Asiatic collaborative network among ampelographic collections. Vitis - Journal of Grapevine Research, 58(1), pp. 37–46. doi: https://doi.org/10.5073/vitis.2019.58.37-46.

Sakiroglu, M., and Brummer, E. C. (2017). Identification of loci controlling forage yield and nutritive value in diploid alfalfa using GBS-GWAS. Theor. Appl. Genet. 130, 261–268. doi:10.1007/s00122-016-2782-3.

Salotti, I. et al. (2022). Information on disease resistance patterns of grape varieties may improve disease management. Frontiers in Plant Science, 13. doi: https://doi.org/10.3389/fpls.2022.1017658.

Sapkota, S. et al. (2023). Discovery and genome-guided mapping of REN12 from Vitis amurensis, conferring strong, rapid resistance to grapevine powdery mildew. Horticulture Research, 10(5). doi: https://doi.org/10.1093/hr/uhad052.

Sapkota, S., Chen, L.-L., Yang, S., Hyma, K. E., Cadle-Davidson, L., and Hwang, C.-F. (2019). Construction of a high-density linkage map and QTL detection of downy mildew resistance in Vitis aestivalis-derived 'Norton.' Theor. Appl. Genet. 132, 137–147.

Sargolzaei, M. et al. (2021). Georgian Grapevine Cultivars: Ancient Biodiversity for Future Viticulture. Frontiers in Plant Science. doi: https://doi.org/10.3389/fpls.2021.630122.

Sargolzaei, M., Maddalena, G., Bitsadze, N., Maghradze, D., Bianco, P. A., Failla, O., et al. (2020). Rpv29, Rpv30 and Rpv31: Three Novel Genomic Loci Associated With Resistance to Plasmopara viticola in Vitis vinifera. Front. Plant Sci. 11. doi:10.3389/fpls.2020.562432.

Schaller, A., Stintzi, A. and Graff, L. (2012). Subtilases - versatile tools for protein turnover, plant development, and interactions with the environment. Physiologia Plantarum, pp. 52–66. doi: https://doi.org/10.1111/j.1399-3054.2011.01529.x.

Schreiber, U.; Quayle, P.; Schmidt, S.; Escher, B.I.; Mueller, J.F. (2007). Methodology and evaluation of a highly sensitive algae toxicity test based on multiwell chlorophyll fluorescence imaging. Biosens. Bioelectron., 22, 2554–2563.

Schwander, F., Eibach, R., Fechter, I., Hausmann, L., Zyprian, E., and Töpfer, R. (2012). Rpv10: a new locus from the Asian Vitis gene pool for pyramiding downy mildew resistance loci in grapevine. Theor. Appl. Genet. 124, 163–176.

Segarra, J.; Jeger, M.J.; Van Den Bosch, F. (2001). Epidemic Dynamics and Patterns of Plant Diseases. Phytopathology, 91, 1001–1010.

Seifi, H.S.; De Vleesschauwer, D.; Aziz, A.; Höfte, M. (2014). Modulating plant primary amino acid metabolism as a necrotrophic virulence strategy. Plant Signal. Behav., 9, e27995. https://doi.org/10.4161/psb.27995.

Semiarti, E., Ueno, Y., Tsukaya, H., Iwakawa, H., Machida, C., and Machida, Y. (2001). The ASYMMETRIC LEAVES2 gene of Arabidopsis thaliana regulates formation of a symmetric lamina, establishment of venation and repression of meristem-related homeobox genes in leaves. Development 128, 1771–1783.

Sharbati-Tehrani, S. et al. (2008). MiR-Q: A novel quantitative RT-PCR approach for the expression profiling of small RNA molecules such as miRNAs in a complex sample. BMC Molecular Biology, 9. doi: https://doi.org/10.1186/1471-2199-9-34.

Shi, X. et al. (2023). The complete reference genome for grapevine (Vitis vinifera L.) genetics and breeding. Horticulture Research, 10(5). doi: https://doi.org/10.1093/hr/uhad061.

Simón, M.R.; Fleitas, M.C.; Castro, A.C.; Schierenbeck, M. (2020). How Foliar Fungal Diseases Affect Nitrogen Dynamics, Milling, and End-Use Quality of Wheat. Front. Plant Sci., 11, 1568.

Slater, G.S.C. and Birney, E. (2005). Automated generation of heuristics for biological sequence comparison. BMC Bioinformatics, 6, pp. 1–11. doi: https://doi.org/10.1186/1471-2105-6-31.

Smithson, M.; Verkuilen, J. (2006). A better lemon squeezer? Maximum-likelihood regression with beta-distributed dependent variables. Psychol. Methods, 11, 54–71.

Soneson, C., Love, M.I. and Robinson, M.D. (2015). Differential analyses for RNA-seq: transcript-level estimates improve gene-level inferences. F1000Research, 4, p. 1521. doi: https://doi.org/10.12688/f1000research.7563.1.

Song, B., Tang, Z., Li, X., Li, J., Zhang, M., Zhao, K., et al. (2020). Mining and evolution analysis of lateral organ boundaries domain (LBD) genes in Chinese white pear (Pyrus bretschneideri). BMC Genomics 21:644. doi: 10.1186/s12864-020-06999-9

Stanke, M. et al. (2006). AUGUSTUS: ab initio prediction of alternative transcripts. Nucleic Acids Research, 34(Web Server), pp. W435–W439. doi: https://doi.org/10.1093/nar/gkl200.

Stratmann, J.W. and Gusmaroli, G. (2012). Many jobs for one good cop - The COP9 signalosome guards development and defense. Plant Science, pp. 50–64. doi: https://doi.org/10.1016/j.plantsci.2011.10.004.

Sun, Y.; Wang, M.; Mur, L.A.J.; Shen, Q.; Guo, S. (2020). Unravelling the roles of nitrogen nutrition in plant disease defences. Int. J. Mol. Sci., 21, 572.

Sweetman, C., Wong, D. C., Ford, C. M., and Drew, D. P. (2012). Transcriptome analysis at four developmental stages of grape berry (Vitis vinifera cv. Shiraz) provides insights into regulated and coordinated gene expression. BMC Genomics 13:691. doi: 10.1186/1471-2164-13-691

Tan, S. et al. (2016). CSN6, a subunit of the COP9 signalosome, is involved in early response to iron deficiency in Oryza sativa. Scientific Reports, 6. doi: https://doi.org/10.1038/srep25485.

Tariq, R. et al. (2022). Genome-wide analyses of the mung bean NAC gene family reveals orthologs, co-expression networking and expression profiling under abiotic and biotic stresses. BMC Plant Biology, 22(1). doi: https://doi.org/10.1186/s12870-022-03716-4.

Team, R. (2020). Rstudio: Integrated Development for r. Rstudio, pbc, boston, ma. Available online: http://www.Rstudio.com.

Teh, S. L., Fresnedo-Ramírez, J., Clark, M. D., Gadoury, D. M., Sun, Q., Cadle-Davidson, L., et al. (2017). Genetic dissection of powdery mildew resistance in interspecific half-sib grapevine families using SNP-based maps. Mol. Breed. 37, 1. doi:10.1007/s11032-016-0586-4.

Teng, R.-M., Wang, Y.-X., Wang, W.-L., Li, H., Shen, W., and Zhuang, J. (2018). Genome-wide identification, classification and expression pattern of LBD gene family in Camellia sinensis. Biotechnol. Biotechnol. Equip. 32, 1387–1397.

Thatcher, L. F., Powell, J. J., Aitken, E. A. B., Kazan, K., and Manners, J. M. (2012). The lateral organ boundaries domain transcription factor LBD20 functions in Fusarium wilt susceptibility and jasmonate signaling in Arabidopsis. Plant Physiol. 160, 407–418. doi: 10.1104/pp.112.199067

The, S.V.; Snyder, R.; Tegeder, M. (2021). Targeting Nitrogen Metabolism and Transport Processes to Improve Plant Nitrogen Use Efficiency. Front. Plant Sci., 11, 628366.

This, P., Lacombe, T. and Thomas, M.R. (2006). Historical origins and genetic diversity of wine grapes. Trends in Genetics, pp. 511–519. doi: https://doi.org/10.1016/j.tig.2006.07.008.

Thom, H. (1958). A note on the gamma distribution. Mon. Weather Rev., 86, 117–122.

Thomidis, T.; Zioziou, E.; Koundouras, S.; Karagiannidis, C.; Navrozidis, I.; Nikolaou, N. (2016). Effects of nitrogen and irrigation on the quality of grapes and the susceptibility to Botrytis bunch rot. Sci. Hortic., 212, 60–68.

Thompson, J. D., Higgins, D. G., and Gibson, T. J. (1994). CLUSTAL W: improving the sensitivity of progressive multiple sequence alignment through sequence weighting, position-specific gap penalties and weight matrix choice. Nucleic Acids Res. 22, 4673–4680. doi: 10.1093/nar/22.22.4673

Thrane, C., Kaufmann, U., Stummann, B., and Olsson, S. (2004). Activation of caspase-like activity and poly (ADP-ribose) polymerase degradation during sporulation in Aspergillus nidulans. Fungal Genet. Biol. 41, 361–368. doi: 10.1016/j.fgb.2003.11.003

Toffolatti, S. L., De Lorenzis, G., Brilli, M., Moser, M., Shariati, V., Tavakol, E., et al. (2020). Novel aspects on the interaction between grapevine and plasmopara viticola: dual-RNA-Seq analysis highlights gene expression dynamics in the pathogen and the plant during the battle for infection. Genes (Basel). 11:261. doi: 10.3390/genes11030261

Toffolatti, S. L., Maddalena, G., Salomoni, D., Maghradze, D., Bianco, P. A., and Failla, O. (2016). Evidence of resistance to the downy mildew agent Plasmopara viticola in the Georgian Vitis vinifera germplasm. Vitis - J. Grapevine Res. 55, 121–128. doi: 10.5073/vitis.2016.55.121-128.

Toffolatti, S. L., Maffi, D., Serrati, L., and Vercesi, A. (2011). Histological and ultrastructural studies on the curative effects of mandipropamid on plasmopara viticola. J. Phytopathol. 159, 201–207.

Toffolatti, S. L., Venturini, G., Maffi, D., and Vercesi, A. (2012). Phenotypic and histochemical traits of the interaction between Plasmopara viticola and resistant or susceptible grapevine varieties. BMC Plant Biol. 12:124. doi: 10.1186/1471-2229-12-124

Toffolatti, S.L.; De Lorenzis, G.; Costa, A.; Maddalena, G.; Passera, A.; Bonza, M.C.; Pindo, M.; Stefani, E.; Cestaro, A.; Casati, P.; et al. (2018). Unique resistance traits against downy mildew from the center of origin of grapevine (Vitis vinifera). Sci. Rep., 8, 12523. doi: https://doi.org/10.1038/s41598-018-30413-w.

Tomasi, N.; Monte, R.; Varanini, Z.; Cesco, S.; Pinton, R. (2015). Induction of nitrate uptake in Sauvignon Blanc and Chardonnay grapevines depends on the scion and is affected by the rootstock. Aust. J. Grape Wine Res., 21, 331–338.

Töpfer, R. et al. (2011). New Horizons for Grapevine Breeding. Fruit, Vegetable and Cereal Science and Biotechnology.

Trenti, M., Lorenzi, S., Bianchedi, P. L., Grossi, D., Failla, O., Grando, M. S., et al. (2021). Candidate genes and SNPs associated with stomatal conductance under drought stress in Vitis. BMC Plant Biol. 21, 7. doi: 10.1186/s12870-020-02739-z.

Trouvelot, S., Varnier, A.-L., Allègre, M., Mercier, L., Baillieul, F., Arnould, C., et al. (2008). A β-1,3 glucan sulfate induces resistance in grapevine against plasmopara viticola through priming of defense responses, including HR-like cell death. Mol. Plant-Microbe Interact. 21, 232–243. doi: 10.1094/MPMI-21-2-0232

Untergasser, A., Nijveen, H., Rao, X., Bisseling, T., Geurts, R., and Leunissen, J. A. M. (2007). Primer3Plus, an enhanced web interface to primer3. Nucleic Acids Res. 35, W71–W74. doi: 10.1093/nar/gkm306

Vadlamudi, T., Patil, B. L., Kaldis, A., Sai Gopal, D. V. R., Mishra, R., Berbati, M., et al. (2020). DsRNA-mediated protection against two isolates of Papaya ringspot virus through topical application of dsRNA in papaya. J. Virol. Methods 275:113750. doi: 10.1016/j.jviromet.2019.113750

Van den Bosch, F.; Zadoks, J.; Metz, J. (1988). Focus Expansion in Plant Disease. II: Realistic Parameter-Sparse Models. Phytopathology, 78, 59–64.

Van Schie, C.C.N. and Takken, F.L.W. (2014). Susceptibility genes 101: How to be a good host. Annual Review of Phytopathology, 52, pp. 551–581. doi: https://doi.org/10.1146/annurev-phyto-102313-045854.

Velt, A. et al. (2023). An improved reference of the grapevine genome reasserts the origin of the PN40024 highly homozygous genotype. G3: Genes, Genomes, Genetics, 13(5). doi: https://doi.org/10.1093/g3journal/jkad067.

Venturini, L. et al. (2013). De novo transcriptome characterization of Vitis vinifera cv. Corvina unveils varietal diversity. BMC Genomics, 14(1). doi: https://doi.org/10.1186/1471-2164-14-41.

Venuti, S., Copetti, D., Foria, S., Falginella, L., Hoffmann, S., Bellin, D., et al. (2013). Historical Introgression of the Downy Mildew Resistance Gene Rpv12 from the Asian Species Vitis amurensis into Grapevine Varieties. PLoS One 8, 1–7. doi: 10.1371/journal.pone.0061228.

Verdenal, T.; Dienes-Nagy, Á.; Spangenberg, J.E.; Zufferey, V.; Spring, J.-L.; Viret, O.; Marin-Carbonne, J.; Van Leeuwen, C. (2021). Understanding and managing nitrogen nutrition in grapevine: A review. OENO One, 55, 1–43.

Veyres, N. et al. (2008). Has Arabidopsis SWEETIE protein a role in sugar flux and utilization? Plant Signaling and Behavior, 3(9), pp. 722–725. doi: https://doi.org/10.4161/psb.3.9.6470.

Vos, P. G., Paulo, M. J., Voorrips, R. E., Visser, R. G. F., van Eck, H. J., and van Eeuwijk, F. A. (2017). Evaluation of LD decay and various LD-decay estimators in simulated and SNP-array data of tetraploid potato. Theor. Appl. Genet. 130, 123–135. doi: 10.1007/s00122-016-2798-8.

Wan, G., Lim, Q.E. and Too, H.P. (2010). High-performance quantification of mature microRNAs by real-time RT-PCR using deoxyuridine-incorporated oligonucleotides and hemi-nested primers. RNA, 16(7), pp. 1436–1445. doi: https://doi.org/10.1261/rna.2001610.

Wang, J. et al. (2017). Overexpression of VpEIFP1, a novel F-box/Kelch-repeat protein from wild Chinese Vitis pseudoreticulata, confers higher tolerance to powdery mildew by inducing thioredoxin z proteolysis. Plant Science, 263, pp. 142–155. doi: https://doi.org/10.1016/j.plantsci.2017.07.004.

Wang, J., and Zhang, Z. (2021). GAPIT Version 3: Boosting Power and Accuracy for Genomic Association and Prediction. Genomics. Proteomics Bioinformatics 19, 629–640. doi: 10.1016/j.gpb.2021.08.005.

Wang, M., Thomas, N., and Jin, H. (2017). Cross-kingdom RNA trafficking and environmental RNAi for powerful innovative pre- and post-harvest plant protection. Curr. Opin. Plant Biol. 38, 133–141. doi: 10.1016/j.pbi.2017.05.003.

Wang, X., Zhang, S., Su, L., Liu, X., and Hao, Y. (2013). A genome-wide analysis of the lbd (lateral organ boundaries domain) gene family in malus domestica with a functional characterization of MdLBD11. PLoS One 8:e57044. doi: 10.1371/journal.pone.0057044

Wang, Y. et al. (2014). Simultaneous editing of three homoeoalleles in hexaploid bread wheat confers heritable resistance to powdery mildew. Nature Biotechnology, 32(9), pp. 947–951. doi: https://doi.org/10.1038/nbt.2969.

Wang, Yantao et al. (2020). The Apple microR171i-SCARECROW-LIKE PROTEINS 26.1 Module Enhances Drought Stress Tolerance by Integrating Ascorbic Acid Metabolism1. Plant Physiology, 184(1), pp. 194–211. doi: https://doi.org/10.1104/PP.20.00476.

Wei, S. et al. (2018). COP9 signalosome subunit 5A affects phenylpropanoid metabolism, trichome formation and transcription of key genes of a regulatory tri-protein complex in Arabidopsis. BMC Plant Biology, 18(1). doi: https://doi.org/10.1186/s12870-018-1347-9.

Welter, L. J., Göktürk-Baydar, N., Akkurt, M., Maul, E., Eibach, R., Töpfer, R., et al. (2007). Genetic mapping and localization of quantitative trait loci affecting fungal disease resistance and leaf morphology in grapevine (Vitis vinifera L). Mol. Breed. 20, 359–374. doi: 10.1007/s11032-007-9097-7.

Wheeler, S.; Pickering, G.J. (2005). Effects of soil management techniques on grape and wine quality. In Fruits: Growth, Nutrition and Quality; Dris, R., Ed.; WFL Publisher: Helsinki, Finland; pp. 195–208.

Wick, R. (2009). Diagnostic tip of the month: clearing and staining roots and other plant tissues. Natl. Plant Diagnostic Netw. Natl. Newsl. 4, 3–5.

Wiedemann-Merdinoglu, S., Prado, E., Coste, P., Dumas, V., Butterlin, G., Bouquet, A., et al. (2006). Genetic analysis of resistance to downy mildew derived from Muscadinia rotundifolia. in Ninth International Conference on Grape Genetics and Breeding, Udine, Italy 2-6 July (Udine, Italy).

Wong, H.-K.; Chan, H.-K.; Coruzzi, G.M.; Lam, H.-M. (2004). Correlation of ASN2 Gene Expression with Ammonium Metabolism in Arabidopsis. Plant Physiol., 134, 332–338.

Woodall, J.; Forde, B.G. (1996). Glutamine synthetase polypeptides in the roots of 55 legume species in relation to their climatic origin and the partitioning of nitrate assimilation. Plant Cell Environ., 19, 848–858.

Xia, N. et al. (2010). Characterization of a novel wheat NAC transcription factor gene involved in defense response against stripe rust pathogen infection and abiotic stresses. Molecular Biology Reports, 37(8), pp. 3703–3712. doi: https://doi.org/10.1007/s11033-010-0023-4.

Xia, Y. et al. (2012). Acyl CoA binding proteins are required for cuticle formation and plant responses to microbes. Frontiers in Plant Science, 3(OCT). doi: https://doi.org/10.3389/fpls.2012.00224.

Xu, B., Li, Z., Zhu, Y., Wang, H., Ma, H., Dong, A., et al. (2008). Arabidopsis genes AS1, AS2, and JAG negatively regulate boundary-specifying genes to promote sepal and petal development. Plant Physiol. 146, 566–575. doi: 10.1104/pp.107.113787

Xu, C., Luo, F., and Hochholdinger, F. (2016). lob domain proteins: beyond lateral organ boundaries. Trends Plant Sci. 21, 159–167.

Yang, H., Shi, G., Du, H., Wang, H., Zhang, Z., Hu, D., et al. (2017). Genome−wide analysis of soybean lateral organ boundaries domain − containing genes: a functional investigation of GmLBD12. Plant Genome 10, 1–19. doi: 10.3835/plantgenome2016.07.0058

Yang, Y. et al. (2012). The ankyrin-repeat transmembrane protein BDA1 functions downstream of the receptor-like protein SNC2 to regulate plant immunity. Plant Physiology, 159(4), pp. 1857–1865. doi: https://doi.org/10.1104/pp.112.197152.

Ye, J., Coulouris, G., Zaretskaya, I., Cutcutache, I., Rozen, S., and Madden, T. L. (2012). Primer-blast: a tool to design target-specific primers for polymerase chain reaction. BMC Bioinformatics 13:134. doi: 10.1186/1471-2105-13-134

Yordanov, Y. S., Regan, S., and Busov, V. (2010). Members of the lateral organ boundaries domain transcription factor family are involved in the regulation of secondary growth in populus. Plant Cell 22, 3662–3677. doi: 10.1105/tpc.110.078634

Younis, A. et al. (2014). RNA interference (RNAi) induced gene silencing: A promising approach of hi-tech plant breeding. International Journal of Biological Sciences, 10(10), pp. 1150–1158. doi: https://doi.org/10.7150/ijbs.10452.

Yu, J., Xie, Q., Li, C., Dong, Y., Zhu, S., and Chen, J. (2020). Comprehensive characterization and gene expression patterns of LBD gene family in Gossypium. Planta 251:81. doi: 10.1007/s00425-020-03364-8

Yu, Y., Zhang, Y., Yin, L., and Lu, J. (2012). The mode of host resistance to Plasmopara viticola infection of grapevines. Phytopathology 102, 1094–1101. doi: 10.1094/PHYTO-02-12-0028-R

Zaidi, S.S. e. A., Mukhtar, M.S. and Mansoor, S. (2018). Genome Editing: Targeting Susceptibility Genes for Plant Disease Resistance. Trends in Biotechnology, pp. 898–906. doi: https://doi.org/10.1016/j.tibtech.2018.04.005.

Zendler, D., Schneider, P., Töpfer, R., and Zyprian, E. (2017). Fine mapping of Ren3 reveals two loci mediating hypersensitive response against Erysiphe necator in grapevine. Euphytica 213, 68. doi: 10.1007/s10681-017-1857-9.

Zhang, S. et al. (2022). Action Mechanisms of Effectors in Plant-Pathogen Interaction. International Journal of Molecular Sciences. MDPI. doi: https://doi.org/10.3390/ijms23126758.

Zhang, Y., Feng, L., Fan, X., Jiang, J., Zheng, X., Sun, H., et al. (2017). Genome-wide assessment of population structure, linkage disequilibrium and resistant QTLs in Chinese wild grapevine. Sci. Hortic. (Amsterdam). 215, 59–64. doi: 10.1016/j.scienta.2016.12.014.

Zhang, Y., Li, Z., Ma, B., Hou, Q., and Wan, X. (2020). Phylogeny and functions of lob domain proteins in plants. Int. J. Mol. Sci. 21:2278. doi: 10.3390/ijms21072278

Zhou, Y. et al. (2019). The population genetics of structural variants in grapevine domestication. Nature Plants, 5(9), pp. 965–979. doi: https://doi.org/10.1038/s41477-019-0507-8.

Zini, E. et al. (2019). R-Loci Arrangement Versus Downy and Powdery Mildew Resistance Level: A Vitis Hybrid Survey. International Journal of Molecular Sciences, 20(14). doi: https://doi.org/10.3390/ijms20143526.

Zou, C. et al. (2020). Haplotyping the Vitis collinear core genome with rhAmpSeq improves marker transferability in a diverse genus. Nature Communications, 11(1). doi: https://doi.org/10.1038/s41467-019-14280-1.

Zou, C. et al. (2023). A Multi-Tiered Haplotype Strategy to Enhance Phased Assembly and Fine-Mapping of a Disease Resistance Locus. Plant Physiology doi: https://doi.org/10.1093/plphys/kiad494.

Zyprian, E., Ochßner, I., Schwander, F., Šimon, S., Hausmann, L., Bonow-Rex, M., et al. (2016). Quantitative trait loci affecting pathogen resistance and ripening of grapevines. Mol. Genet. Genomics 291, 1573–1594. doi: 10.1007/s00438-016-1200-5.

Acknowledgments

Ten years of studies, five years within the marvelous world of grapes…and here we are, the end of a chapter, the beginning of a new one.

I want to thank all the people who helped, encouraged, and sustained me along this journey.

First of all, my acknowledgments go to all the colleagues and professors of the Agriculture, Environment, and Bioenergy Course of the Department of Agricultural and Environmental Sciences (DiSAA) - University of Milan, where I had the opportunity to carry out my Ph.D. studies.

I want to thank my PhD supervisor, Professor Gabriella De Lorenzis, for all the teachings, the support, and the opportunities I had the chance to receive because of her dedication. With her, I want to thank Elisabetta Sergi, without whom my Ph.D. work wouldn't have been as enjoyable (and probably bearable hehe) as it was.

Special thanks go to Dr. Remo Chiozzotto, a constant presence who helped solve the everyday challenges of laboratory activities. With him, I thank all the Professors, colleagues, and friends who were there, with me and for me, along the journey. All the Viticulture group, Prof. Brancadoro, Prof. Failla, and Dr. Cola, Davide B., Davide M., Martino, Beatrice, Francesca, Giacomo and Carola. All the Arboriculture – Barley people, all the professors, Irina, Alessandro, Roberta (amazing roommate too), Valerio and James, Irene, Denise, Elisa, Massimo. All the researchers and all the students.

Thank you to Prof. Dario Cantù and his lab members for hosting me at the University of California, Davis, and for teaching me exciting new tools to broaden my studies.

Thank you to my reviewers and the evaluation committee.

Thank you to all my friends and my roommates. You were always there for fun and support.

And finally, an enormous thank you to my family. Because of you and your sacrifices, I became motivated and brave enough to face this journey.

I hope I didn't forget anyone. If that is the case, I hope you can forgive me. I'm very emotional. You know too well how this affects me. Just know that you have all my gratitude.
If I am who I am, it is because of all of you, there for me.